TUMOR-INITIATING CELLS

IN

MALIGNANT BRAIN TUMORS

A Dissertation

Presented to

The Faculty of the Graduate School

University of Missouri-Columbia

In Partial Fulfillment

of the Requirements for the Degree

Doctor of Philosophy

---

by

PRAKASH RATH

Dr. Mark Kirk, Dissertation Advisor

Dr. Huidong Shi, Dissertation Advisor

December 2009

The undersigned, appointed by the Dean of the Graduate School, have examined the thesis entitled

TUMOR-INITIATING CELLS IN MALIGNANT BRAIN TUMORS

Presented by Prakash Rath

A candidate for the degree of Doctor of Philosophy of Biological Sciences

In addition, hereby certify that their opinion it is worthy of acceptance

_____

Professor Mark D Kirk

_____

Professor Huidong Shi

_____

Professor Joel A Maruniak

_____

Professor Frederick S vom Saal

_____

Professor N Scott Litofsky

I would like to dedicate this to my

friends and family for their endless support.

In memory of my extraordinary grandparents

and my wonderful dog.

ACKNOWLEDGEMENTS

I have been fortunate to meet and collaborate with many amazing people during my Ph.D studies, for which I am truly grateful. I moved around to many labs and locations during my five years and I would like to thank my mentors Dr. Mark Kirk and Dr. Huidong Shi for making the transitions periods as smooth as possible. I would also like to thank them for supporting my research and ideas, which are the most any graduate student can ask for. They have been instrumental in shaping the way I think and encouraging me to succeed. I would like to thank my committee members, Dr. Joel Maruaniak for being a true student advocate, Dr. Scott Litofsky for insightful discussions and constant support, and Dr. Fred vom Saal for his openness and help throughout the dissertation process. I would like to thank my 'special interest committee' Dr. Douglas Anthony and Dr. Douglas Miller for always having an open door and providing excitement in the field of neuro-oncolgy. I would like to thank my friends, particularly Martin, Davide and Sarai, who have supported me in countless ways through the toughest of times. Finally, I would like to thank my brother Dipak for his unique inspiration, my mom Sipra for instilling in me the will to go forward, and my Dad Narayan for his tireless encouragement, long hours of science talk, and pushing me to be a scientist just like him. It is the best thing I've ever done and I can't thank you enough.

TABLE OF CONTENTS

LIST OF FIGURES

Page

LIST OF TABLES

ABSTRACT

Stem cells have the unique ability to differentiate into the many specialized cells of the body. During adulthood, stem cells remain in the organism and maintain the ability to repair and replenish injured or dead cells when necessary. In some cancers however, stem cells are implicated as the driving force of tumorigenesis. The cancer stem cell (CSC) hypothesis states that only a small fraction of cells within a tumor has the capacity to regenerate and maintain the heterogeneity seen in the tumor they were derived from.

Cancer stem cells were first identified as being associated with an acute myeloid leukemia model 15 years ago, and since then, have been detected in a variety of tumors. In malignant gliomas such as glioblastoma multiforme (GBM), a GBM-CSC population with increased levels of resistant to chemotherapy and radiation therapy is thought to be responsible for malignancy and tumor recurrence.

To test the CSC hypothesis, it is necessary to identify these cells. If the model proves to be valid, developing CSC specific therapies would target the root of cancer growth. Overall, understanding the cells involved in brain tumor development, dispersal, and prevention, is the focus of this dissertation.

CHAPTER 1

INTRODUCTION

1.1 Stem Cells

Embryonic Stem Cells (ESCs)

By definition, stem cells maintain two fundamental characteristics: the ability of self-renewal, and the capacity to differentiate into the specialized cells of an adult organism. As development progresses, thousands of genes turn on and off, directing the morphological and biochemical changes occurring in the cell. As the cells move towards their fate, some retain their stem cell properties while other terminally differentiate.

Development begins at the union of the sperm cell and the ovum. After fertilization is complete, the zygote, also known as the totipotent stem cell, will begin to differentiate into the more than 200 tissue types in the adult mammalian body **(Figure 1)** (Smith, 2001). The zygote divides through a series of cleavage divisions, from one cell, to two cells, to four cells and so forth, resulting in densely packed cells called the morula around day three. The outer cells begin to pass fluid into the morula, resulting in the formation of the fluid-filled blastocoel cavity. At around day five, two distinct regions are present, the outer trophoblast layer, and the inner cell mass, collectively referred to as the blastocyst. The inner cell

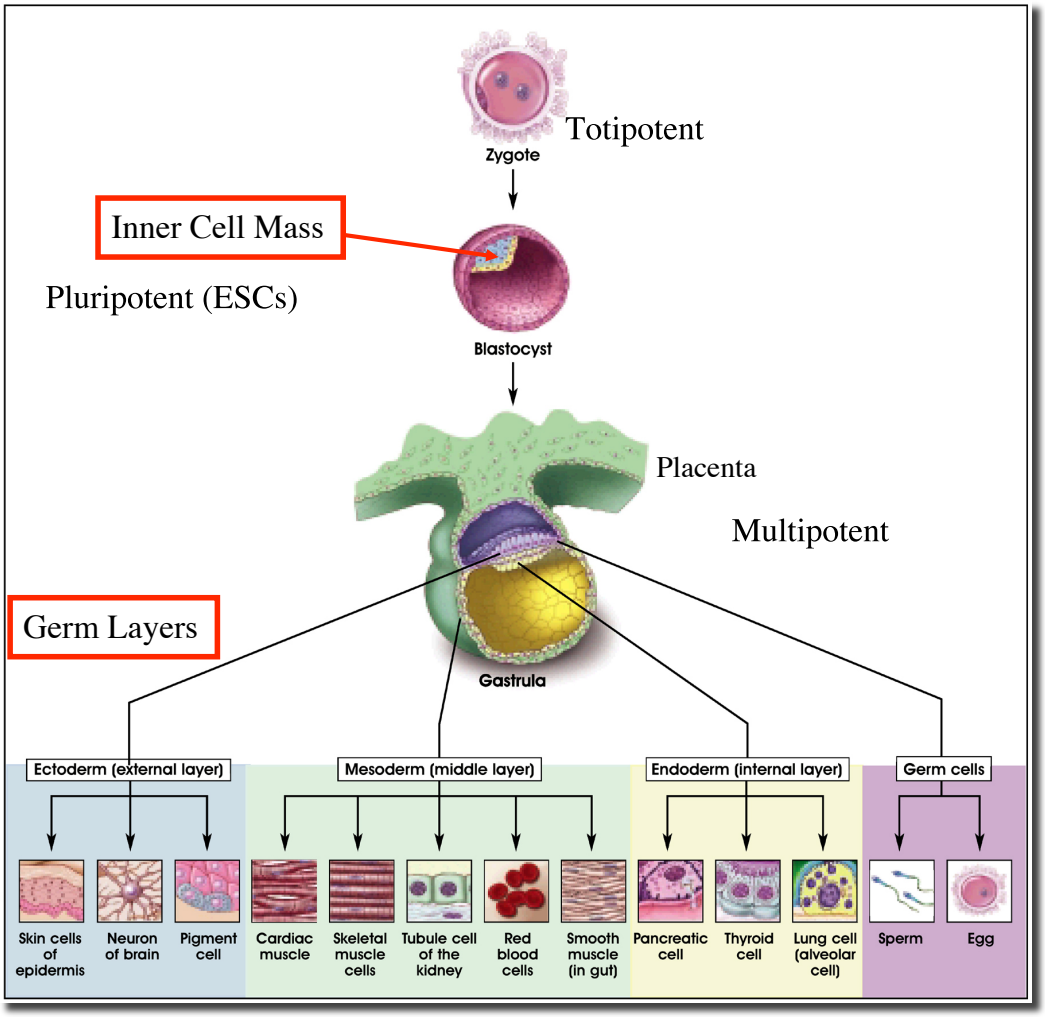

Figure 1. Stem cell differentiation and development

Totipotent stem cells give rise to all the specialized cells of an organism, including the placenta. During the developmental process, the differentiation potential of a cell reduces in a linear fashion: totipotent ⇒ pluripotent ⇒ multipotent ⇒ unipotent ⇒ differentiated cell. ESCs can be obtained from the embryo via immunosurgical and mechanical isolation methods. They can be cultured in defined media in an undifferentiated state for indefinite periods of time, or induced down specific lineages (Koestenbauer et al., 2006). Figure adapted from (Reports, 2006).

mass, better known as the embryonic stem cells (ESCs), are also considered the pluripotent stem cells. ESCs will give rise to the three germ layers: ectoderm, mesoderm, and endoderm. Cells restricted to the ectodermal layer will become skin cells and form the central nervous system. Mesodermal layer cells will become blood, muscle, bone, and fat cells, and endodermal layer cells become lung cells, and cells of the gut (Scott, 2006). As cells become more specialized, their characteristics change accordingly to reflect the extent of their differentiation. A cell that has the ability to form multiple cell types in a specific lineage is known as a multipotent stem cell or progenitor cell, and is generally found within organs or clumps of specialized tissue. Unipotent stem cells, also referred to as precursor cells, are found in developed tissues and differentiate to form only one or two specialized cell types. In contrast to multipotent stem cells, unipotent stem cells have the capacity for a limited number of divisions until they terminally differentiate.

ESC Growth Requirements

Self-renewal is a key feature of stem cells. It is a necessary component of the developing embryo and for the maintenance of adult tissues. Stem cells can undergo asymmetric or symmetric division to produce daughter cells. In asymmetric division, unequal daughter cells are generated in which one cell maintains the parents' developmental features, while the other cell develops into a more specialized cell. Symmetric division results in the generation of two identical daughter cells, both maintaining the developmental potential of the parent cell.

Human ESCs (hESCs) and mouse ESCs (mESCs) respond differently to extrinsic signals, and therefore, different culture requirements are necessary for maintaining them in an undifferentiated state.

Mouse ESCs can be maintained in an undifferentiated state on mouse embryonic fibroblasts feeder cells or by exogenous factors. Studies have shown that mESC self-renewal and inhibition of differentiation depends on leukemia inhibitory factor (LIF) or a cytokine related family member such as interleukin-6 (IL-6). These cytokines act via the gp130/LIF receptor, where upon activation, downstream JAK/STAT3 signaling regulates stem cell differentiation in a myc-dependant fashion (Smith, 2001).

Human ESCs utilize a more complex process to proliferate in an undifferentiated state. Growth factors such as fibroblast growth factor 2 (FGF2), epidermal growth factor (EGF), and transforming growth factor (TGF-ß), have been shown to be mitogenic regulators critical for stem cell self-renewal and inhibition of differentiation (Gritti et al., 1999; Vescovi et al., 2006). FGF2 for example, can maintain hESC self-renewal through the activation of the PI3K/Akt/PKB signaling, where inhibiting this pathway can lead to hESC differentiation (Kim et al., 2005).

Until recently, hESCs were co-cultured on mouse feeder layers (or conditioned medium from feeder layers) in the presence of bovine serum to maintain their undifferentiated state. However, the concern of interspecies pathogen transfer, led to the development of serum-free and feeder-free culture conditions. Studies have shown that hESC differentiation can be inhibited when

they are grown in feeder-free culture conditions supplemented with FGF alone, or in combination with noggin and activin A (Oh and Choo, 2006). In another model for maintaining hESC pluripotency, exogenous noggin was used. Noggin functions to sequester the action of bone morphogenetic protein 4 (BMP4). BMP4 traditionally binds to its receptors, BMPRI and II, whose downstream Smad 1/5/8 activation promotes differentiation. Another peptide Activin A, inhibits differentiation by activating Smad 6/7 to block Smad 1/5/8, and leads to self-renewal by activating Smad 2/3/4. Activin A belongs to the BMP family and acts as an agonist for BMPRI and II, as well as activating its own activin type I and II receptors (Oh and Choo, 2006).

ESC Differentiation

To induce mESCs down specific lineages, mESCs are plated in non-adherent conditions, which facilitates the formation of aggregates termed embryoid bodies (EBs). EBs are grown as suspension cultures in the presence of serum and the absence of LIF. If left in culture, these EBs would spontaneously differentiate into many cell types including neuronal, cardiac, and hematopoietic cells (Chen et al., 2006). This process leads to a heterogeneous conglomeration of differentiated and undifferentiated cells. To specify unique differentiation outcomes, small molecules are used for modulating particular cell fates. For example, retinoic acid (RA) can modulate gene expression and is widely used to induce neuronal differentiation of mESCs (Meyer et al., 2004). During hindbrain development and patterning of the retina, ESCs respond to various concentrations of RA. RA signaling begins by binding to its cognate

retinoic acid receptors (RARs), which dimerize and translocate to the nucleus where they bind to RAR response elements on DNA.

To generate specific cell fates such as motor neurons, combinations of neural inductive signals can be applied in a stepwise fashion. To demonstrate this, Wichterle et al. first treated mESC derived EBs with neural inductive signals (that mimic RA) generated by stromal cells. Further treatment with RA, hedgehog, or hedgehog agonists, creates various types of motor neurons, spinal progenitor cells, and dorsal progenitor cells (Wichterle et al., 2002).

ESC Molecular Markers

Stage-specific embryonic antigens (SSEA) are carbohydrate-conjugated antigens that exist in three forms, the oligosaccharide antigen SSEA-1, and the glycolipid antigens SSEA- 3 and 4. All three SSEA markers are expressed by hESCs and mESCs but differ in the time point in which they appear during development.

Similarly, both hESCs and mESCs express the surface markers CD9 and osteopontin. CD9 is a transmembrane receptor whose expression is linked to the LIF pathway, and proposed to be involved in cell adhesion, migration, proliferation, and fusion (Draper et al., 2002).

Three central proteins that influence gene expression during early development include Oct ¾, Sox-2, and Nanog. They regulate surface marker expression, transcriptional activation, and chromatin remodeling as part of maintaining the pluripotency of stem cells. The expression patterns of these TFs are virtually identical throughout early development and generally regarded as

the markers characteristic of ESC pluripotency in humans and mice (Draper and Fox, 2003).

Sox-2 and Oct ¾ expression is seen during embryonic development in post-migratory primordial germ cells, and down regulated during differentiation. Oct ¾ and Sox-2 bind to an enhancer region and act synergistically downstream of the coding region for target genes, such as the osteopontin gene. In the enhancer region of the osteopontin gene, Sox-2 acts to repress the transactivation of Oct ¾. In contrast, when Sox-2 binds to the FGF4 enhancer region, it acts to suppress the activities of Oct ¾. Sox gene family members facilitate protein-protein interactions on enhancer regions (Koestenbauer et al., 2006).

The TF Nanog, expressed in pluripotent ESCs, plays an essential role in the early development of the embryo and in propagation of undifferentiated ESCs. Nanog and Oct ¾ overlap in function, but their expression does not seem to rely on one another. In a landmark study by Takashashi and Yamanaka et al., the state of ESC pluripotency was induced from mouse embryonic fibroblasts by introducing Oct ¾, Sox-2, c-Myc, and Klf4 (Kruppel-like factor 4; tumor suppressor protein), but not Nanog (Takahashi and Yamanaka, 2006). This study opened the path for creating a pluripotent stem cell state from a seemingly differentiated cell. Induced pluripotent stem cell (iPS) research is an active area of research in many labs across the world because of its potential to bypass the use of ESCs.

Adult Stem Cells (ASCs)

ASCs are considered multipotent cells that differentiate into the specialized cell types of the tissues they reside in. ASCs can be isolated from fetal and adult tissues such as the brain, bone marrow, blood, heart, muscle, skin, liver, fat, amniotic fluid, and gut (Scott, 2006). In most cases, they are slow cycling cells that function to repair tissue when signaled by a disease state or tissue injury.

Perhaps the most well described ASCs are the hematopoietic stem cells (HSCs), which give rise to cells of the myeloid and lymphoid lineages. They are located primarily in the bone marrow but can be found in the spleen, lymph nodes, and circulating blood. Also located in the bone marrow are mesenchymal stem cells (MSCs), which give rise to osteocytes and chondrocytes. In the brain, neural stem cells (NSCs) give rise to neurons, astrocytes, and oligodendrocytes and will be discussed in depth in the sections below (Reports, 2006).

Although ASCs are generally thought to be restricted to a particular lineage, it has been shown that ASCs exhibit remarkable plasticity and can differentiate into cell types other than that of the tissue in which they reside. Examples of this include HSCs differentiating into brain, skeletal muscle, cardiac, and liver cells, and NSCs differentiating into blood and skeletal muscle cells (Grove et al., 2004; Reports, 2006). Similarly, D'Ippolito et al., demonstrated that human bone marrow stomal cells, from which they termed 'marrow-isolated adult multilineage inducible' (MIAMI) cells, had the potential to differentiate into osteoblasts, chondrocytes, adipocytes, and neural stem cells (D'Ippolito et al.,

2004). These cells were proposed to be ideal candidates for the treatment of multiple ailments because they could be coaxed to differentiate into various cell lineages, be readily isolated from peripheral blood, stably transduced with lentiviral vectors, and unlike ESCs, were free of ethical concerns.

Mammalian Stem Cell Niches

To provide support for tissue homeostasis in the event of apoptosis, injury, or tissue regeneration, stem cells must be readily available to mobilize when needed. The regions where stem cells reside in the adult organism are referred to as the 'niche'. This microenvironment, found in various tissues throughout the body, supports the function of stem cells. When called upon to perform their reparative duties, stem cells rely on their intrinsic genetic program, and respond to the environmental signals and supporting cells in the niche (Li and Xie, 2005).

Neural Stem Cell Niche

For most of the twentieth century, the idea that neurogenesis occurred in the brain was largely unaccepted. However, through cellular and molecular studies, it has been shown that neural stem cells reside in two well-characterized germinal regions in the adult brain: the subventricular zone (SVZ) of the lateral ventricle, and the subgranular zone (SGZ) of the dentate gyrus (**Figure 2**). The SVZ is the area situated between the lateral ventricles and the parenchyma of the striatum and is considered the larger of the two identified regions of neurogenesis in the brain. Neurogenesis in the SGZ occurs between the hippocampal granular layer and the hilus (Vescovi et al., 2006).

In the SVZ, cells resembling astrocytes (type B cells) are postulated to be the *bona fide* NSC. These small subsets of astrocytes are relatively quiescent cells with a proposed cell-cycle time of 28 days. Eventually, these cells give rise to neurons and oligodendrocytes. In the sub-ventricular zone, type B SVZ astrocytes are located adjacent to the ependymal cells where they extend a single cilium through the ependymal layer that reaches the lateral ventricle region. Type B SVZ astrocytes express GFAP, vimentin, nestin, and PDGFRα. SVZ astrocytes give rise to fast cycling transiently amplifying precursor cells (type C cells) with a cell-cycle time of about 12 hours. The C cell precursor is characterized as a nestin positive, mitotically active cell. Type C cells further generate mitotically active migrating neuroblasts (type A cells). Neuroblast cells express PSA-NCAM1 (polysialic acid neural cell adhesion molecule 1) and type III B-tubulin. Type A neuroblasts migrate through the rostral migratory stream (RMS) to the olfactory bulb and express HAS (heat-stable antigen). Eventually, neuroblasts differentiate into mature cells such as mitral cells, glomerular, granular cells and interneurons as they integrate in the olfactory bulb. They label positive for neurofilament and MAP2 (microtubule-associated protein) (Li and Xie, 2005) (Vescovi et al., 2006).

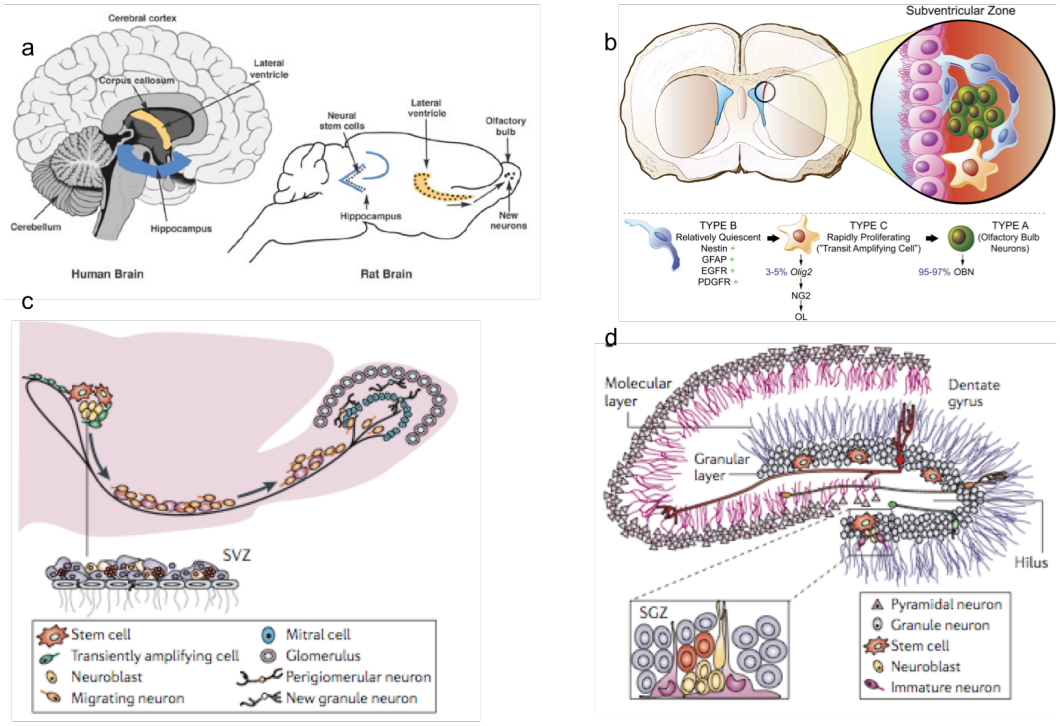

Figure 2. Neural stem cell niche

(a) Sagittal section of a human and mouse brain shows two areas of neurogenesis; 1) the sub ventricular zone located adjacent to the lateral ventricles (yellow), and 2) the sub granular zone of the dentate gyrus (blue). **(b)** Coronal section of a mouse brain depicts the niche architecture of the cells in the SVZ. **(c)** Type A cells migrate tangentially from the SVZ through the rostral migratory stream towards the olfactory bulb where they eventually integrate as interneurons. **(d)** Architecture of the SGZ neural stem cell niche. Figures adapted from: (NIAAA.NIH.GOV.; Vescovi et al., 2006),(Stiles and Rowitch, 2008).

Similar to the cell hierarchy of the SVZ, SGZ astrocytes (equivalent to type B cells) in the hippocampal area are thought to be the true NSC. They are found in direct contact with endothelial cells of blood vessels located in the SGZ. SGZ type B cells eventually generate an intermediate cell (type D cell) that gives rise to functionally integrated granular neurons (type G cell) in the dentate gyrus. In contrast to SVZ neurogenesis, neural precursors in the SGZ migrate short distances before they integrate into the granule-cell layer (Li and Xie, 2005).

For both the SVZ and the SGZ, basal laminal contact and signals from the endothelial cells of adjacent blood vessels is critical for maintaining self-renewal and differentiation of primitive neural stem cells. Some niche signals include: FGF2, IGF1 (insulin-like growth factor 1), VEGF (vascular endothelial growth factor), TGFa (transforming growth factor-alpha), BDNF (brain-derived neurotrophic factor), Noggin, and (bone morphogenetic proteins) BMPs. The type B cells seem to be responsive to these signals, directing the self-renewal and maintenance cues. For example, NSC maintenance occurs by BMP actions that inhibit neuronal differentiation and favors an astrocytic fate. Noggin on the other hand, acts as an antagonist to BMP to promote neurogenesis (Stiles and Rowitch, 2008).

Stem Cell Migration and Migratory Pathways in the Brain

As described above, SVZ-originating neuroblasts migrate throughout the brain, generally along the pathway known as the rostral migratory stream (RMS) towards the olfactory bulb (OB) (Gage, 2000). In response to injury, SVZ originating cells also migrate in many directions through the gray and sub-cortical

white matter, including non-OB regions of the cerebral cortex, the corpus callosum, and to subcortical structures such as the striatum, septum, thalamus and hypothalamus (Goings et al., 2004; Ramaswamy et al., 2005). Migration to adjacent areas of the primary injury site could be due to signaling by areas because of retrograde degeneration, or signal related function of recovery and neural reorganization following injury (Ramaswamy et al., 2005).

In the absence of tumor influence, cells traveling in the brain do so by local and distant cues generated by glial and endothelial cells that populate the microenvironmental regions of the brain. The microenvironment is involved with providing support for neuron development, maintaining homeostasis, and regulating stem cell migration *in vivo* (Muller et al., 2006). In areas of the central nervous system, NSCs use each other for guidance. Two forms of migration in the brain have been studied: radial migration in which neurons climb on radial cells, and tangential migration, where neurons move parallel and perpendicular to radial glial fibers (Lois et al., 1996). The movement known as tangential migration has been defined in the developing brain when cells migrate dorsally on a path from the basal ganglia to the cerebral cortex and hippocampus (Marshall et al., 2003). Lois et al., described another type of migration in adult mice called chain migration, in which SVZ-originating cells migrate to the OB grouped in chains (Lois et al., 1996). During chain migration, glial processes and cell bodies from a type of glial cell in the RMS flank the migrating cells. This glial support provides microenvironmental cues permissive for migration, suggesting that neural precursors move in an independent fashion not guided by radial glia

or axonal fibers. This mechanism of chain migration could explain why NSCs are able to reach pathological regions of the brain such as tumors or inflammation caused by strokes, etc. when traveling in non-typical migratory pathways.

The migratory capacity and potential of NSCs and NPCs (neural progenitor cells; more differentiated than NSCs) has been recently compared (Soares and Sotelo, 2004). Adult SVZ neurosphere-derived stem and progenitor cells were grafted into the SVZ on *ex vivo* organotypic brain slice cultures and mouse brains *in vivo*. Based on criteria evaluating cell survival, integration, and migration, both progenitor and stem cells were relatively equal, with the exception of migratory ability. In forebrain slices, the migratory distance covered by neurosphere-derived progenitor cells was two-fold longer than that of neurosphere-derived neural stem cells. Overall, taking into account the various paradigms outlined in this study, they suggested that although neurosphere-derived progenitor cells exhibited a greater migratory ability, they have a limited migratory potential and neurosphere derived stem cells have broader migratory potential. However, the progenitor cells were grafted in an area containing neurophilic pathways, which happens to be a substrate that favors NPCs. The placement in this area would explain why NPCs had a broader migratory capacity but a lower migratory potential than the NSCs (Soares and Sotelo, 2004). Due to this experimental bias, NSCs may be better suited for brain migration because of their ability to travel on both neurophilic and gliophilic pathways, which suggests that they have the ability to mimic the migratory capacity of tumor cells.

1.2 Brain Tumors

The brain is composed of two main types of cells; neurons and glial cells. Neurons function to transmit signals through the body, and glia supports the structure and function of neurons in the brain. Glial tumors are the most common primary tumor of the brain and are derived from the three main glial cells: astrocytes, oligodendrocytes, and ependymal cells. The World Health Organization (WHO) has set criteria for classifying brain tumors. Neoplasms are histologically graded based on nuclear atypia, mitotic rate, vascular proliferation, and necrosis (**Table 1)**. Benign tumors (grade I) are slow growing, well-differentiated neoplasms. Anaplastic or intermediate grade tumors (grade II) are moderately differentiated with elevated mitoses. Malignant tumors (grade lll-IV tumors) are identified by poorly differentiated or undifferentiated cells and marked endothelial hyperplasia and/or hyperplasia (Vescovi et al., 2006).

The most malignant glioma (WHO grade IV), known as glioblastoma multiforme (GBM), is an aggressive tumor that orginate *de novo* (called primary GBM) or progress from a lower grade tumor (called secondary GBM). Survival rate for GBM patients is approximately one year after diagnosis, a two-year survival of less than 10%, and a five-year survival of less than 4% even with conventional therapies (resection, chemotherapy, radiation therapy) (CBTRUS: 2007-2008 Statistical report: primary brain tumors in the United States; Dirks, 2008; Lipinski et al., 2005). Patients diagnosed with malignant gliomas often succumb to uncontrolled growth of the tumor cells in the limited space of the skull. The foremost treatment is surgical resection, but due to the

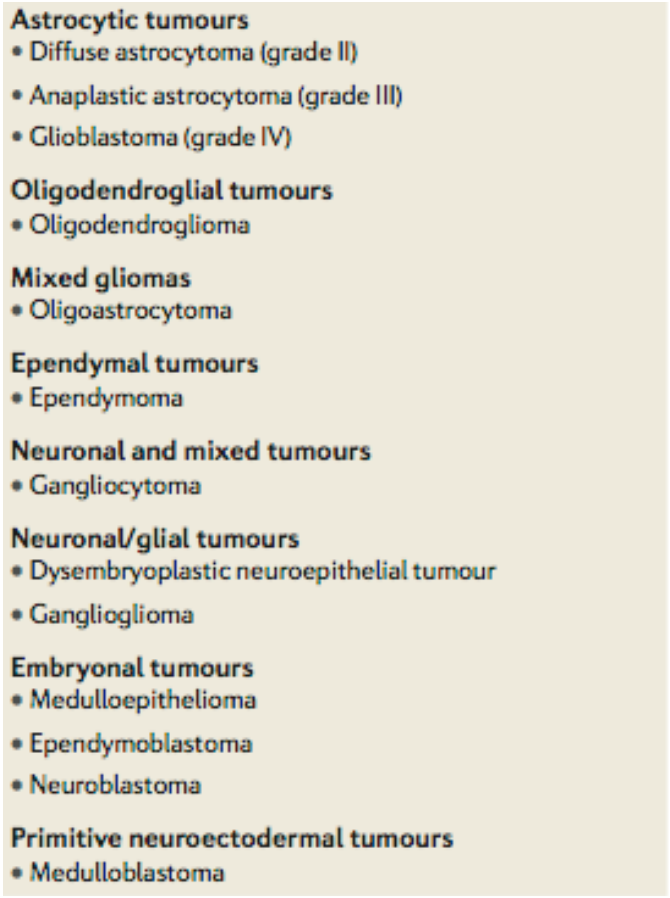

Table 1. WHO classification of brain tumors

Brain tumors are named according to: (1) the cell type they arise from (such as oligodendrogliomas arising from oligodendrocytes), (2) their pathologic evaluation based on World Health Organization (classification grade is based on a I to IV scale from least to most aggressive), (3) sometimes their location (a supratentorial glioma is named because of its location above the tentorium cerebri structure in the forebrain). Due to the heterogeneity of tumors, grade is based on the most malignant cell type in the mass. (Vescovi et al., 2006)

infiltrative growth pattern into normal brain, total removal is never considered complete. GBMs are difficult to treat because of their non-uniform cell cluster formation, with individual cells having varying levels of resistance to radiation and chemotherapy (Bao et al., 2006).

GBMs are defined by their migratory capabilities and characterized by their local or distant migration from the primary tumor site. Pathological hallmarks of GBMs include hyperplasia, vasculation, marked necrosis, and neoplastic cells palisading around the area of necrosis. GBM cells are considered anaplastic with unrecognizable cellular structures and patterns (**Figure 3a)** (Claes et al., 2007).

The cells that break off the primary tumor mass and infiltrate the normal brain, or remain in the walls of the tumor cavity after surgical removal of the bulk tumor, contribute to tumor recurrence. (**Figure 3b)**. These cells have been hypothesized to be the 'cancer stem cell' of the glioma, with the capability of evading conventional treatment modalities (Bao et al., 2006). Note: The literature refers to this sub-population as 'cancer stem cells', 'tumor-initiating cells', 'cancer cells with stem-like properties' etc., here they will be referred to as CSC's.

The 'cancer stem cell' hypothesis states that only a rare subset of cells that reside within the tumor population has the capacity to initiate and sustain the growth and progression of the tumor **(Figure 4a).** Studies have suggested that CSCs are able to mirror the organization and hierarchical structure of normal stem cells. Furthermore, CSCs may undergo asymmetric division with the

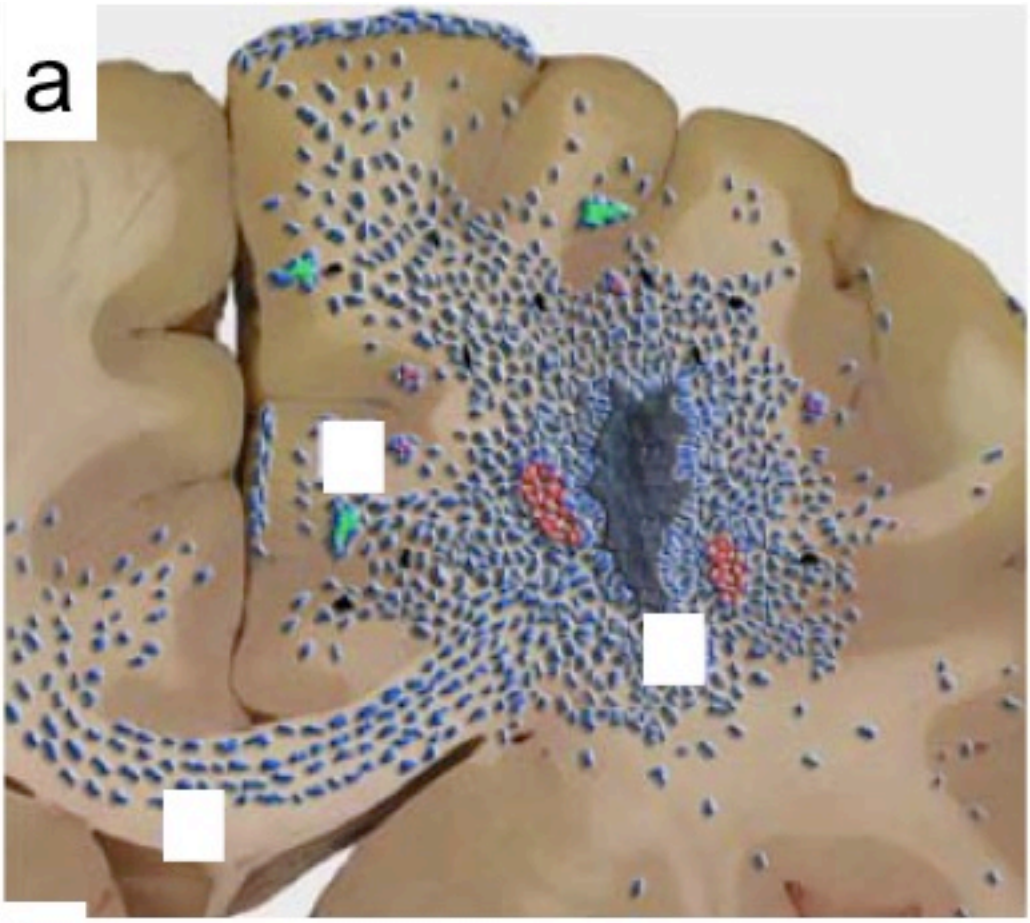

b

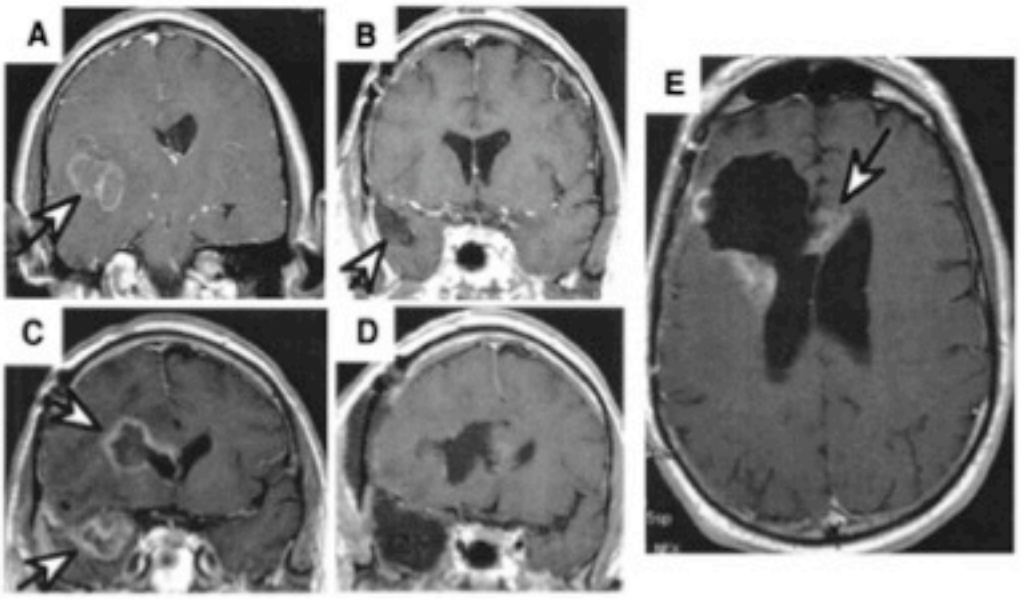

Figure 3. Distinctive features of GBMs

(a) The growth pattern of GBMs is distinct with well-defined characteristics such as: 1) vascular proliferation (blood vessels are in red) 2) tumor cells (blue) accumulation around the vasculature, 3) necrotizing areas (necrosis in dark grey) surrounded by a pseudopalisading tumor cells 4) mitotically active cells (black) 5) 'butterfly structure' of satellite cells seen migrating around neurons (perineuronal satellitosis in green) and contralaterally via the corpus callosum **(b)** MRI scans of a patient with recurring GBM (A) arrow head points to the site of the GBM pre-operation. (B) Scan shows the cavity of the tumor after tumor removal and radiation therapy (C) scan at 6 months post-operation. The arrowheads point the GBM recurrence at the initial site of removal and another site of recurrence. (D) Second operation shows the GBM was removed from both sites. (E) 3 months post second operation showed that the tumor recurred at the margin of the second cavity. Figures adapted from (Claes et al., 2007) and (Holland, 2000).

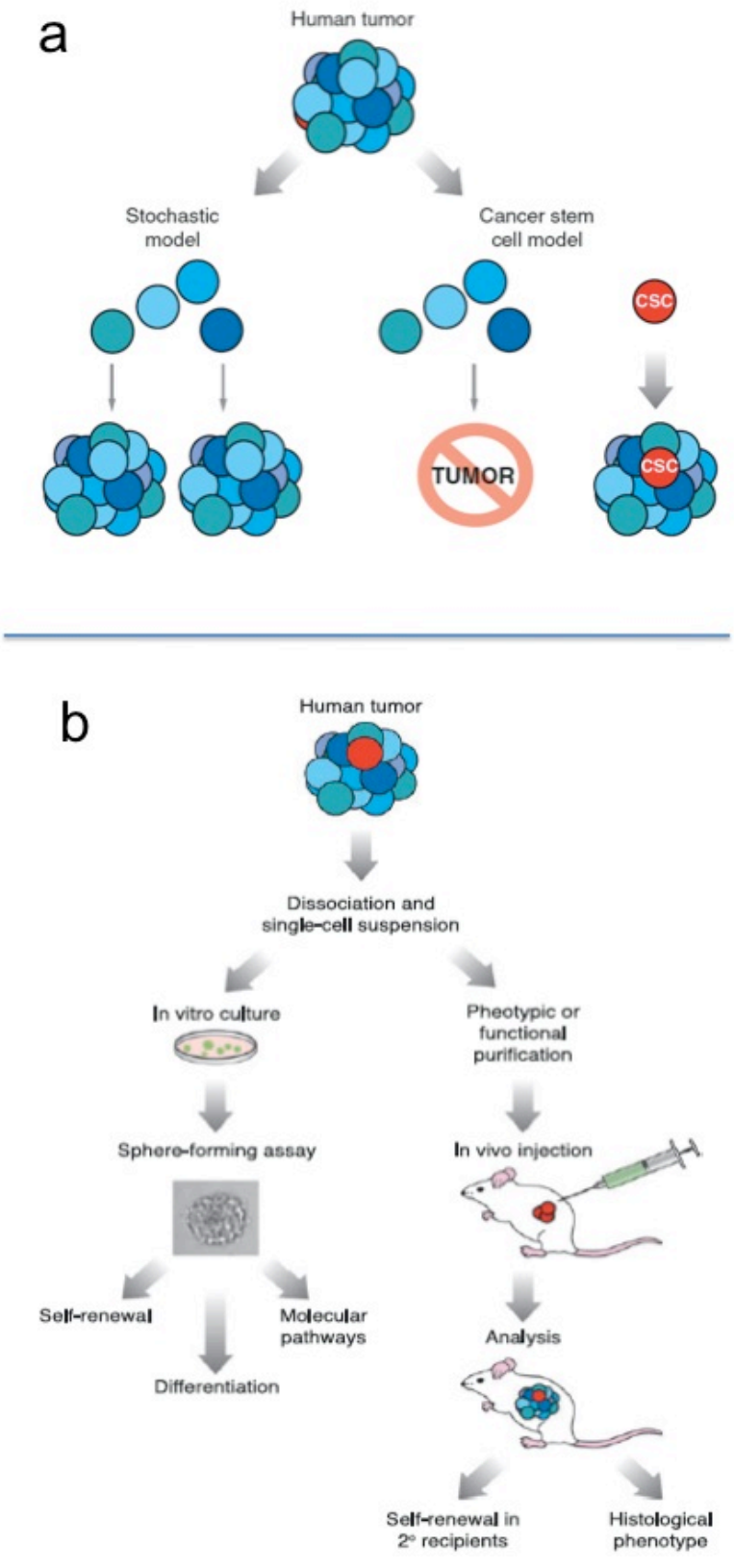
a
Human tumor
Stochastic model
Cancer stem cell model
CSC
TUMOR
CSC
b
Human tumor
Dissociation and single-cell suspension
In vitro culture
Pheotypic or functional purification
Sphere-forming assay
In vivo injection
Self-renewal
Molecular pathways
Differentiation
Analysis
Self-renewal in 2° recipients
Histological phenotype

Figure 4. Stochastic versus cancer stem cell model for tumor growth

(a) Human tumors are composed of heterogeneous population of cells. The stochastic model predicts that if a tumor is dissociated into single cell populations and transplanted *in vivo,* every cell would result in the tumor that recapitulates the heterogeneity of the parental tumor, based on the assumption that all cells have equal capacity. The cancer stem cell hypothesis predicts that only a small fraction of cells (cancer stem cell or CSC in red) in the parental tumor has the ability to regenerate and sustain tumor growth, whereas the rest of the cells would not be able to form a tumor. **(b)** Stem cell properties can be assessed by self-renewal, and differentiation assays. Transplanting fresh dissociated or enriched cultures *in vivo* is performed in order to assess the tumorigenicity of the cells. The xenograft tumor is analyzed to identify if it can recapitulate the phenotype seen in the parental tumor. Expanding cells *in vitro* is necessary to obtain a sufficient amount of cells for further analysis such as the identification of the molecular pathways, phenotypic characterization, and tumorigenesis. It is imperative that defined media containing mitogens is used to propagate the stem cells population. Studies have shown that GBM cells grown in serum (such as the case with many of the established cell glioma lines i.e. U87, N1321 etc.) have additional chromosomal changes and do not well represent the tumor they were initially derived from (Lee et al., 2006) Figures adapted from (Ward and Dirks, 2007).

capability of producing progenitor cells, and have the ability to self-renew and differentiate to form the heterogeneous tumor (Vescovi et al., 2006; Ward and Dirks, 2007). Foremost, the existence of CSCs suggests that developing targeted therapies against this sub-population is necessary to prevent the recurrence of tumor growth.

To identify CSCs, experimental approaches such as sphere-forming assays and transplant models are utilized to determine the ability of self-renewal, differentiation, and tumor regeneration (**Figure 4b).** To isolate CSCs from the brain, the primary tumor is dissociated either mechanically or enzymatically with trypsin or accutase (**Figure 5)**. The cells are placed in serum-free defined medium supplemented with mitogens such as EGF, bFGF, and LIF. LIF was once thought to only effect mouse embryonic cells but recently, the self-renewal of glioma-initiating cells could be induced by TGF-β and LIF (Penuelas et al., 2009). CSCs grow as spherical structures, similar to neurospheres. The removal of mitogens results in the differentiation of precursor cells to neuronal lineages, astrocytes, oligodendrocytes, and neurons.

Under these growth conditions, tumorspheres express nestin and CD133. The surface marker CD133 is perhaps the most-well known marker associated with brain tumor stem cells. CD133 is a trans-membrane protein with unknown function, and found on hematopoietic stem cells as well as neural stem cells. The percentage of cells positive for CD133 in a glioma is though to depend on the aggressiveness of the tumor and can range from 1%-30% of the cells in the

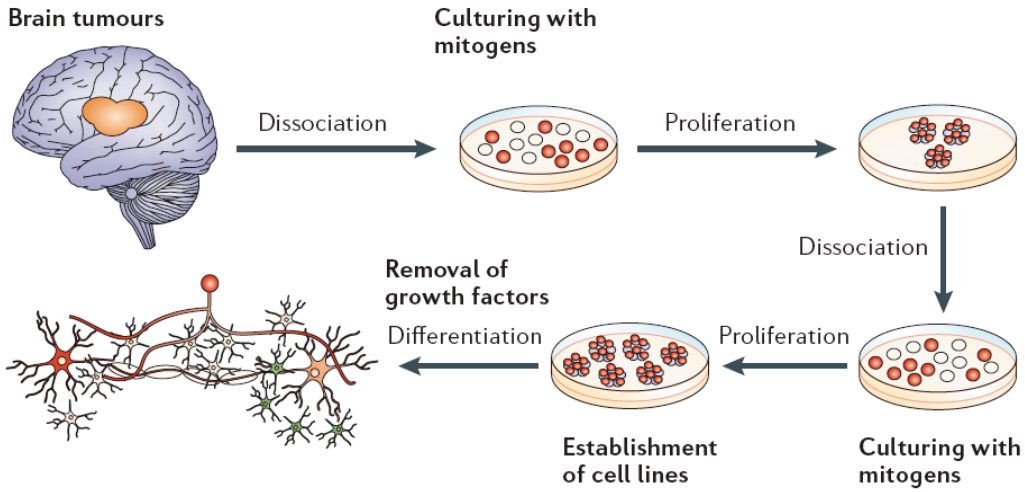

Figure 5. Brain tumor stem cell isolation from primary tumors Schematic representation of a serum-free culture system that allows for the enrichment of CSC population. Growing cells as non-adherent cultures allows the CSCs to float to the top and proliferate, while the non-CSC portion settles to the bottom and differentiates. The tumor spheres can be passaged and eventually, only the non-adherent portion of the tumor remains, representing the enriched CSC population. To study the differentiation capacity, cells may be placed in serum-containing medium, removing of growth factors, or by the addition of chemicals such as retinoic acid or differentiation factors such as BMP or CTNF. Figure from (Vescovi et al., 2006).

tumor (Dirks, 2008). Many studies have documented the isolation of CSCs based on magnetic or flow sorting of cells for CD133. Transplanting 100-1000 CD133+ cells sorted from a GBM can result in a tumor that recapitulates the heterogeneity of the parental tumor, whereas transplanting the CD133- fraction does not result in a tumor (Dirks, 2008). For many years CD133 was thought to be the putative brain tumor stem cell marker, but this notion has been challenged by a study by Beier et al, showing that the CD133- fraction of GBMs maintains stem cell-like properties, and may represent a unique CSC subtype within GBMs (Beier et al., 2007). Additionally, not every CD133+ demonstrates the ability to initiate a GBM and contain stem cell properties. Moreover, Son et al. reported that stage-specific embryonic antigen 1 (SSEA-1), may be present on embryonic stem cells, and utilized as a general CSC enrichment marker in GBMs. They went on to show that SSEA-1+ cells contain all the properties associated with a putative brain tumor stem cell: self-renewal by giving rise to a SSEA-1- population of cells, multilineage differentiation ability, and *in vivo* tumorogenicity (Son et al., 2009).

1.3 Genetics and Epigenetics of GBMs

The driving force of cancer is the genetic and epigenetic alterations. Copy number aberrations, single nucleotide polymorphisms, inversions, translocations, gene fusion events, and DNA methylation events are some of the inherent processes that contribute to cancer. Recently, there have been many large scale studies designed to understand the fundamental mechanisms of GBMs. The aim

of these seminal studies was to identify a 'genetic signature' common to GBMs with the notion that exposing these widespread occurrences will direct the development of better-targeted therapies. The Cancer Genome Atlas Research Network provided the first comprehensive assessment of GBMs (2008). This study reports the integrative analysis of DNA copy number, gene expression, and DNA methylation alterations of 206 primary human GBMs. Through this approach, they were able to pinpoint deregulated events and provide a quantitative measure for these occurrences. The well-known events included the homozygous deletion of CDKN2A/B in over 50% of the samples, as well as MGMT hypermethylation in over 50% of the samples (discussed in more detail below). Three critical signaling pathways were identified to contain frequent genetic alterations: RTK/RAS/PI(3)K (in 88% of the GBMs), p53 (87%), RB (78%). Strikingly, they observed that 74% of the GBMs contained alterations in all three pathways, which suggests that this may be a requirement in glioblastoma pathogenesis.

With this information at hand, another group set out to identify what they called the 'genetic landscape' of GBMs, i.e. the association between the chromosomal alterations (Bredel et al., 2009). They began by analyzing 45 gliomas specimens for chromosomal alterations, and then mined the TCGA study to corroborate their findings. They identified the frequency of chromosomal alterations and reported a high-rate in regions of chromosomes 1p, 7, 8q, 9p, 10, 12q, 13q, 19q, 20, and 22q **(Figure 6)**. To understand the interactions of the

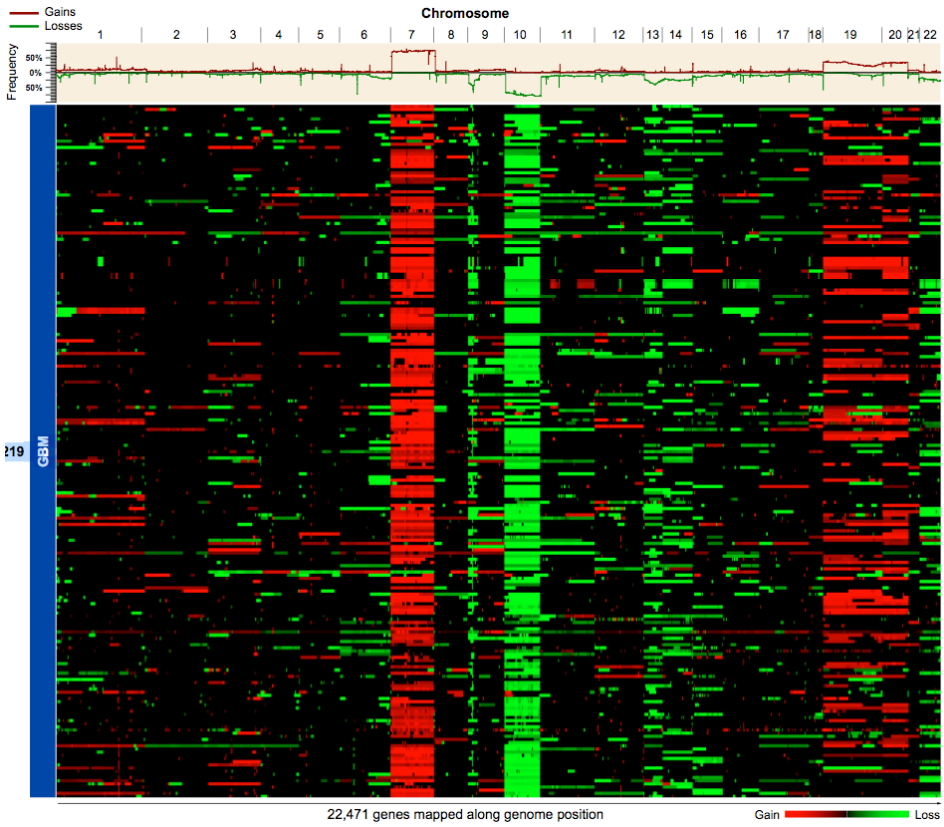

Figure 6. Genome-wide copy number alterations in gliomas

Line diagram show the frequency of CN events for gliomas (based on TCGA study) plotted by chromosome position across the genome. Chromosomes 1p, 7, 8q, 9p, 10, 12q, 13q, 19q, 20, and 22q consistently show a high frequency of alterations. The heat map indicates the frequency of gains (red) and deletions (green) across for individual samples in the data set. The most noticeable occurrence is ch.7 and ch.10 monosomy. Recently, a very nice paper reported the synergism between the amplification of *EGFR* on ch. 7 and the deletion of *ANXA7* on ch. 10, suggesting that the haploinsufficiency of *ANAX7* modulates *EGFR* signaling (Yadav et al., 2009). Figure from (Bredel et al., 2009).

genes that are frequently altered, they performed a pathway analysis, which showed significant interactions amongst genes such as EGFR, MYC, and PTEN. Collectively, these studies provide the framework for understanding the important genetic events that underlies GBMs.

Epigenetics refers to the heritable changes that effect gene expression without altering the DNA sequences and include histone modifications and DNA methylation. Not all genes are expressed at the same time; there are precise mechanisms that ensure that certain cells at certain times express certain genes. DNA methylation and histone modification are mechanisms that regulated cellular processes such as embryonic development, genetic imprinting, x chromosome inactivation, transcription, and chromosomal stability (Robertson, 2005). Epigenetic modifications are reversible, dynamic process, and it is well recognized that epigenetic errors contribute to cancer. DNA is wound around clusters of histone proteins to form nucleosomes. These DNA packaging proteins contributes to chromatin compaction and the regulation of gene expression (**Figure 7)**. The structure of histones can be changed by various biochemical modifications such as acetylation, methylation, and phosphorylation. The modifications dictate whether the chromatin is in a relaxed (open state) or condensed (closed state) state. Active gene expression is associated with the open state of chromatin whereas the repression is associated with the closed state. Addition of a methyl group to the 5-carbon position of a cytosine that precedes guanine in CpG dinucleotides is catalyzed by DNA methyltransferases.

a

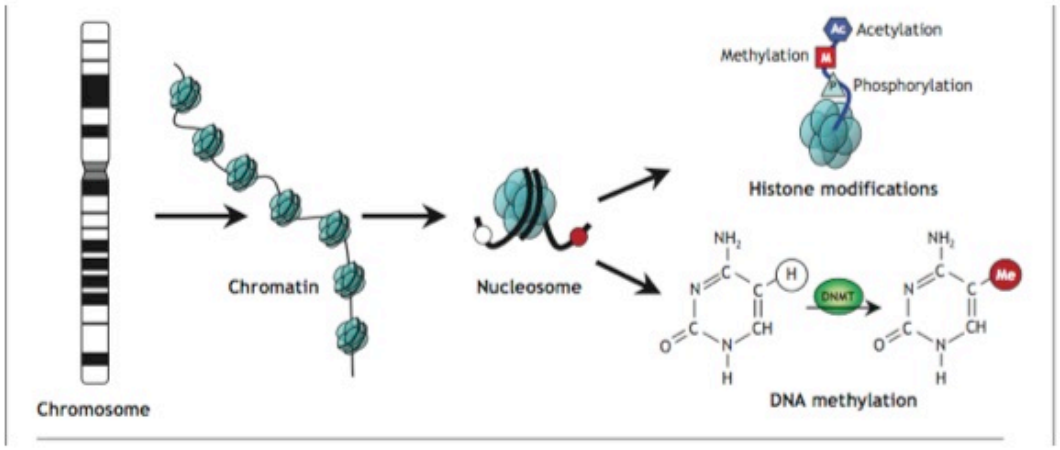
Acetylation
Methylation
Phosphorylation
Histone modifications
Chromosome
Chromatin
Nucleosome
DNMT
DNA methylation

b

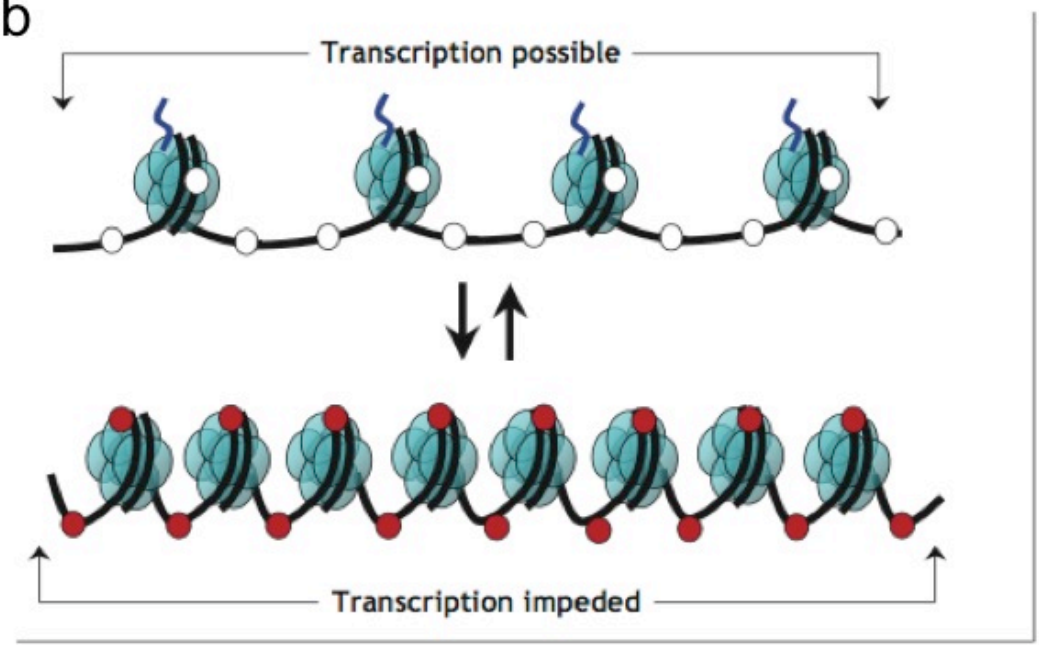
Transcription possible
Transcription impeded

Figure 7. Histone modification and DNA methylation

(a) DNA (black lines) is neatly coiled around nucleosome complexes, each consisting of four core histone proteins: H2A, H2B, H3, and H4 (turquoise circles). Histones function to package DNA as well as regulate gene expression. They are subject to post-translational modifications including the acetylation of histone lysines (blue hexagon) arginine and lysine methylation (red square), and serine phosphorylation (light blue triangle). These modifications facilitate transcriptional activation or repression (blue line represents the amino-terminal tails of the histones) **(b)**. For example, acetylated histones and methylation of lysine (K) 4 residues on H3 is associated with transcriptional activation. Deacetylated histones and methylation of H3 at K9 or K27 is associated with transcriptional repression. Histone modification is a dynamic process and occurs through the actions of histone deacetylases (HDACs) and histone acetyltransferases (HATs) (not shown) (Esteller, 2008). DNA methylation is another type of epigenetic modification in which DNA methyltransferases (DNMTs) catalyze the methylation (red circle) of cytosines at the carbon-5 position. DNA methylation at CpG islands (specifically in promoter to first exon regions) is associated with gene repression, whereas unmethylated areas (white circle) do not impede gene activation. Figures modified from (Rodenhiser and Mann, 2006).

DNA methylation predominantly occurs in CpG dense regions known as CpG islands. CpG islands are distributed throughout the genome and are found in approximately 40% of the promoter regions of genes (Esteller, 2008). In normal cells, CpG islands located in the promoter to first exon regions are generally not methylated. In cancer, hypermethylation in these regions impinges transcription factors from binding, and associated with the silencing of tumor suppressor genes **(Figure 8)**. Conversely, hypomethylation in regions that are normally methylated may result in the expression of genes that are usually turned off.

In GBMs, the methylation status of genes has been correlated with aggressiveness, progression, and sensitivity towards therapeutic agents. An important biomarker is the methylation status of O6-methylguanin-DNA methyltransferase (MGMT), a DNA repair protein that functions to protect normal cells from carcinogens. In cancer cells however, MGMT may protect them from chemotherapy based alkylating agents, which cause DNA damage. In GBMs, promoter hypermethylation of MGMT is associated with deficiency in DNA mismatch repair function and correlates with a longer survival in patients treated with temozolomide. Hence, the methylation status is a predictor for the use of some drugs. CpG island promoter hypermethylation is a frequent event in gliomas and is seen in tumor suppressor proteins such as *TP53, CDKN2A/B, RB* and *PTEN* (Nagarajan and Costello, 2009).

Global DNA hypomethylation on the other hand has been shown to be associated with ~80% of primary GBMs. For example, the frequent

demethylation of the putative oncogene *MAGEA1,* is associated with GBM proliferation (Cadieux et al., 2006). Regarding tumor-initiating cells derived from GBMs, one elegant study by Lee et al, showed that BMP receptor 1A (BMPR1A) epigenetic silencing prevents astroglial differentiation. They went on to show that BMPR1A silencing could be reversed by the addition of a DNA demethylating agents (Lee et al., 2008).

Overall, these examples highlight that genetic and epigenetic events are fundamental mechanisms in the development of cancer and more importantly, these events may be used as biomarkers to predict tumor aggressiveness, or exploited for designing novel therapies.

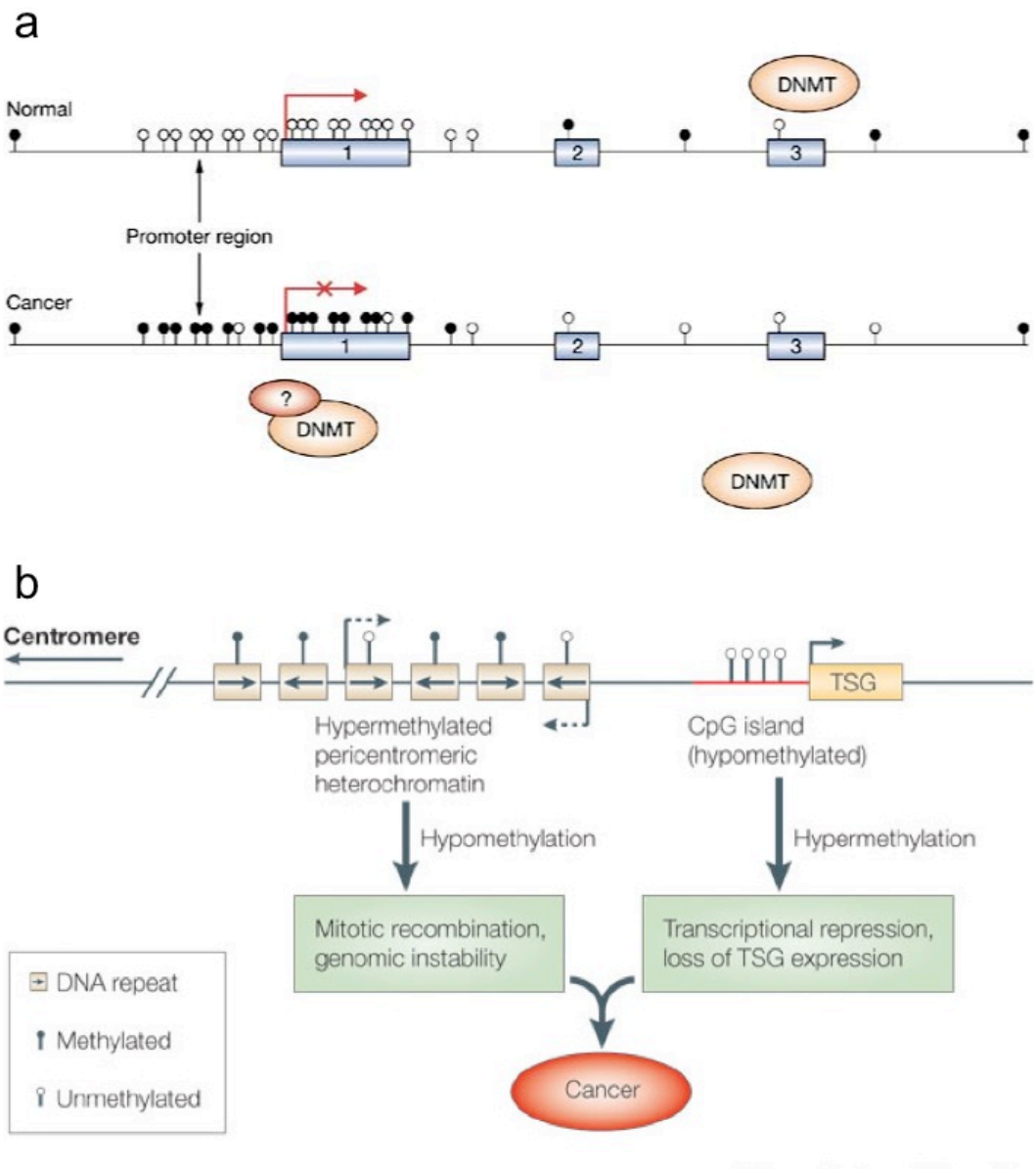
a
Normal
DNMT
1
2
3
Promoter region
Cancer
1
2
3
?
DNMT
DNMT
b
Centromere
TSG
Hypermethylated
pericentromeric
heterochromatin
CpG island
(hypomethylated)
Hypomethylation
Hypermethylation
Mitotic recombination,
genomic instability
Transcriptional repression,
loss of TSG expression
Cancer
DNA repeat
Methylated
Unmethylated

Figure 8. DNA methylation in normal and cancer cells

(a) Schematic representation of the distribution of methylated CpG sites. CpG islands are located throughout the genome but for about have of the genes, they can be found clustered in the promoter regions of genes. In normal cells, the promoter regions are not methylated (white circles), allowing for the transcription of that gene (arrow). In cancer, promoter regions can be methylated (black circles) resulting in the transcriptional silencing of that gene (red x). **(b)** Pericentromeric heterochromatin is transcriptionally silent and heavily methylated. Hypomethylation in this region can lead to instability and may lead to cancer. Correspondingly, methylation of the promoter regions of regulatory genes such as tumor suppressor genes (TSG), may lead to transcriptional silencing and contribution to the development of cancer. Figures adapted from (Baylin, 2005) (Robertson, 2005).

CHAPTER 2

STEM CELLS AS VECTORS TO DELIVER HSV/TK GENE THERAPY FOR MALIGNANT GLIOMAS

Portions Published: Rath, P., Shi, H., Maruniak, J. A., Litofsky, N. S., Maria, B. L., Kirk, M. D., 2009. Current Stem Cell Research & Therapy. 4, 44-9.

2.1 Abstract

The prognosis of patients diagnosed with malignant gliomas including glioblastoma multiforme (GBM) is poor and there is an urgent need to develop and translate novel therapies into the clinic. Neural stem cells display remarkable tropism toward GBMs and thus may provide an effective platform to deliver oncolytic agents to improve survival. First, we provide a brief review of clinical trials that have used intra-tumoral herpes simplex virus thymidine kinase (HSV/tk) gene therapy to treat brain tumors. Then, we review recent evidence that neural stem cells can be used to deliver HSV/tk to GBMs in animal models. While previous clinical trials used viruses or non-migratory vector-producing cells to deliver HSV/tk, the latter approaches were not effective in humans, primarily because of satellite tumor cells that escaped surgical resection and survived due to low efficiency delivery of HSV/tk. To enhance delivery of HSV/tk to kill gliomas cells, recent animal studies have focused on the ability of neural stem cells, transduced with HSV/tk, to migrate efficiently and selectively to regions occupied

by GBM cells. This approach holds the promise of targeting GBM cells that have infiltrated the brain well beyond the original site of the tumor epicenter.

2.2 Introduction

Glioblastoma multiforme (GBM) is the most common primary central nervous system tumor in adults. GBMs are associated with a short life expectancy and high levels of morbidity (Hassler et al., 2006). Conventional treatments including surgical resection, irradiation and chemotherapy may extend survival by weeks, but GBMs are notoriously resistant to adjuvant therapies (Noble, 2000). Infiltrative GBM cells that escape the surgical debulking of the tumor account for tumor recurrence in virtually all cases. The infiltrative GBM cells are highly resistant to treatment so that new therapies must target malignant behaviors of these cells whether they reside at the edge of the surgical cavity or have invaded one or both hemispheres.

Recent *in vitro* and *in vivo* studies highlight the ability of neural stem cells to migrate selectively to brain tumors and to factors secreted by gliomas and cells in their microenvironment (Aboody et al., 2000; Barresi et al., 2003; Serfozo et al., 2006; Shah et al., 2005; Willis et al., 2005) **(Figure 9).** The tropic properties of stem cells, specifically that of neural stem cells (NSCs) (Gage, 2000; Muller et al., 2006) to target brain tumors, suggests that they could serve a role in delivering cytotoxic therapies to gliomas. However, this approach requires

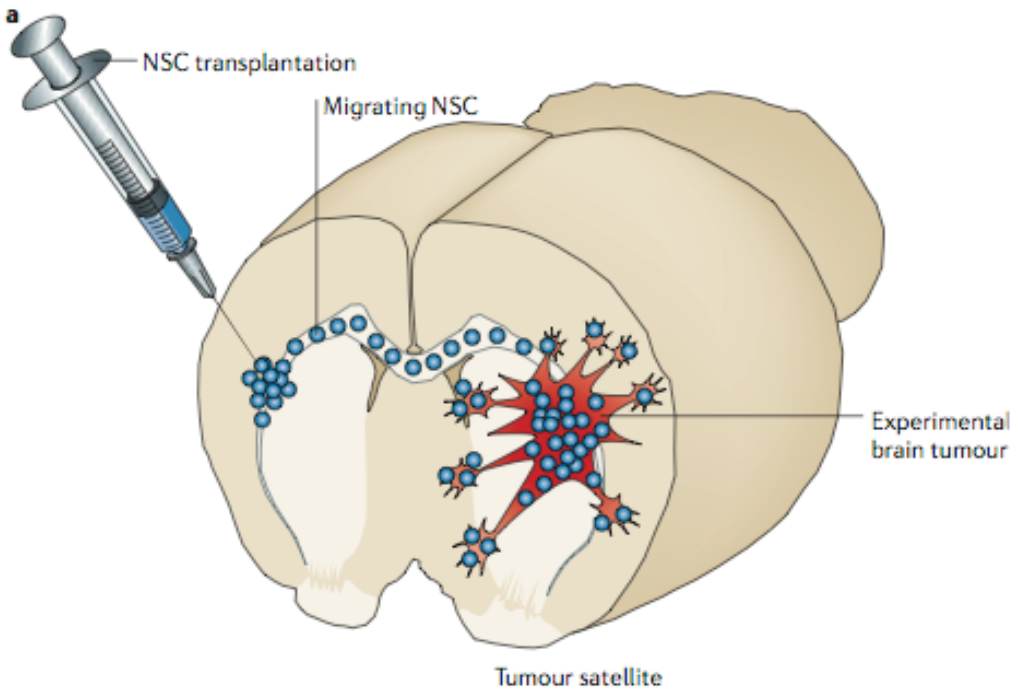

Figure 9. Neural stem cells as vectors to deliver therapy for brain tumors

NSCs show remarkable tropism towards experimental gliomas when transplanted in the brain of rodent models. In malignant gliomas, the cells that break off from the main tumor mass are 1) difficult to identify due to their microscopic size and 2) difficult to and treat due to their seamless infiltration into normal tissue. Neural stem cells are utilized as vectors to deliver chemotherapeutic agents because of their innate migratory capacity in the brain and their ability to respond to the chemokines secreted by the glioma cells. Figure from (Muller et al., 2006).

a better understanding of migratory NSCs, their derivation, administration, and application techniques before it can become useful clinically.

Due to their gliomatropic behavior, NSCs are considered advantageous for delivering anti-tumor agents as an adjuvant for cancer therapy. Various prodrug systems have been designed in which a non-toxic compound (prodrug) is activated within the tissues to become a cytolytic agent when acted upon by a converting enzyme. Examples of prodrug/enzyme gene therapy methods, some of which have employed NSCs as a converting enzyme vehicle for intracranial and disseminated tumor treatment, include 5-fluorocytosine/cytosine deaminase, Camptothecin-11/rabbit carboxylesterase, and Ganciclovir (GCV)/Herpes Simplex Virus-thymidine kinase (HSV/tk) (Aboody et al., 2000; Barresi et al., 2003; Boucher et al., 2006; Danks et al., 2007; Herrlinger et al., 2000; Willis et al., 2005). In this review, we focus on HSV/tk/GCV and on the potential use of NSCs as vehicles to deliver chemotherapy directly to brain tumor cells.

2.3 Methods and Materials

Culture and Neural Induction of Mouse Embryonic Stem Cells

Mouse ES cell line (B5-S129 background; kindly provided by Dr. Andras Nagy, Mount Sinai Research Institute, Toronto, Canada) engineered to express enhanced green fluorescent protein (EGFP) were cultured as undifferentiated colonies in embryonic stem cell growth medium (ESGM) and maintained at 37˚C, 5% CO_2 in a humidified incubator. ESGM consists of Dulbecco's Modified Eagle Medium (DMEM), 10% Fetal Bovine Serum, 10% Newborn Calf Serum,

nucleosides, 1mM leukemia inhibitory factor (LIF), and 7μM ß-mercaptoethanol. Cells were passaged using 0.25% trypsin until they reached ~70% confluence.

To induce the cells down a neural lineage, we used the 4-/4+ induction protocol, which refers to four days in the absence then presence of retinoic acid (Bain et al., 1995) (Meyer et al., 2006). The ES cells were dissociated and seeded onto uncoated petri dishes where they remained for four days in embryonic stem cell induction medium (ESIM is ESGM lacking ß-mercaptoethanol and LIF) to aggregate and form free-floating embryoid bodies (EBs). The medium was changed every other day and after four days, the ESIM was supplemented with 500 nM all-*trans* retinoic acid during induction (Bain et al., 1995; Meyer et al., 2004).

Our lab has previously shown that *in vitro* retinoic acid 4-/4+ treatment will induce B5 EBs to generate neural progenitors, immature and mature neurons and glial cells as seen by marker expression (Meyer et al., 2004). This induction process may be important because embryonic stem cells (ESCs) and neuralized ESCs cells have different capacities for pathotropism and migratory potential (Aboody et al., 2000; Serfozo et al., 2006).

Tumor Cell Culture

We used the SF767 human malignant glioblastoma cell line (kindly provided by Dr. Joseph Loftus, Mayo Clinic, Scottsdale, Arizona), which has been stably transduced to constitutively express red fluorescent protein (RFP), as described (Lipinski et al., 2005). The cells were cultured in DMEM

supplemented with 10% fetal bovine serum and maintained at 37˚C, 5% CO_2 in a humidified incubator.

Organotypic Brain Slices and Donor Cell Application

Organotypic slice cultures were used to visualize migration of the neuralized ESCs to the tumor cells, as *ex vivo* conditions mimic well the *in vivo* environment **(Figure 10)**. This protocol was developed in the Kirk Lab by modifying existing procedures (Benninger et al., 2003; Lipinski et al., 2005; Stoppini et al., 1991). Organotypic slices from whole brains of post-natal day 10 Sprauge-Dawly Rats were maintained for up to 8 weeks, with their organization and cytoarchitecture intact.

Rats were sacrificed by chloroform inhalation according to protocols established by ACUC at the University of Missouri. Briefly, the brains were removed from the skull and immediately placed in ice-cold medium composed of 50% MEM with 15mM Hepes, 25% Horse Serum, 25% HBSS, 6.5 mg/ml glucose, 10µl/ml Penicillin/Streptomycin, 10µl Fungizone, pH 7.2. The brains were then placed in room temperature 4% agarose and put on ice to gel. The brains (containing both hemispheres) were coronally sectioned with a vibratome (VIBRATOME Series 1000) at 400µm and aseptically placed onto Millicell ® trans-well membranes (Millipore, Billerica, MA) in 35 mm petri dishes, or agar plates made with the medium, and maintained in a 37ºC, 5% CO_2 humidified incubator. Culture medium was replaced daily until day 5, then replaced once weekly with serum-free medium composed of 95% DMEM-F/12, 2% B27, 1% N_2 1% Penicillin/Streptomycin, and 1% Fungizone.

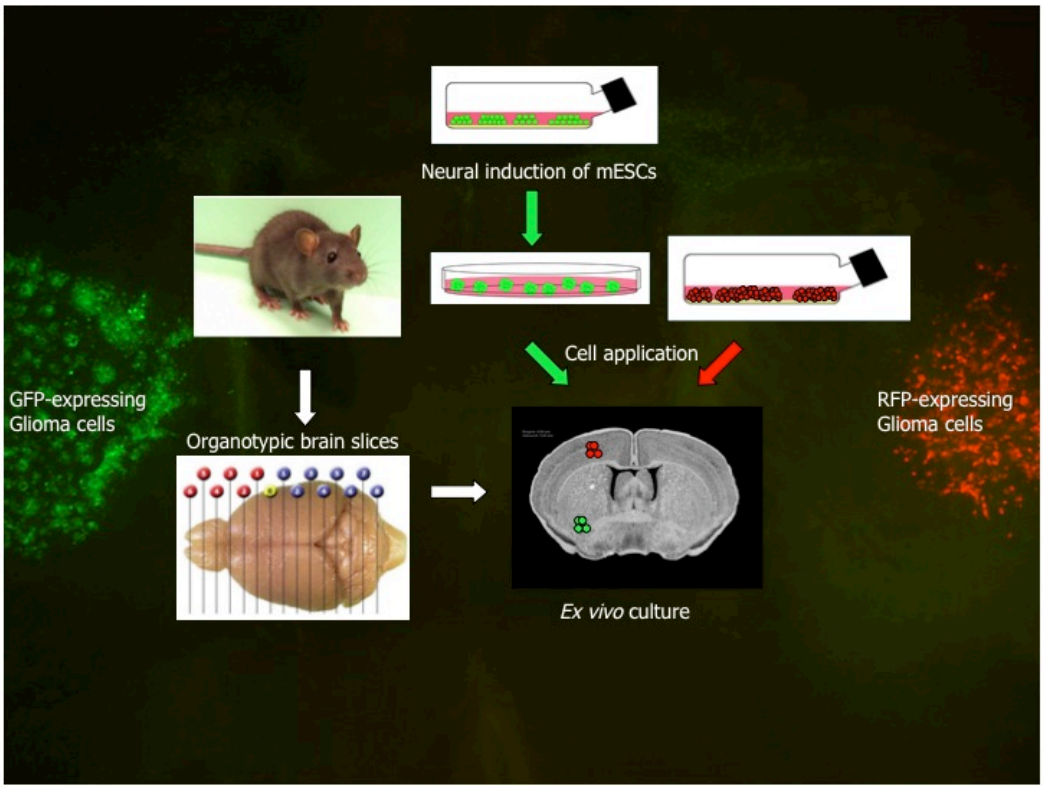

Figure 10. Workflow for studying stem cell migration *ex vivo*

Organotypic brain slices provide a good model system for studying migration because it is cost-effective and allows for real-time monitoring of stem cell migration at multiple time points. Organotypic brain slices well represent the cellular composition, morphology, and physiological properties of the brain environment. Furthermore, the interaction between the cells and the extracellular matrix is an important component to establish the tumor microenvironment and migration. The background image is stereomicroscopic view of green fluorescent protein (GFP)-expressing neuralized mouse embryonic stem cells placed adjacently to red fluorescent protein (RFP)-expressing SF767 glioma cells on an organotypic brain slice. Mouse figures from (http://www.mbl.org/).

On the day of the brain explants, 5,000-20,000 cells (in 0.2 µl) of GFP-expressing neuralized B5 mESCs were added via borosilicate glass pulled pipettes to an area at the bottom left quadrant of the brain slice. One day later, RFP-expressing 5,000-20,000 SF767 glioblastoma cells were added to the top right quadrant of the brain slice.

2.4 Results and Discussion

HSV/tk/GCV – Mechanisms of Action

The HSV/tk targeted gene therapy approach for treating malignant gliomas is a well-characterized gene therapy (Culver et al., 1992; Hurwitz et al., 2003; Moolten and Wells, 1990; Namba et al., 2001; Ram et al., 1997). It is known as a suicide gene therapy because upon exposure to GCV it kills rapidly dividing cells transduced with HSV/tk and rapidly dividing bystander cells (see below). This form of gene therapy was developed as a human cancer therapy because of its efficacy in preclinical studies (Boucher et al., 2006; Kokoris and Black, 2002). The key enzyme, thymidine kinase, has a crucial function in DNA synthesis and is therefore exploited in anti-viral drugs designed to target constantly replicating viruses. Previous therapies involving HSV/tk for cancer treatment used retroviruses to insert the HSV/tk DNA directly into the genome of cancer cells. Conversely, when stem cells are used as therapeutic platforms, the HSV/tk protein in transduced stem cells converts a prodrug to an oncolytic factor, and the latter is transferred from the stem cell to tumor cells via gap junctions; this requires effector and target cells to be contiguous.

In normal cells, tk functions by catalyzing the phosphorylation of thymidine to produce deoxythymidine mono-, di-, and tri- phosphate (dTMP, dTDP, dTTP), and dTTP inserts itself into nascent DNA during cell division (Reardon, 1989). Unlike human tk, HSV/tk has broad substrate specificity with the ability to phosphorylate pyrimidines (thymidine), pyrimidine analogs (such as azidothymidine or AZT, the popular drug used to combat HIV), purines (guanosine), and purine analogs (such as GCV). Ganciclovir is a commonly used drug for treatment of Herpes infection and as the prodrug used in combination with the HSV/tk method for cancer therapy. GCV is administered intravenously and freely diffuses across the blood-brain-barrier. Initially, the non-toxic nucleoside analog GCV is referred to as the prodrug, that upon phosphorylation by the enzyme HSV/tk produces a cytotoxic metabolite that accumulates in the cell (Kokoris and Black, 2002; Reardon, 1989).

As mentioned above, HSV/tk transduced stem cells kill neighboring non-transduced, rapidly dividing cells (e.g. gliomas) through the transfer of the oncolytic agent between nearby or contiguous target cells; this is known as the "bystander effect" **(Figure 11)**. After migration to the glioma, the HSV/tk transduced stem cells form gap-junction channels with adjacent tumor cells, and the gap junctions enable transfer of phosphorylated GCV metabolites from one cell to the other (Mesnil et al., 1996; Namba et al., 2001). Gap junction formation provides adhesive contacts important for neuronal migration and has been

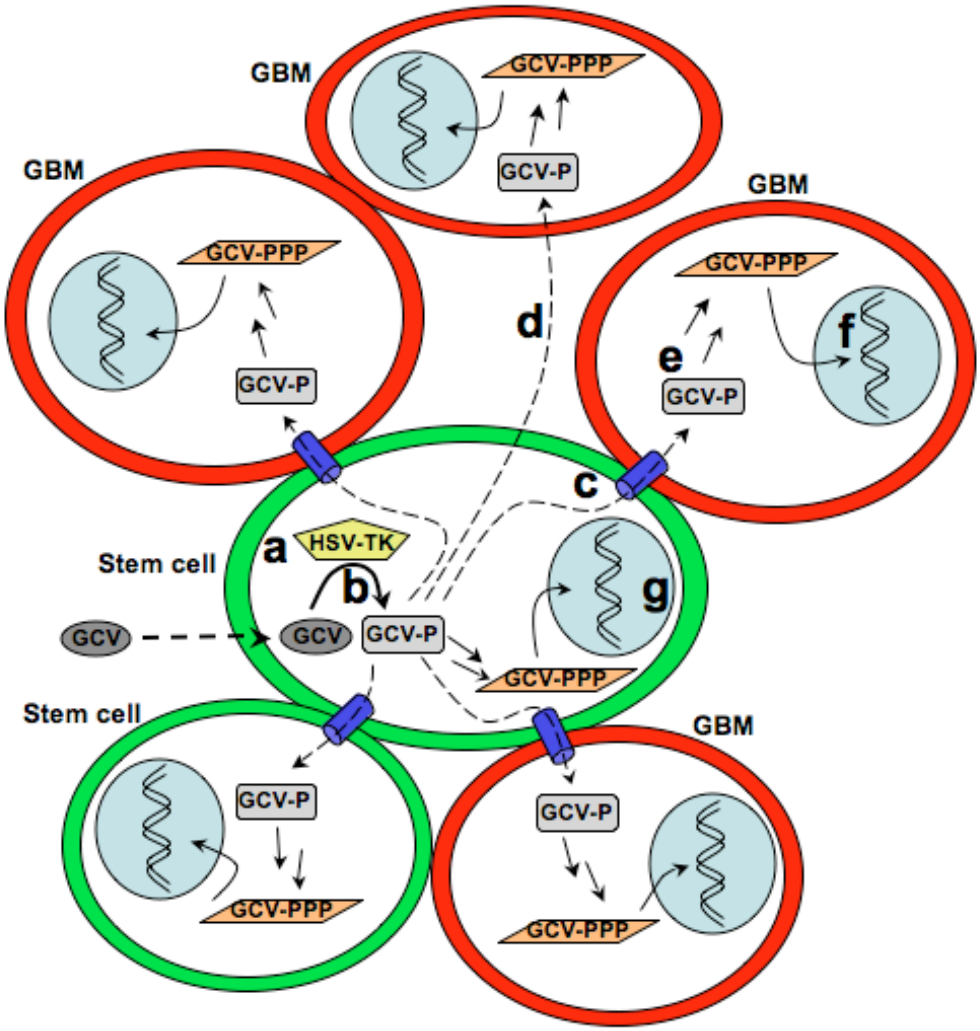
GBM
GCV-PPP
GCV-P
GBM
GCV-PPP
GCV-P
GBM
GCV-PPP
e
GCV-P
f
d
c
a
HSV-TK
b
Stem cell
g
GCV
GCV
GCV-P
GCV-PPP
Stem cell
GBM
GCV-P
GCV-PPP
GCV-P
GCV-PPP

Figure 11. Suicide gene therapy and the bystander effect.

(**a**) Transduced stem cells (green) that express constitutively Herpes Simplex Virus thymidine kinase (HSV-TK) migrate to the vicinity of GBM cells (red). (**b**) Upon systemic administration of the non-toxic, antiviral drug ganciclovir (GCV), GCV is mono-phosphorylated (GCV-P) by the viral TK enzyme in the stem cells. (**c**) Gap junctions present between cells facilitate the passive transport of GCV-P to adjacent non-transduced target GBM cells. (**d**) GCV-P may also be transported to GBM cells via a gap junction-independent pathway. (**e**) Endogenous mammalian kinases within the GBM cells further phosphorylate GCV-P to its toxic product (GCV-PPP). (**f, g**) GCV-PPP acts as a purine analog incorporating itself into nascent DNA where it interferes with replication, resulting in apoptosis of rapidly dividing cells. The death of non-transduced cells due to the transfer of an oncolytic agent is referred to as the bystander effect and in conjunction with concurrent suicide of transduced cells by the same mechanism involving GCV-PPP, is collectively known as suicide gene therapy. Figure adapted from (Hurwitz et al., 2003)

implicated in modulating the adhesiveness and invasion of malignant gliomas (Elias et al., 2007; Lin et al., 2002). Regarding the HSV/tk gene therapeutic approach, intercellular communication via gap junctions has been linked to a strong tumoricidal bystander effect, particularly involving connexin 43 (Sanson et al., 2002).

The specific mechanisms whereby GCV/tk delivered by stem cells kills rapidly dividing cells are as follows. Initially, the HSV/tk present in the stem cells converts GCV into monophosphorylated GCV-P that then traverses into neighboring cells through the gap junctions (Sanson et al., 2002). Alternatively, it is possible for GCV-P to be transferred by efflux from HSV/tk-expressing cells with subsequent uptake by neighboring cells in a gap junction independent manner (Drake et al., 2000). After GCV-P is transferred, it is further phosphorylated by host cell thymidine kinase to create the cytotoxic metabolite GCV-triphosphate (GCV-PPP). The GCV-PPP inhibits competitively incorporation of deoxyguanosine triphosphate (dGTP), and cells undergoing DNA replication (e.g., rapidly dividing glioma cells) integrate GCV-PPP into newly synthesized DNA, causing premature chain termination that leads to cell death via apoptosis (Beltinger et al., 1999; Boucher et al., 2006; Moolten and Wells, 1990).

Stem Cells as Therapeutic Platforms to Deliver Oncolytic Agents

Neural stem cells are primitive, self-renewing cells that can differentiate to form mature cells of neuronal or glial lineage. Neural stem cells can be obtained from neurogenic regions in the brain such as the subventricular zone (SVZ) or

can be derived from induced embryonic stem cells (Alvarez-Buylla and Doetsch, 2002). Neural stem cells are considered good candidates as therapeutic vectors for malignant cancer therapy because they possess a number of unique characteristics. Perhaps the most important feature of NSCs in this context is a large migratory capacity that enables them to traverse brain hemispheres, a necessary characteristic when considering a cell-based therapeutic method that is capable of 'tracking down' diffuse infiltrative gliomas such as GBM satellite cells (Muller et al., 2006; Srivastava et al., 2006). This ability of transplanted NSCs to migrate towards contralateral tumor insults in the brain has been demonstrated in many studies and was first observed in rat models by Snyder and colleagues (Aboody et al., 2000). Since then, many stem cell types including embryonic, mesenchymal and neural stem cells have shown glioma tropism in the central nervous system (CNS) as well as the ability to deliver prodrug/enzyme therapies to cancers (Aboody et al., 2000; Aboody et al., 2006; Chen et al., 2007; Nakamizo et al., 2005; Srivastava et al., 2006).

Throughout adulthood neuroblasts originating from the SVZ migrate along the rostral migratory stream and enter the olfactory bulb (Gage, 2000; Goings et al., 2004). However, in response to injury, SVZ-derived neuroblasts can migrate in many directions through gray matter and sub-cortical white matter, including regions of the cerebral cortex and the corpus callosum and to subcortical structures such as the striatum, septum, thalamus and hypothalamus (Goings et al., 2004; Ramaswamy et al., 2005). For example, Glass and colleagues observed that endogenous SVZ stem cells can migrate toward a glioma graft

(Glass et al., 2005). In addition to being able to migrate in the brain, another benefit of using NSCs is that they are destined inherently (or primed in the case of induced embryonic cells) to become mature neural cells. Neural cells may be more suitable for engrafting, navigation, and integrating into a neural environment but most importantly, to deliver chemotherapy to the GBM in the brain parenchyma.

Neural Stem Cell Homing and Pathotropism

The innate attraction and migration to areas of inflammation due to CNS pathologies such as brain tumors make NSCs unique candidates for therapeutic platforms. Therefore, several preclinical studies have explored the use of NSCs as drug-delivery vehicles to treat brain cancer (Aboody et al., 2000; Tang et al., 2003; Willis et al., 2005). The chemokines and receptors that direct NSC pathotropism are not defined completely but involve signals released at the site of insult (cancer, lesion, etc.) and transient reparative signals expressed by cells in the microenvironment (Imitola et al., 2004; Muller et al., 2006). Some chemoattractants that may induce NSC tropism include stem cell factor (SCF), stromal cell derived factor-1 (SDF-1), vascular endothelial growth factor (VEGF), fractalkine, monocyte chemoattractant protein 1 (MCP-1), hepatocyte growth factor (HGF), and many of the CXC motif chemokines (Imitola et al., 2004; Kendall et al., 2008; Muller et al., 2006; Yip et al., 2006).

Stem cell tropism towards various types of cancers involves different subsets of stem cells and occurs following xenotransplantation of stem cells (Aboody et al., 2006; Nakamizo et al., 2005; Srivastava et al., 2006). Cross-

species interactions may be an important point when considering treatment and tolerance in humans; for instance as described later, human clinical trials have tested mouse fibroblasts as drug delivery biopumps.

We examined cross-species interactions using *ex vivo* post-natal day 10 rat organotypic brain slices as a model system for migration. Neuralized mouse embryonic stem cells that were implanted on the slices, migrated and co-localized with human glioblastoma cells within one-week **(Figure 12)**. This migration of murine stem cells toward human glioma cells on *ex vivo* rat slices is similar to *in vivo* results of transplanted syngeneic NSC migration to induced brain tumors in rodent models (Li et al., 2005). In both *in vivo* and *ex vivo* studies, transplanted stem cells surrounded the tumor graft and were not detectable in other areas of the brain, suggesting a very directed migration of the stem cells that resulted in co-localization with the glioma cells **(Figure 12D)**. This well-orchestrated movement is consistent with a specific chemokine-mediated gliomatropic response and illustrates the compatibility of signaling mechanisms between species, albeit in the absence of an immune response in these *ex vivo* studies. Most importantly, tumor infiltration by stem cells seen over time appears sufficient to confer a cytotoxic transfer between the stem and tumor cells via the bystander effect **(Figure 13)**.

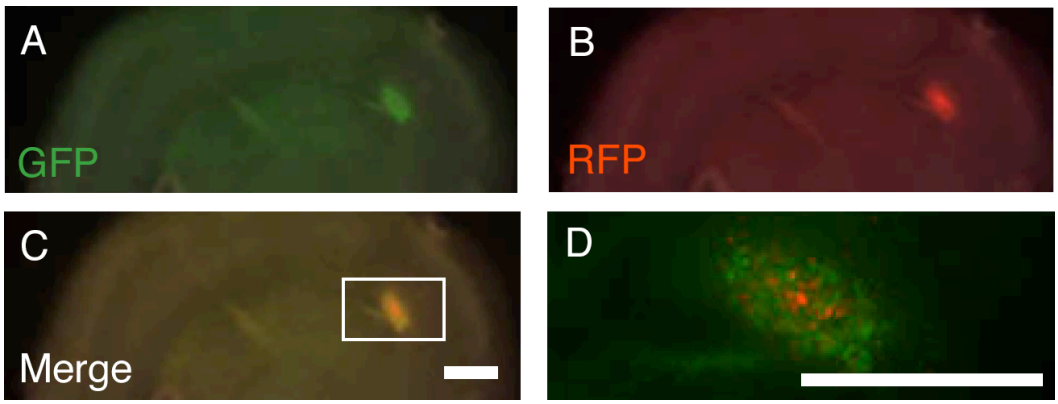

Figure 12. nESCs co-localize with glioma cells

GFP-expressing neuralized mouse embryonic stem cells (nESCs) co-localize with RFP-expressing human tumor cells in an organotypic brain slice. Stereoscopic epifluorescent images show tumor mass infiltration by nESCs. GFP-expressing nESCs and RFP-expressing human glioma cells were introduced on the surface of the organotypic rat brain slice. The living brain section was obtained from a 300-micron thick coronal slice just anterior to bregma obtained from a fresh rat brain embedded in agarose and cut with a vibratome. Initially, 10 ml (~8,000 cells/ µl) of both cell types were simultaneously implanted at separate locations on the surface of a one-week old slice. Aliquots of the two cell types were applied approximately 10 mm from each other across the width of the organotypic slice. Images shown here were taken one week after implantation of the nESCs and glioma cells. Stereomicroscopic epifluoresent images show that stem cells placed distant from the tumor cells co-localized to with tumor cells and were not detectable in other regions of the brain slice. Scale bars = 1 mm; Scale bar in C applies to A-C.

It will be of interest to determine the specific mechanisms that lead to stem cell proliferation and migration when attacking brain tumors. For instance, further studies are needed to analyze whether the stem cells proliferate before migration, or whether the tumor microenvironment influences stem cell migration before proliferation. Molecular and cellular mechanisms underlying stem cell mobilization are relatively unknown and understanding how stem cells mobilize may improve strategies for optimizing where and when to administer stem cells, and in the context of GCV/tk, how to improve GCV administration for more efficient bystander killing.

Our migration data illustrate that *ex vivo* culturing provides the opportunity to view cells in a neural environment that closely mimics *in vivo* conditions, a limitation that *in vitro* migration assays have yet to achieve. Organotypic cultures further highlight the potent ability of signaling molecules to regulate stem cell migration, and highlight the conservation of stem cell and glioma cell signaling molecules across species (i.e., human and mouse). This may also prove to be a useful model system for investigating pathotropism and for testing various types of stem cells as potential delivery vehicles for prodrug/enzyme therapies.

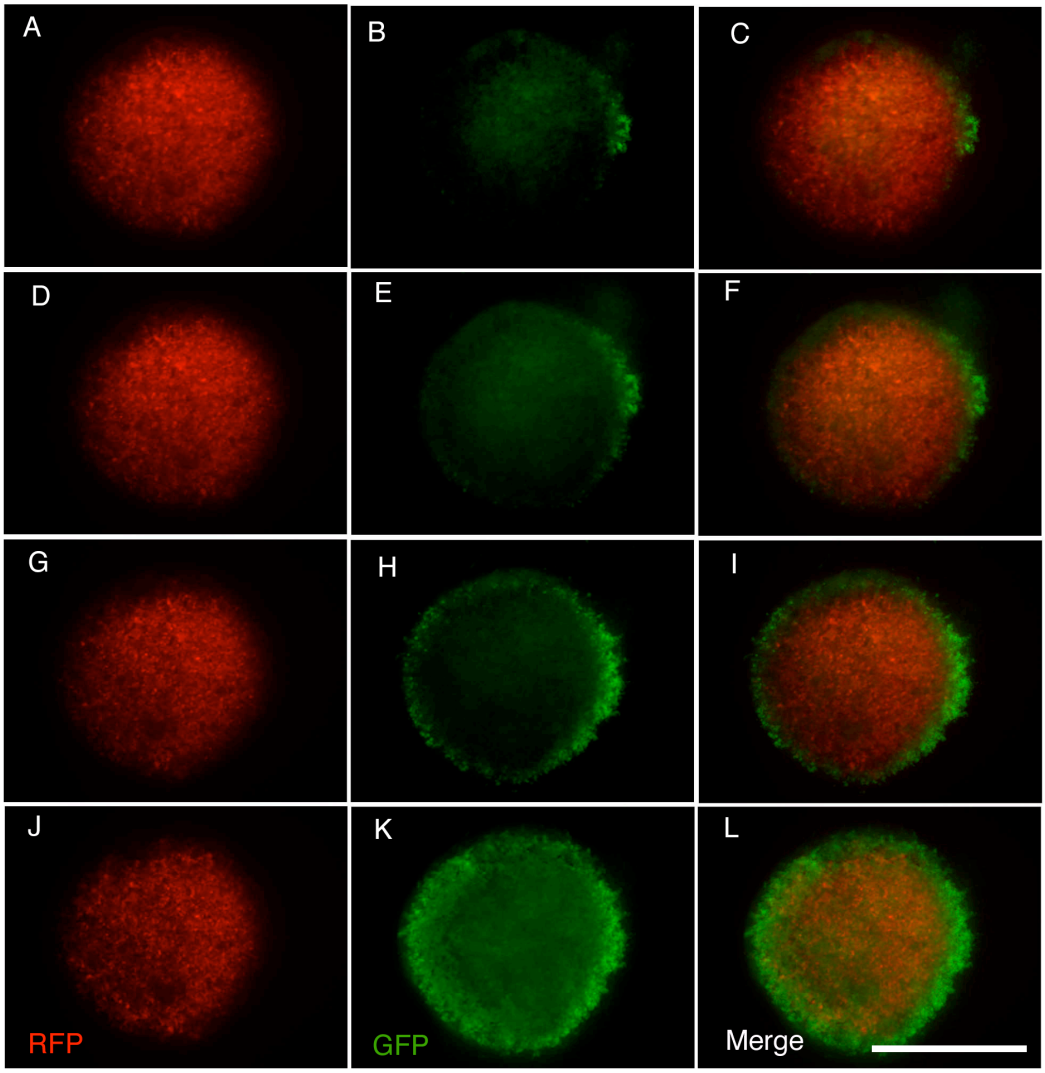
A
B
C
D
E
F
G
H
I
J
K
L
RFP
GFP
Merge

Figure 13. Time course of tumor infiltration by neuralized embryonic stem cells on an organotypic brain slice.

These stereoscopic epifluorescent images show the progression of tumor mass infiltration by nESCs over the course of a several weeks in an organotypic brain slice culture. GFP-expressing nESCs and RFP-expressing human glioma cells were introduced on the surface of an organotypic rat brain slice as described in figure 2. **(A-C)** Starting at 2 weeks post-implantation, nESCs are found at the tumor mass. At 3 weeks **(D-F)** and 4 weeks **(G-I)** post-implantation, the tumor mass becomes infiltrated progressively by nESCs. At 6 weeks **(J-L)**, the tumor mass becomes encapsulated completely by the stem cells, suggesting contiguity between nESCs and glioma cells. Scale bar = 1 mm; Scale bar applies to all panels.

Advances in Pre-clinical and Clinical Studies

Development of a GCV/tk mediated gene therapy has been a focus of cancer research for many years with the central issue being the effectiveness of transgene delivery to non-transduced cancer cells. In the past, viral vectors have been used predominantly to deliver gene products directly to tumor cells but have met with limited success. Therefore, novel strategies employing cell-mediated delivery of GCV/tk are being investigated.

There has been success in developing and characterizing neural stem cells as vehicles to deliver GCV/tk for cancer gene therapy (Willis et al., 2005); recently, pre-clinical studies have reported substantial progress in eliminating brain tumors in rat models. Li and colleagues (Willis et al., 2005) demonstrated complete elimination of glioma xenografts by HSV/tk engineered neural stem cells in combination with GCV treatment (termed NSC/tk therapy). This study reported that NSC/tk therapy completely abolished tumors that were induced 7 days before the intra-tumoral administration of NSCs, and remarkably, rodents remained glioma-free for up to 10 weeks before sacrifice. These encouraging findings show the potential of NSC/tk therapy even though direct intra-tumoral delivery of HSVtk-producing fibroblast vector producer cells was ineffective in human clinical trials. Nonetheless, these exciting results still leave one of the most important questions regarding the feasibility of this application unanswered before translating into clinical trials: Will NSC/tk therapy target invading GBM cells at some distance from the tumor's epicenter? Since xenografts, including human orthotopic xenografts, form relatively well-circumscribed GBMs, genetic

mouse models that result in spontaneous tumor occurrence may be better suited to addressing this important question.

In a Phase III clinical trial, fibroblasts were used to deliver HSV/tk intra-tumorally to GBM patients as an adjuvant to conventional therapy (surgical resection and radiotherapy) (Rainov, 2000). In this multi-center controlled trial, randomized patients received vector-producing mouse fibroblasts cells (cell line PA317) engineered to deliver the HSV/tk gene in a retrovirus-mediated fashion to tumor cells. The vector producer cells were injected into the wall of the cavity formed by surgical tumor debulking. Study patients then received intravenous GCV and radiation versus radiation alone. Unfortunately, median patient survival was not significantly different compared to the radiation-treated control group. Most of the recurrences were adjacent to the wall of the cavity and in patients who succumbed before they were treated with GCV; vector producer cells were seen at autopsy within a few millimeters of needle tracks. It is not known whether the outcome resulted from the use of murine-derived cells, non-migratory fibroblasts, or was a combination of various technical factors. Before an NSC/tk therapy can be employed in a human clinical trial, preclinical testing will need to be completed in genetic mouse models of GBM or human orthotopic xenografts that more closely mimic the human disease. After GCV administration, it is expected that all the transplanted tk+ stem cells and the targeted tumor cells would succumb to self-induced death. Ideally, GCV will need to be administered when the maximum number of stem cells have honed to GBM cells within the brain.

Unpublished observations - Intracranial Transplant Models

To understand the *in vivo* migration capacity of the stem cells towards the tumor cells, we utilized methods established by Li et al. with modifications (Li et al., 2005). For preliminary studies, we transplanted neuralized mouse embryonic stem cells and glioma tumor cells intracranially in wild-type C57 mice, similar to the methods described for the organotypic brain slices **(Figure 14)**. Animal studies were performed in accordance with approved protocols outlined by the Institutional Animal Care and Use Committee of the University of Missouri. Briefly, before cell injections, mice were anesthetized and placed in a stereotactic apparatus to secure the cranium. For reference and locations of cell placement, we referred to the text of 'The Mouse Brain in Stereotaxic Coordinates' (Paxinos and Franklin, 2004). The skin covering the skull was parted and a burr hole was created. Transplantation coordinates for cortical cell placement just above the corpus callosum in adult mice was as follows: 0.5mm anterior of bregma, 2mm lateral from bregma in left or right hemispheres. A 31.5 gauge 10 µl Hamilton microsyringe (Hamilton Company, Reno, NV) was inserted into the brain to the point of 4mm ventral from the dura, and allowed to sit for one minute, retracted to 3mm ventral from the dura then removed upon one minute after injection (Li et al., 2005).

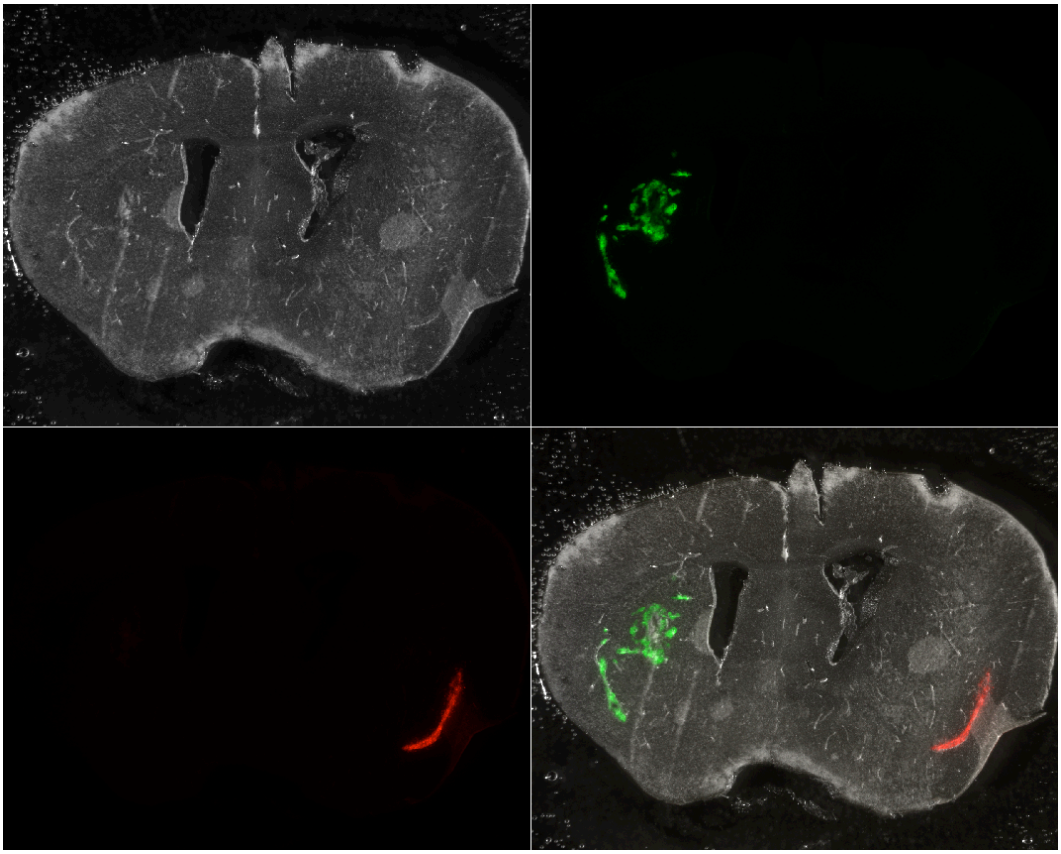

Figure 14. Intracranial transplant model

As proof of principle, GFP-expressing neuralized mouse embryonic stem cells (green signal) and RFP-expressing glioma cells (red signal) were intracranially transplanted into the cerebral cortex of rats. After a few days, the brains were removed and sectioned to visualize migration. In this section, the stem cells can be seen in the striatum and the external capsule, and the tumor cells have migrated on the external capsule down towards the lateral septal nucleus.

For experiments, tumor and stem cells were injected on the same day in contralateral hemispheres and, and sacrificed 4 days post-transplant. We transplanted approximately two million cells (~500,000 cells/ul) of B6 mouse ESCs in the left hemishphere and one million SF767 cells (500,000 cells/ul) in the right hemisphere. Upon removal of brains, the brain was fixed in 4% paraformaldehyde and sucrose protected in increasing concentrations of sucrose, then OCT embedded. The brains were cryosectioned at approximately 20 μm for visualization.

Brain slices containing the cells were viewed with an epi-fluorescence Leica stereoscope to determine the migratory capacity of the GFP-expressing neuralized ESCs towards the RFP-expressing tumor cells (**Figure 14).** For some experiments, the animals were sacrificed at between 1-2 weeks post-transplant. Stem cells were seen co-localized with tumor cells in some sections indicating that neuralized embryonic stem cells have the capacity to migrate contralaterally towards glioma cells *in vivo.*

HSV/tk Vector

The coding sequence for HSV/tk was excised from plasmid pAd-HSV-tk (Aldevron) and cloned into the Xho1-BamH1 sites of pcDNA3.1 (Invitrogen) to produce pcDNA/tk **(Figure 15)**. The HSV/tk vector can be transfected into B5 embryonic stem cells and GFP-expressing fibroblast cells (as controls) with Lipofectamine reagent (GIBCO/BRL), and selected with geneticin (G418).

Migration of Neuralized mESCs

Cell migration in the brain occurs on migratory pathways such as the corpus callosum, or the rostral migratory stream (RMS) as is the case for SVZ born neuroblasts. Studies have shown that neural stem cell lines transplanted into mouse brain associate with blood vessels and often migrate along blood vessels (Honda et al., 2007). This relationship has also been described in the rostral migratory stream. Whitman et al., show that blood vessels and astrocytic arborizations run parallel to neuroblast migration in the RMS. The contribution of glia to the structure of the RMS is important, and this study suggests that the dense vasculature in the RMS plays an important role in modulating the migratory microenvironment (Whitman et al., 2009). As demonstrated here, neuralized mESCs have the ability to migrate towards human glioma grafts on organotypic rat brain slices. Our observations suggest that the stem cells migrate along the vasculature as well as the fiber tracts **(Figure 16).**

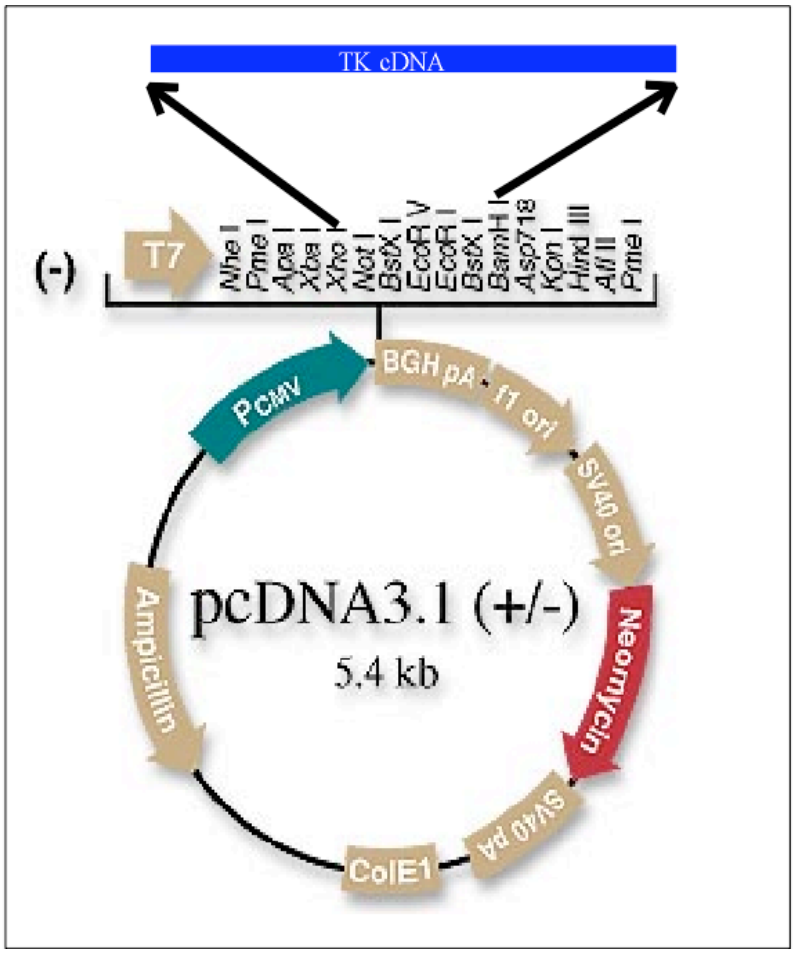

Figure 15. TK **vector construction**

The TK sequence was cloned into a plasmid containing a *neo* gene. This plasmid can be transfected into ESCs before neuralization. Transfected cells can be selected for with G418. Cell suicide can be tested with the addition of GCV to determine the optimal dosage concentration for *in vivo* studies.

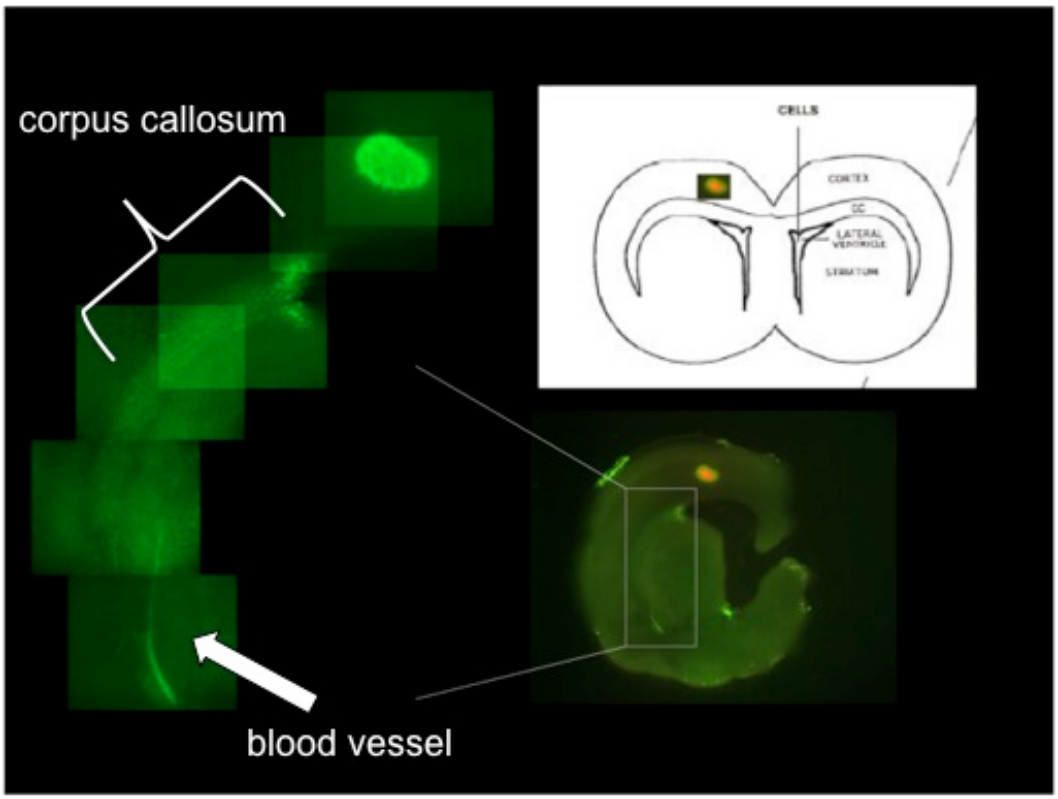

Figure 16. Migratory pathways of nESCs

The glioma cells were placed in the top right quadrant of the brain slice, and the stem cells were placed in the bottom left quadrant of the slice as described in the methods. After one week in culture, the stem cells formed a distinct linear organization in the direction of the glioma cells, appearing to surround a blood vessel (which are in abundance and noticeable in this region during slice preparation). The mESCs are also seen in the fiber tracts of the corpus callosum. Regardless of the substrate, the mESCs efficiently navigate towards the glioma cells. Coronal slice image provided as reference, from (Belicchi et al., 2004).

Conclusions

Clinical studies support the feasibility and biosafety of an HSV/tk-based gene therapy. It remains to be determined in humans if efficient gene transfer to tumor cells can be achieved using stem cells as a delivery platform. Additional research is required to elucidate the utility of transplanted stem cells, before neural, mesenchymal or embryonic cells can be used safely and effectively in the clinical setting. Neural stem cells transduced with HSV/tk combined with GCV administration provide a promising new treatment option that may one day extend significantly the life of patients with GBM.

Acknowledgements

This work was supported by the National Institutes of Health (NS045813 to MDK) and a Flo-Dickey Funk Fellowship (to PR). The authors especially thank Dr. Joseph Loftus at the Mayo Clinic Scottsdale, AZ for kindly providing the SF767 cell line. The authors also thank Dr. Elmer Price for assistance with vector construction, Laura Engel, Jason Kern, Jason Morrison and the Molecular Cytology Core at the University of Missouri for experimental support.

CHAPTER 3

ISOLATION AND CHARACTERIZATION OF A POPULATION OF STEM-LIKE PROGENITOR CELLS FROM AN ATYPICAL MENINGIOMA

Submitted: Prakash Rath, Douglas C. Miller, N. Scott Litofsky, Douglas C. Anthony, Qi Feng, Craig Franklin, Lirong Pei, Alan Free, Mark D. Kirk, Huidong Shi.

3.1 Abstract

The majority of meningiomas are benign tumors associated with favorable outcomes; however, the less common aggressive variants with unfavorable outcomes often recur and may be due to sub-populations of less-differentiated cells residing within the tumor. These sub-populations of tumor cells, termed tumor-initiating cells, may be isolated from heterogeneous tumors when sorted or cultured in defined medium designed for enrichment of the tumor-initiating cells. We report the isolation and characterization of a population of tumor-initiating cells derived from an atypical meningioma. These meningioma-initiating cells (MICs) self-renew, differentiate, and can recapitulate the histological characteristics of the parental tumor when transplanted into athymic nude mice. Immunohistochemistry reveals protein expression patterns similar to neural stem

and progenitor cells while genomic profiling verified the isolation of cancer cells (with defined meningioma chromosomal aberrations) from the bulk tumor. Furthermore, microarray analysis of gene expression reveals that many epithelial to mesenchymal transition genes are upregulated in the MICs, consistent with the presence of both neural stem cell and mature neural cell molecular markers seen in the derived cultures. Pathway analysis identifies biochemical processes and gene networks related to aberrant cell cycle progression, particularly the loss of heterozygosity of tumor suppressor genes *CDKN2A ($p16^{INK4A}$), $p14^{ARF}$, and CDKN2B ($p15^{INK4B}$).* Flow cytometric analysis revealed the expression of CD44 and activated leukocyte adhesion molecule (ALCAM/CD166); these may prove to be markers able to identify this cell type. In conclusion, we identify a tumor-initiating population from an atypical meningioma that displays a unique phenotype and these results provide increased understanding of atypical meningioma progression.

3.2 Introduction

Meningiomas are common intracranial neoplasms that account for approximately 30% of all reported brain tumors (CBTRUS: 2007-2008 Statistical report: primary brain tumors in the United States). Most meningiomas are attached to the dura and press on the brain or spinal cord through the arachnoid, although unusual examples can arise within the brain's ventricles or in the leptomeninges without a dural attachment. These tumors express a phenotype similar to meningothelial (arachnoid cap) cells both histologically and

immunohistochemically, and the majority are sporadic, slow growing, and are classified as benign (WHO grade I) (Willis et al., 2005). However, more aggressive variants such as atypical (WHO grade II) and anaplastic (WHO grade III) meningiomas may express a mesenchymal-like phenotype, and these often recur and invade the brain following initial removal, or even disseminate to distant sites (WHO grade III) resulting in a lower median survival compared to their benign counterparts (Willis et al., 2005). Unusual examples of meningiomas are associated with genetic syndromes (e.g., Neurofibromatosis Type II, NF2) or are induced by radiation (Simon et al., 2007).

Whole genome gene expression profiling has provided insight into the genetic alterations and pathway deregulation of meningiomas, providing a better understanding of the molecular signature for meningioma variants. Mutations and aberrant DNA methylation patterns in the well-studied tumor suppressor gene NF2, located on chromosome 22, have been implicated in more than half of spontaneous meningiomas suggesting a role for NF2 involvement in meningiomas and as a target for therapy (Hanemann, 2008; Liu et al., 2005). However, additional genetic components contribute to the more aggressive meningioma variants and include frequent chromosomal aberrations such as the loss of chromosomal regions 1p, 6q, 10, 14q, 18q, 22q, or the gain of 1q, 9q, 12q, 15q, 17q and 20q (Keller et al., 2009; Watson et al., 2002; Weber et al., 1997; Wrobel et al., 2005). These include the inactivation of cell cycle genes either due to homozygous deletion or truncated expression due to mutation, and may contribute to the malignant growth and progression of meningiomas through

the deregulation of the cell cycle. Deletions in tumor suppressor genes *CDKN2A* ($p16^{INK4A}$), $p14^{ARF}$, and *CDKN2B* ($p15^{INK4B}$) have been investigated in high-grade meningiomas and are known to cause cell-cycle deregulation at the G1/S phase checkpoint (Bostrom et al., 2001; Simon et al., 2007).

Over the past few decades, many studies have identified and characterized small populations of cells that are present within various tumors. Designated tissue-specific cancer stem cells (CSCs) or tumor-initiating cells (TICs) with stem-like properties, these cells are characterized by their *in vitro* properties of self-renewal and differentiation, and *in vivo* tumorigenic capabilities (Dalerba et al., 2007; Fang et al., 2005; Lapidot et al., 1994; Singh et al., 2004; Zhang et al., 2008). First described in acute myeloid leukemia (Lapidot et al., 1994), these "cancer stem cells" are now recognized in a variety of tumors (Hill and Wu, 2009). According to the cancer stem cell hypothesis, sub-populations of cells reside within tumors to regenerate and sustain the heterogeneity of the tumor and its growth. CSCs or brain tumor-initiating cells (BTICs) share properties of neural stem/progenitor cells (NSPCs) with regard to their ability to self-renew and differentiate, their enrichment in defined culture conditions, and their identification based on the molecular markers they express (Singh et al., 2003).

Identification of CSCs or BTICs has been an active area of research in cancer biology and understanding these cells may be a first step toward targeting the underlying causes of recurrent tumors. In the brain, CD133 is a putative though not exclusive stem cell marker used to identify BTICs and is associated

with NSPCs, mesenchymal stem cells, progenitor cells, and hematopoietic stem cells. Additionally, CD133 is expressed by many tumor types such as carcinomas of colon, liver, lung, ovary, pancreas and prostate (Fabian et al., 2009). A CSC, or initiating population within tumors and tissues have been identified based on the presence or absence of various molecular markers such as: CD44+/CD24- for breast cancer, CD44+/CD24+ for pancreatic cancer, CD44+/ CD133+/- CD166+ for colon cancer, CD44+/ CD133+/ Sca-1+/ CD117+ for prostate cancer, CD44+/ CD117+ for ovarian cancer, CD20+ for melanoma, and CD90+ for liver and lung (Chu et al., 2009; Fabian et al., 2009; Fang et al., 2005; Zhang et al., 2008). It is important to note that the overlap of markers and the lack of consensus in various studies regarding the combination of markers to identify progenitor cell populations within tumors are due to tissue-specificity, and can be attributed to the heterogeneous nature of the primary tumor, the culture medium, or the developmental state of the cells.

In this study, we report the establishment of a cell line with properties of BTICs, derived from an atypical meningioma. These meningioma-initiating cells (MICs) have been enriched using serum-free cell culture medium in the presence of mitogens, initially designed for the isolation and propagation of NSPCs and BTICs *in vitro* (Reynolds and Weiss, 1992; Singh et al., 2003). These cells exhibit a capacity for self-renewal, differentiation, and recapitulate hallmarks of the parental tumor when transplanted into athymic nude mice. Gene expression microarray analysis in conjunction with flow cytometry and fluorescent immunohistochemistry revealed CD133, CD44, and CD166 surface marker

expression as properties of this meningioma-initiating cell (MIC). Array Comparative Genomic Hybridization (aCGH) identified genomic commonalities of the MICs with high-grade meningiomas. Additionally, we provide evidence supporting the presence of MICs found early in the hierarchal lineage of an atypical meningioma.

3.3 Methods and Materials

Patient tissue specimens

Tissue samples from the primary atypical meningioma and NSPC samples were provided via appropriate Institutional Review Board-approved protocols of the Department of Surgery, Division of Neurological Surgery; and Pathology and Anatomical Sciences, both in the School of Medicine at the University of Missouri. The tumor was located in the left fronto-parietal area, attached to the sagittal sinus and upon removal, was placed in culture medium as described below. The NSPC sample was obtained from telencephalon and diencephalon regions of the cerebral hemispheres from a fresh fetal autopsy at 17 weeks gestational age.

Cell culture

Fresh tissue from the atypical meningioma and NSPC samples were mechanically dissociated, washed with PBS, and red blood cells were removed with Histopaque (Sigma). To promote growth of progenitor cells, the cells were grown as non-adherent cultures in uncoated petri dishes in serum-free growth medium containing DMEM-F12 (lacking phenol red) supplemented with 20ng/ml

epidermal growth factor (EGF; Invitrogen), 20ng/ml basic fibroblast growth factor (bFGF; Invitrogen), 1:50 B27 supplement (Invitrogen), 1:100 N2 supplement (Invitrogen), and 10ng/ml leukemia inhibitory factor (LIF; Chemicon) as a permissive factor to facilitate the proliferation of progenitor cells, hereafter known as "DN2L medium" (i.e. mitogen-containing medium). For differentiation experiments, the cells were dissociated and grown on laminin (Sigma) coated 8-well chamber slides (BD Biosciences) at a density of 100,000 cells/well in the presence of DMEM-F12 ("mitogen-free medium") as described by the manufacturer (Human Neural Stem Cell Characterization Kit, Chemicon). Cells were incubated at 37°C with 5% CO_2.

Flow Cytometry

For fluorescence-activated cell sorting (FACS), cells grown in DN2L media were dissociated with cell dissociation buffer (Sigma) into single cell suspensions and labeled according to the procedures specified by the manufacturer of the antibodies (R&D systems). Antibodies used were: anti-human ALCAM (CD166)-PE conjugated (R&D Systems) and anti-human CD44 APC-conjugated (BD Biosciences). The corresponding isotype controls were: IgG_1 Isotype Control PE-conjugated (R&D Systems) and $IgG2b_K$ Isotype Control APC-conjugated (BD Biosciences) **(Figure 17 a,b).** Upon removal of xenograft tumors, the tissue was mechanically dissociated and placed into DN2L medium (for MIC enrichment) for 1 week before FACS analysis. Cells were sorted using the CyAn ADP high-performance flow cytometer (Beckman Coulter) and data analyzed with Summit software (Dako).

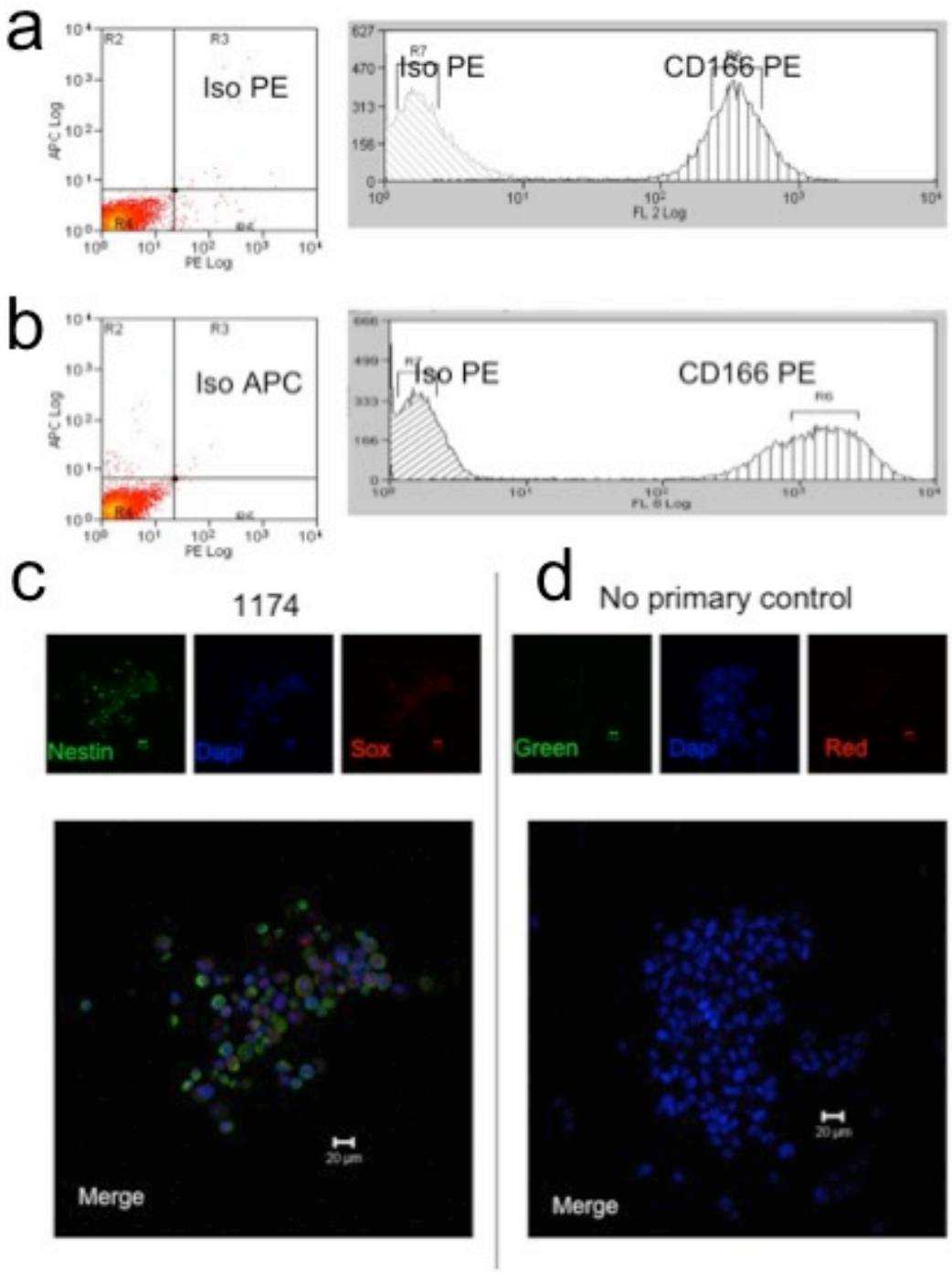

Figure 17. Flow cytometry and IHC Controls

(a) CD166 **(b)** CD44 flow cytometry control antibodies **(c)** IHC reference **(d)** IHC control

Animal Xenografts

Animal studies were performed in accordance with approved protocols outlined by the Institutional Animal Care and Use Committee of the University of Missouri. For *in vivo* tumorigenicity studies, cells grown in DN2L medium were dissociated, counted, resuspended at $5x10^6$ cells in 150 μl 1:1 DN2L media/Matrigel (BD Biosciences), and injected subcutaneously into seven left or right flank regions of 6- to 7-week old female athymic nude mice (Hsd:Athymic Nude *Foxn1*^{nu}; Harlan). Tumor size was measured weekly using a digimatic caliper (Mitutoyo) until sacrifice during the fourth week post-transplant for each group. The volume (*V*) of the flank tumor was calculated by multiplying the longest dimension (*l*) of the tumor by the shortest dimension (*w*), by the height (*h*), multiplied by 0.5263 (π/6), the standard formula for determining spherical and elliptical shaped tumors, $V = (l)(w)(h)(\pi/6)$, as described (Ying et al., 2007). Mice were sacrificed at 4-5 weeks post-transplant and xenograft tumors were removed. Portions of the xenograft were snap frozen for DNA isolation (for aCGH), cryosectioning for immunohistochemistry (IHC), or fixed in 4% paraformaldehyde and embedded in paraffin for histology, or dissociated and placed in DN2L medium for MIC enrichment and FACS analysis.

Histology and Immunohistochemistry

For histology, tumor specimens and xenografts were fixed in either 10% buffered formalin or 4% paraformaldehyde, processed routinely, and embedded in paraffin. Sections were cut at 8 μm thickness and mounted on slides for standard Hemotoxylin and Eosin (H&E) staining and histologic assessment.

Primary antibodies used for IHC were: anti-Vimentin, anti-EMA, anti-GFAP, anti-S100, anti-HMB45, anti-MelanA (A-103), anti-Synaptophysin (Dako), NF-M (RMDO20) (Invitrogen), anti-NeuN (Chemicon), anti-Nestin (Santa Cruz). Avidin-biotin immunoperoxidase detection methods were used for visualization. For fluorescence IHC, cells were prepared and processed according to the manufacturer's protocol (Human Neural Stem Cell Characterization Kit; Chemicon). Tumor cell clusters and neurospheres were embedded in OCT, sectioned at 10 μm sections in a cryostat, and labeled with antibody as previously described (Bleau et al., 2008). Primary antibodies used for fluorescent IHC were: anti-Nestin, anti-Sox2, anti-βIII-tubulin, anti-GFAP, anti-Neurofilament 150kd (Chemicon), anti-CD133, anti-CD166, (Abcam), anti-Vimentin (Dako), anti-Snai1, and anti-Twist1 (ABNOVA). Fluorescently tagged secondary antibodies used were goat anti-mouse Alexa Fluor 488, goat anti-rabbit Alexa Fluor 546, and goat anti-rabbit Alexa Fluor 488 (Invitrogen). Sections were counterstained with Vectashield (Vector Labs) mounting medium (which contains the DNA counterstain DAPI) before visualization. Negative controls were processed as described above with no primary antibody **(Figure 17 c,d).**

Imaging

Brightfield images of cultured cells were captured with a Nikon D100 camera through an Olympus CKx41 upright microscope. Histology photomicrographs were captured with an Optronics Macrofire digital photomicroscope camera mounted on an Olympus BX51 microscope. Confocal

images were captured with a Zeiss 510 META NLO and a Zeiss 5 live microscope and processed with LSM 5 Image Examiner software.

Microarrays

Tissue was disrupted using the TissueLyser apparatus (Qiagen). Isolation of RNA (from cells grown in DN2L media) and DNA (from the primary tumor, cells in DN2L medium, xenograft, and post-transplant cells in DN2L medium) were performed using RNeasy and DNeasy mini kits (Qiagen). Subsequent samples were run on microarrays to assess copy number (CN), loss of heterozygosity (LOH), and significant differences in gene expression. Sample data generated for CN and LOH came from an Affymetrix Human SNP 5.0 array interrogating 500,568 SNP probes and 420,000 additional non-polymorphic probes (Affymetrix, Inc.). Data for gene expression was derived from an Illumina Human WG-6 v3 Expression BeadChip interrogating ~48,000 transcripts (Illumina, Inc.). Both array formats are whole genome arrays and the assays were performed in accordance with the respective manufacturer's protocol.

Data Acquisition and Analysis

Arrays were scanned to obtain raw data that was imported into Partek Genomics Suite to generate relevant CN, LOH, and Gene Expression data. CN values were created using comparisons against a 270 HapMap CN sample dataset (a value of 2 being a normal diploid CN value). Genetic CN events were reported as amplifications (CN values >2.3) and deletions (CN values <1.7) using Partek's Genomic Segmentation algorithm. Single nucleotide polymorphism (SNP) genotype data was obtained through Affymetrix's Genotyping Console to

create heterozygous and homozygous calls for each SNP, which is then imported into Partek and compared against a 270 HapMap genotype sample dataset to generate a list of potential regions with a loss in heterozygosity. Gene Expression values were created by ANOVA (analysis of variance) 1-way contrast in Partek to create a differential expression table which is imported and analyzed in Ingenuity Pathway Analysis (IPA) for functional network and pathway relevance (Ingenuity® Systems, www.ingenuity.com). A fold change cutoff of +/-2 and p-value cutoff of 0.01 were set to identify significant changes in global gene expression, and correlated with the CN and LOH data to identify the genes of interest that were significantly differentially expressed as compared to the NSPCs. These "focus genes" were overlaid onto a global molecular network developed from information contained in the Ingenuity Pathways Knowledge Base, a repository of molecular interactions, events, and associations used for pathway construction. Specific networks of these focus genes were then algorithmically generated based on their connectivity. For functional analysis, the most significant genes from the dataset that met the cutoff and were associated with biological functions and/or diseases in the Ingenuity Pathways Knowledge Base were considered for the analysis. Fischer's exact test was used to calculate a p-value determining the probability of each biological function and disease assigned to the data set. Similarly, pathway analysis identified the pathways from the Ingenuity Pathways Analysis Library of Canonical Pathways, derived from Ingenuity Pathways Knowledge Base, that were most significant to the data set. Illumina BeadStudio module was used to generate histograms of

the average signal. A detailed description of the data generation and analysis can be found in the supplementary material (Supplementary Information S1). Raw microarray data have been uploaded to the Gene Expression Omnibus database and can be accessed via accession # (pending upon acceptance) (http://www.ncbi.nlm.nih.gov/geo/)

Microarray Data Generation and Analysis

Raw data was imported into Partek Genomics Suite to generate relevant CN, LOH, and Gene Expression data. CN values were created by logging (base 2) all of the ~900K raw probe fluorescent values compared against a 270 HapMap Sample baseline CN dataset and converting this information into the corresponding CN values (a value of 2 being a normal diploid CN value). Genetic CN events were reported as amplifications (CN values >2.3) and deletions (CN values <1.7) using Partek's Genomic Segmentation algorithm. A resulting CN event was required to have a minimum of 10 correlated neighboring probes with a p-value threshold of 0.001 for the significance of the difference from two neighboring probes.

SNP genotype data was created by running the ~500K SNP probes through Affymetrix's Genotyping Console using the BRLMM genotyping algorithm to create heterozygous and homozygous calls for each SNP probe. The data file is imported into Partek and compared against a 270 HapMap genotype sample dataset for LOH analysis which generates a list of potential regions with a loss in heterozygosity using a threshold approaching "zero" value (roughly, less than

0.07) based upon a heterozygous rate of the probes in the region. Normal regions have a heterozygous rate around 0.3.

Gene Expression values were created by first normalizing the arrays using a Quantile Normalization in Partek to remove statistical variation. The raw probe fluorescent values were then logged (Base 2) and contrasted by generating Log_2 ratios from the test sample compared to a normal group using an ANOVA (analysis of variance) 1-way contrast in Partek. This creates a differential expression table where the log_2 ratios were considered significant if the change from normal was >2 or <-2 and reported as a fold change table. This fold change table was then restricted to transcripts that had a p-value significance less than 0.01. The resulting data sets from CN, LOH, and Gene Expression analysis were integrated in Partek to compare the effect of CN and LOH data on the overall Gene Expression. The resulting table of correlated genes was imported and analyzed in IPA for functional network and pathway relevance to compare against the global Gene Expression data generated in the previous step. The data sets containing the respective gene identifiers and corresponding expression values were uploaded into IPA. Each gene identifier was mapped to its corresponding gene object in the Ingenuity Pathways Knowledge Base. A fold change cutoff of +/-2 and p-value cutoff of 0.01 were set to identify the global gene expression and correlated with the CN and LOH data to identify the genes of interest that were significantly differentially regulated.

Fischer's exact test was used to calculate a p-value determining the probability that each biological function and disease assigned to the data set is

due to the effect of the condition as opposed to the biological function designation occurring by random chance. Canonical pathways were analyzed to identify the pathways of significance from the Ingenuity Pathways Analysis library. Significance of the associated pathway was measured by a ratio of the number of genes from the data set that map to the pathway divided by the total number of genes involved in respective pathway. Secondly, a Fischer's exact test was performed to assess the significance of the association of the focus genes to the pathway of interest.

3.4 Results

Cells derived from primary atypical meningiomas self-renew and differentiate along neuronal and glial lines *in vitro*.

Fresh primary atypical meningioma specimens, upon dissociation and RBC removal, were placed in mitogen-containing DN2L media and grown as non-adherent cell clusters. The cells were sub-cultured weekly for approximately 1 month until it was apparent that only non-adherent cells remained in the dish. These cells aggregated as small clusters or single cells **(Figure 18*A top*),** compared with the tight spherical formations normally associated with NSPC neurospheres or tumorspheres, such as those derived from high-grade gliomas (data not shown). The cells rapidly proliferated and expressed the NSPC molecular markers Nestin, SRY-related HMG box gene 2 (Sox2), and CD133 **(Figure 18*B, left and middle*),** and expressed the intermediate filament proteins Vimentin and Glial Fibrillary Acidic Protein (GFAP) **(Figure 18*B, right*).** Upon

dissociating the aggregates and plating on laminin-coated slides in the absence of mitogens, we observed outgrowth of cellular processes and morphologies consistent with a differentiated cellular phenotype **(Figure 18*A, bottom*)**. The cells were immunoreactive for the mature neuronal markers Neurofilament-M (NF-M, 150kD) and βIII-tubulin **(Figure 18*C, left and middle*)**, and retained the expression of Vimentin and GFAP **(Figure 18*C, right*)**. The expression of Nestin, Sox2, and CD133 was similar to the staining patterns seen in NSPCs grown in the DN2L medium (data not shown). Furthermore, upon the withdrawal of mitogens, the NSPCs differentiate and express mature cell markers (data not shown) in a manner similar to that shown here for the meningioma-derived cells. These results indicate that these tumor-derived cells, or meningioma-initiating cells (MICs), can self-renew, and following withdrawal of mitogens, differentiate into neural lineages similar to that of a brain-progenitor cell-type. However, unlike the NSPCs, these MICs grown in the DN2L medium expressed the mature cell marker NF-M (**Figure 19).**

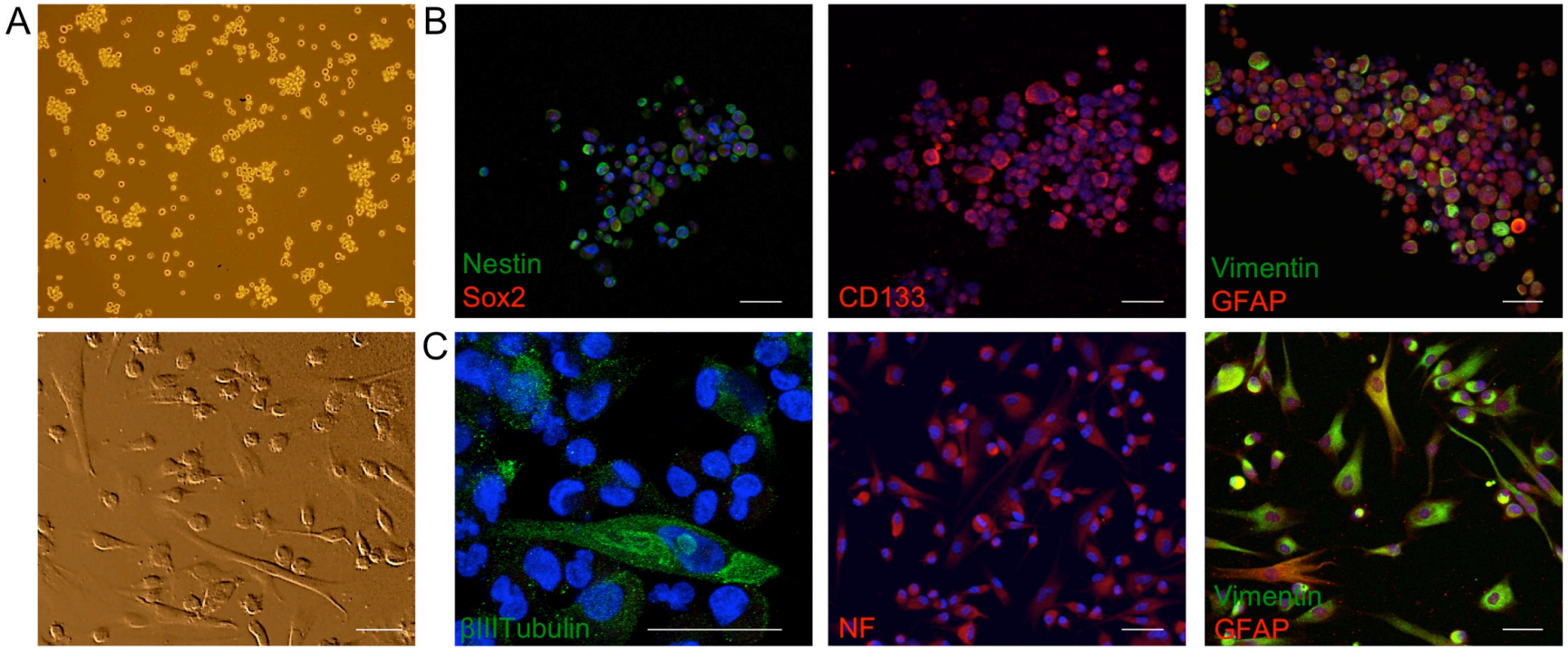
A
B
Nestin
Sox2
CD133
Vimentin
GFAP
C
βIIITubulin
NF
Vimentin
GFAP

Figure 18. Mitogen withdrawal induces differentiation of MICs *A,* MICs cultured in serum-free medium supplemented with mitogens grow as non-adherent asymmetrical clusters of cells (*top*), and following withdrawal of mitogens in adherent culture conditions, extend processes and exhibit morphologies similar to neurons and astrocytes (*bottom*). *B,* In the presence of mitogens, the majority of undifferentiated cells were immunoreactive for neural stem/progenitor cell markers Nestin and SRY-related HMG box gene 2 (Sox2) (*left)*, the stem cell marker CD133 (*middle*), and the intermediate filament proteins Vimentin and GFAP (*right*). *C,* In the absence of mitogens, adherent cultures expressed the mature cell markers βIII-tubulin (*left)*, Neurofilament-M (*middle*), and retained the expression of Vimentin and GFAP (*right*). Nuclei were counterstained with DAPI (blue). Scale bars for all images 50μm.

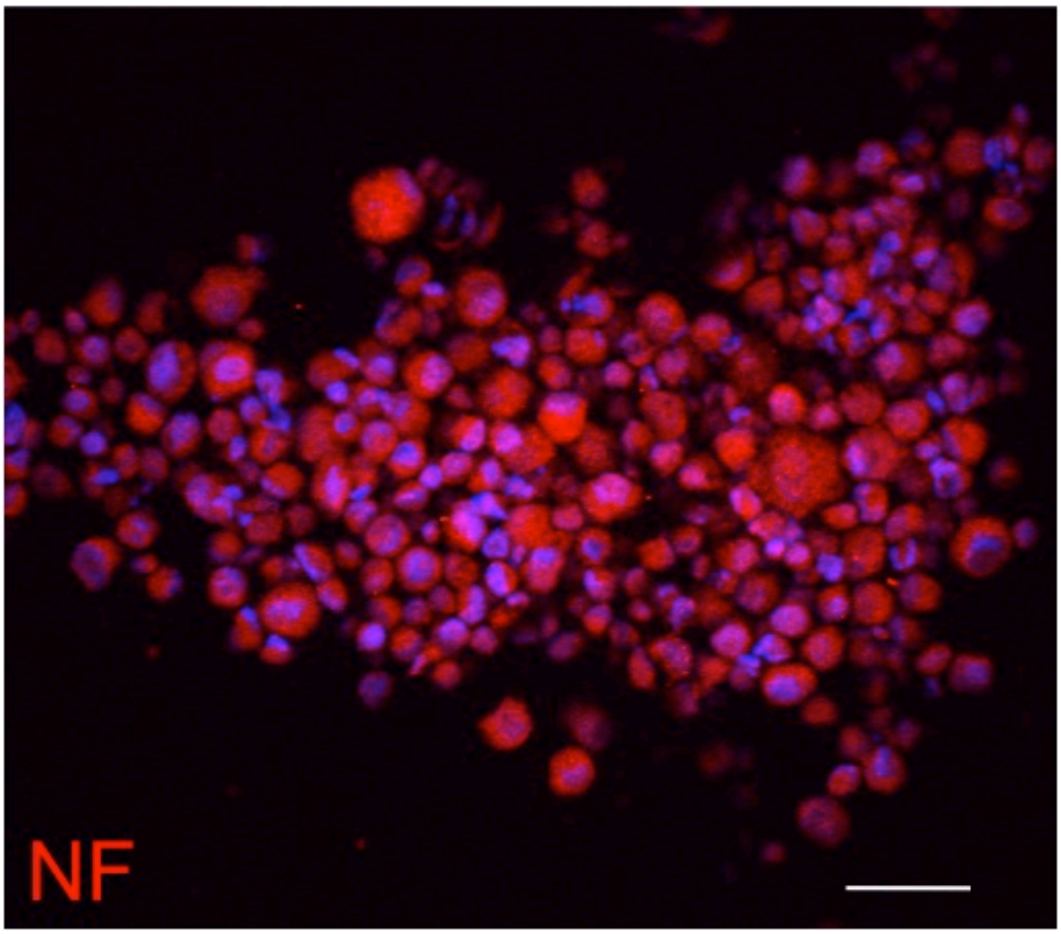

Figure 19. MICs express NF

MICs cultured in DN2L media express the mature cell marker Neurofilament with DAPI as a nuclear counterstain (blue). Scale bar 50μm.

MICs are tumorigenic and histologically resemble the primary tumor.

The primary tumor was a dural-based frontoparietal convexity mass excised at surgery **(Figure 20).** Sections of routinely processed tumor showed a meningioma with lobular growth patterns containing epithelioid clusters and sheets of cells, most sharply demarcated from underlying cerebral cortex **(Figure 21).** The tumor had a variety of histological features characteristic of meningiomas, including classical meningotheliomatous meningioma with areas of sheet-like growth of small to mid-size bland monotonous cells, and other areas with markedly pleiomorphic cells with large nuclei and large prominent nucleoli. Several foci contained small cells with hyperchromatic nuclei and scant cytoplasm **(Figure 21** ***A, top, left-right).*** There were zones with considerable fibrous tissue between the cells, particularly in the more pleiomorphic areas. The tumor showed areas with multiple mitotic figures, which in these areas exceeded 4 mitotic figures in 10 high power (400x) fields. Additionally, the tumor focally invaded the underlying brain.

The tumor cells were strongly and diffusely immunopositive for vimentin and in patches had a delicate surface membrane immunopositivity for Epithelial Membrane Antigen (EMA) and was GFAP immunonegative (with adjacent immunopositive gliotic brain) **(Figure 21** ***A bottom, left-right)*****.** There was nuclear immunoreactivity for Progesterone Receptors in a small minority of tumor cells and no immunopositivity for S100 protein, HMB45, MelanA (antibody A-103), or pan-cytokeratin (data not shown). Based on the immunofluorescence, subsequent immunostains were performed on cultured cells (see above), which

demonstrated no immunoreactivity for the neuronal markers Synaptophysin, Neurofilament Protein (antibody RMDO20 to NF-M), or Neu-N, or for the neural precursor marker Nestin (data not shown).

To examine the tumorigenicity of the non-adherent MIC's (DN2L medium) we xenografted these cells subcutaneously to the flank regions of athymic nude mice. After four weeks of growth **(Figure 22 *B, top left)*,** we observed tumors that had histological features similar to those of the primary tumor, such as areas with whorl formation and areas that resembled the more atypical areas of the parental tumor with more pleiomorphic nuclei and mitotic figures **(Figure 22 *B, top right)*.** Similar to the primary parental tumor, the xenograft had diffuse areas of Vimentin positivity and regions of patchy EMA cell-surface positivity **(Figure 22 *B bottom, left, middle*)**. However, there were areas of patchy GFAP immunopositivity in tumor cells, consistent with the immunofluorescence results from cultured cells derived from the primary tumor **(Figure 22 *B bottom, right*).** Unlike the primary tumor, the mouse xenograft had strong labeling of Nestin and areas of patchy immunopositivity for Neu-N, Synaptophysin, and NF-M **(Figure 23)**

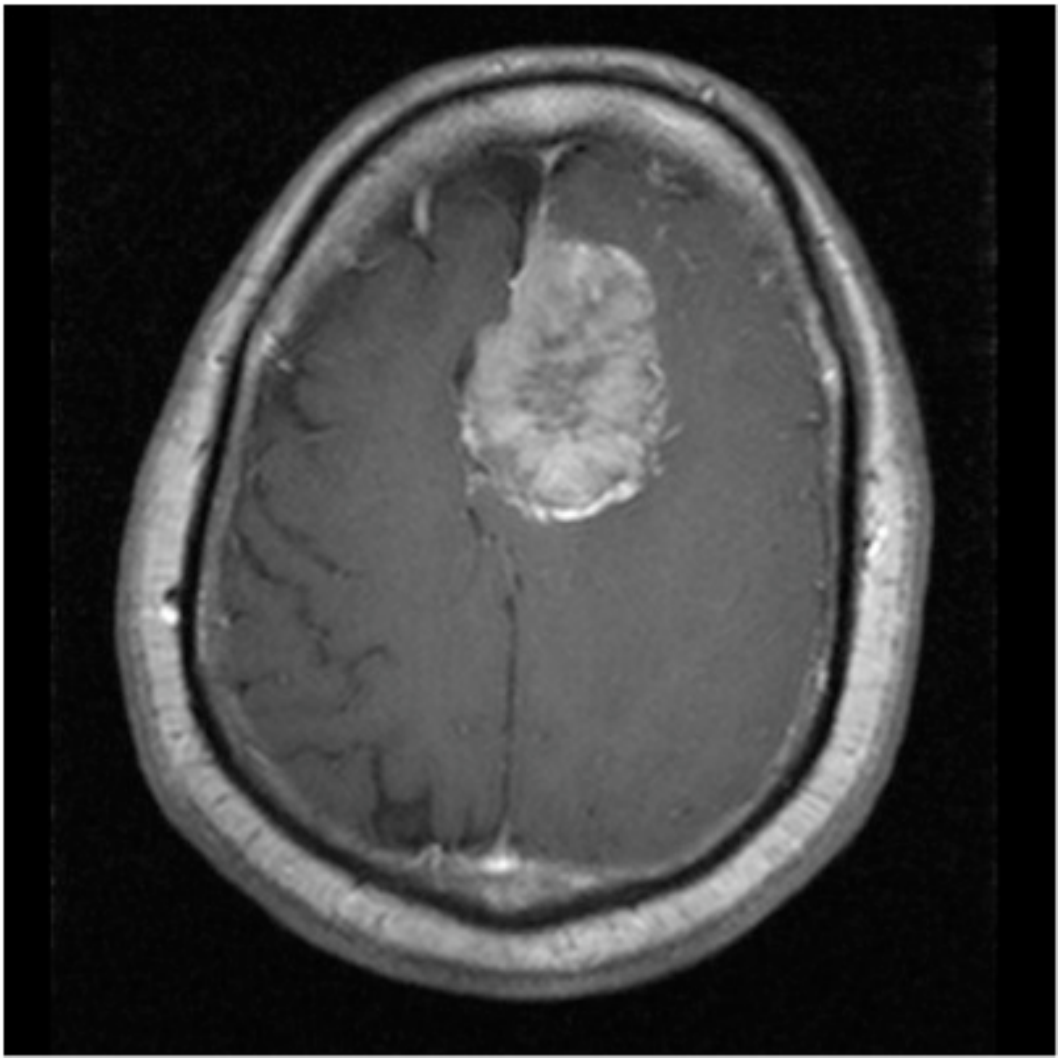

Figure 20. MRI image of primary atypical meningioma

Malignant meningiomas account for 4% of all meningiomas. The tumor was located in the left fronto-parietal area, attached to the sagittal sinus.

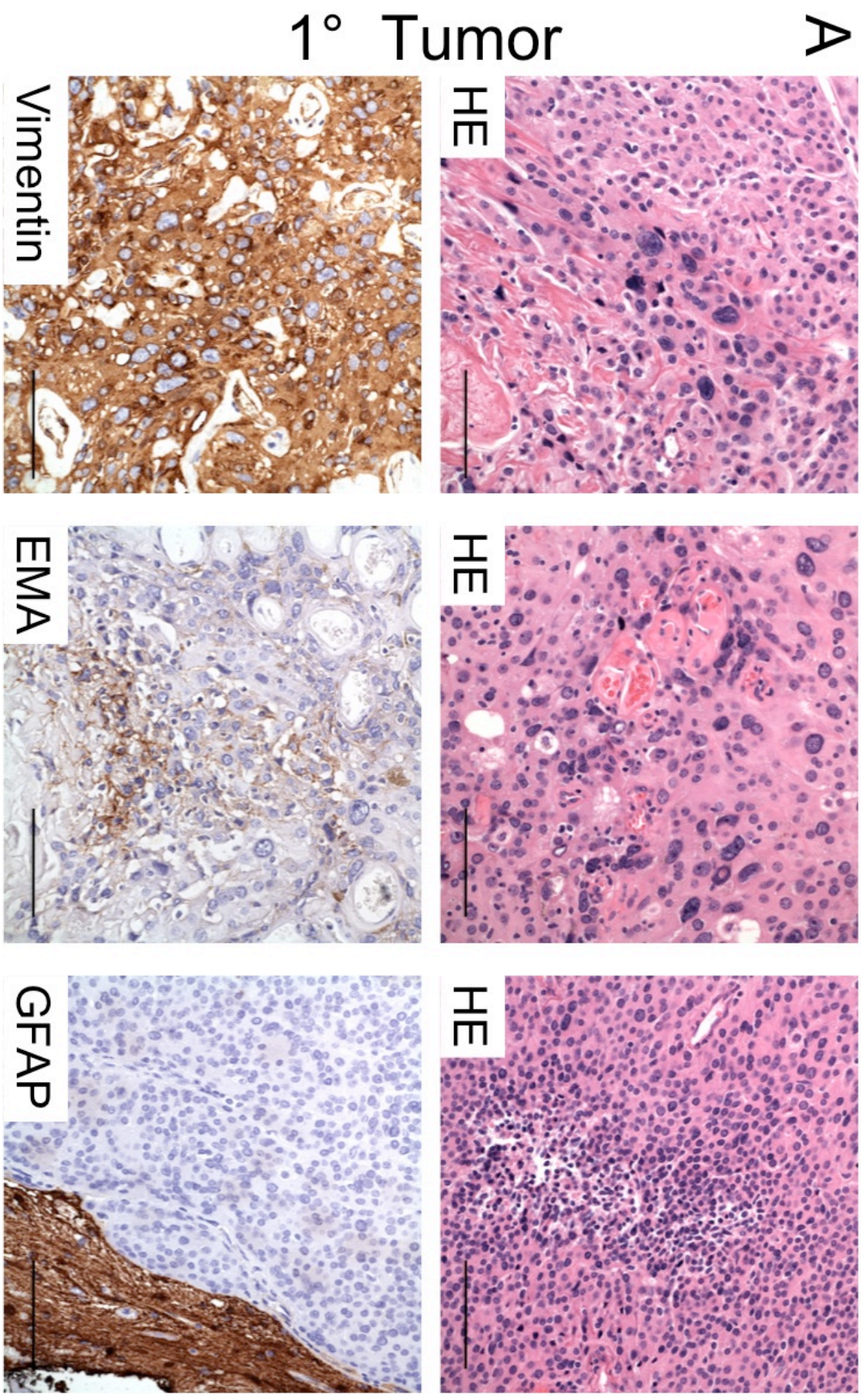
1° Tumor
A
Vimentin
HE
EMA
HE
GFAP
HE

Figure 21. Histological assessment of 1° parental tumor

A, top panel, representative H&E staining of the parental atypical meningioma exhibiting a variety of histological patterns including areas of atypical cluster formation (*left*), highly atypical areas (*middle*), and small anaplastic cells (*right*). ***A, bottom panel****,* immunolabeling shows strong, diffuse immunopositivity in virtually all tumor cells for Vimentin (*left*), a membranous staining pattern for EMA with variable intensity (*middle*), and tumor cells without GFAP staining (*right*) with GFAP immunopositivity in adjacent brain. Scale bars for all images 50μm.

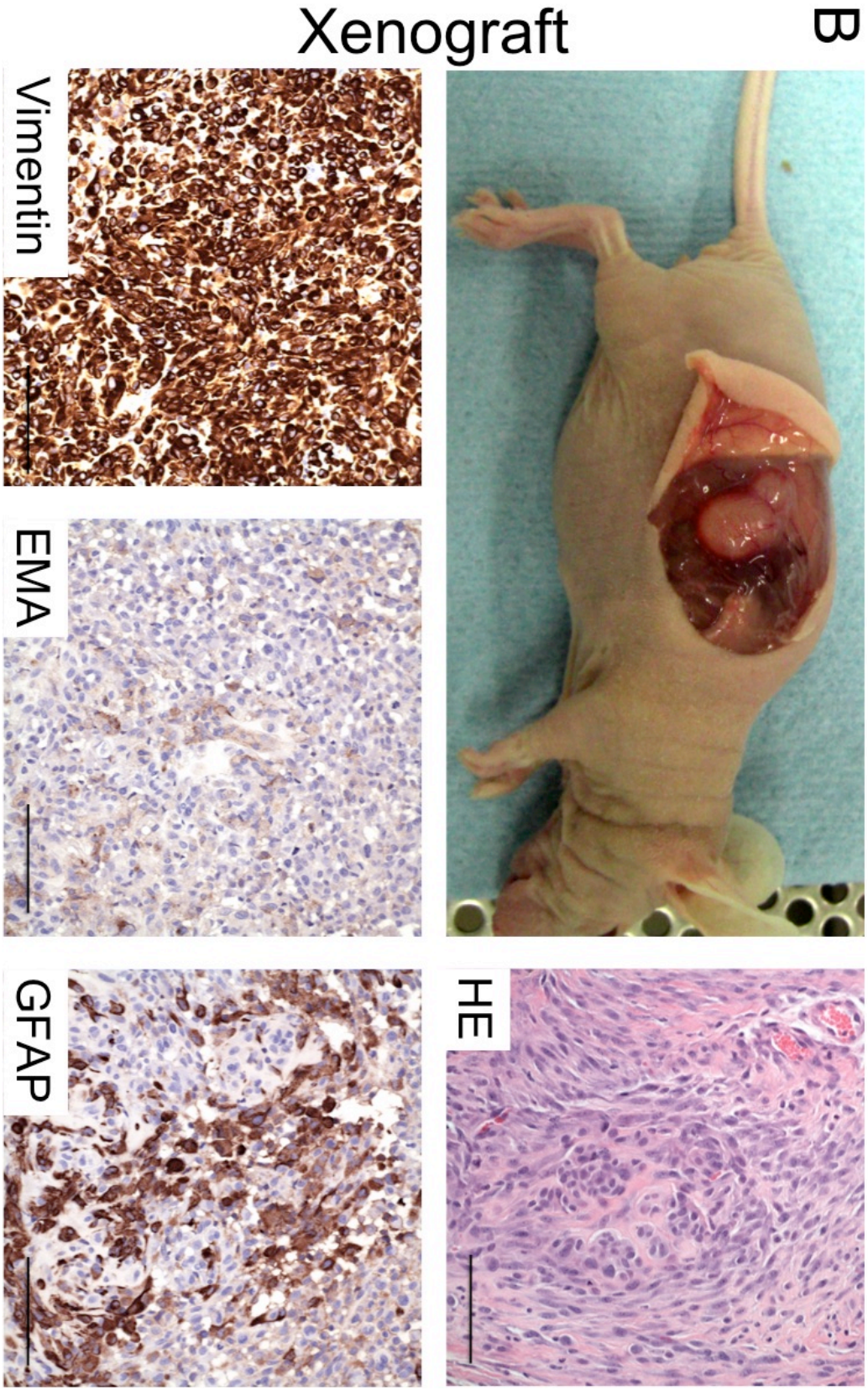
Xenograft
B
Vimentin
EMA
GFAP
HE

Figure 22. **Xenograft of MICs recapitulates features of 1° parental tumor**

B, top left*, r*epresentative image of xenograft tumor 4 weeks after subcutaneous injection of undifferentiated MICs enriched from the parental atypical meningioma tumor. Xenograft tumors recapitulate meningioma features and have areas with whorl formation (*top right*) and histological patterns similar to the parental tumor. ***B, bottom left****,* mouse xenograft tumor labeled immunopositive for Vimentin, EMA (*bottom middle)*, GFAP (*bottom right)*. Scale bars for all images 50μm.

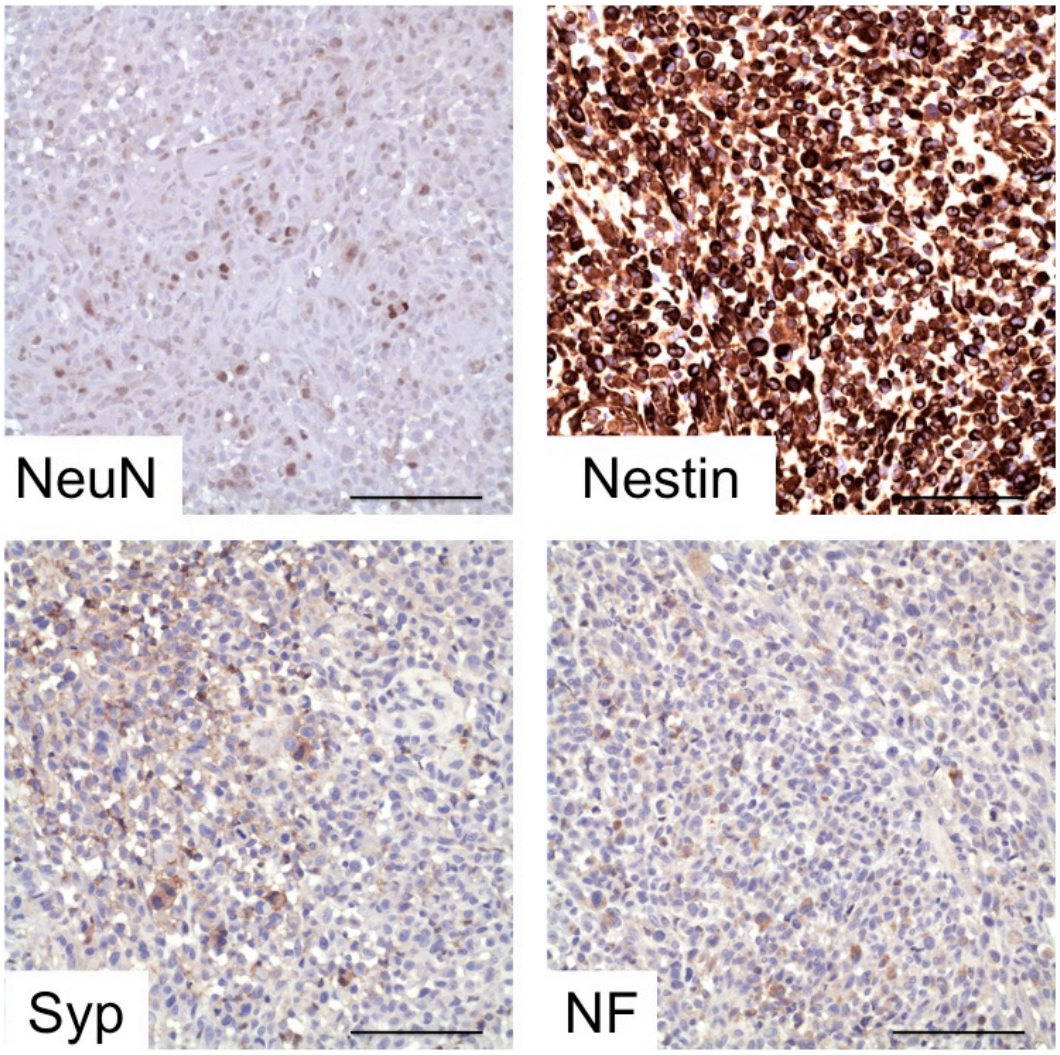

Figure 23. H&E staining of the mouse xenograft tumor

The xenograft tumor showed immunopositive labeling for NeuN (top *left)*, Nestin (*top right)*, Synaptophysin (Syp) (*bottom left), and* Neurofilament (RMDO20) (*bottom right*). Scale bars for all images 50μm.

ALCAM/CD166 and CD44 are expressed before and after xenograft.

Surface markers that are associated with progenitor and tumor-initiating cell populations in other tumor types are used to identify and isolate these cells from the bulk tumors. Analysis of the gene expression profile revealed that hyaluronate receptor (CD44) and activated leukocyte cell adhesion molecule (ALCAM or CD166) is upregulated in the MICs as compared to the NSPCs (data not shown). This expression profile suggested that these markers might be enriched because of placement in the DN2L medium. Therefore, we tested whether this phenotype is present in the primary tumor and could be re-isolated or re-enriched following xenotransplantation. Fluorescent IHC revealed that the primary tumor contained scattered cells that were immunopositive for the expression of ALCAM **(Figure 24 *A left*),** whereas nearly all the cells had expression when cultured in the DN2L medium before transplantation (**Figure 24 *A middle).*** Flow cytometric analysis confirmed that the cells grown in the DN2L medium homogeneously express the surface markers ALCAM and CD44 before transplantation **(Figure 24 *B left*).** After removal and dissociation of the xenograft, the cells were placed into DN2L medium for one-week before analysis, the length of time necessary to re-isolate the non-adherent only population of cells from the dissociated bulk tumor. Fluorescent IHC indicated that the majority of cells post-transplantation expressed ALCAM **(Figure 24 *A right*),** and flow analysis confirmed the expression of ALCAM, as well as CD44 in nearly all of the cells **(Figure 24 *B right*).** The lower expression level in the primary parental tumor as compared to the pre-transplant cells suggests the enrichment in culture

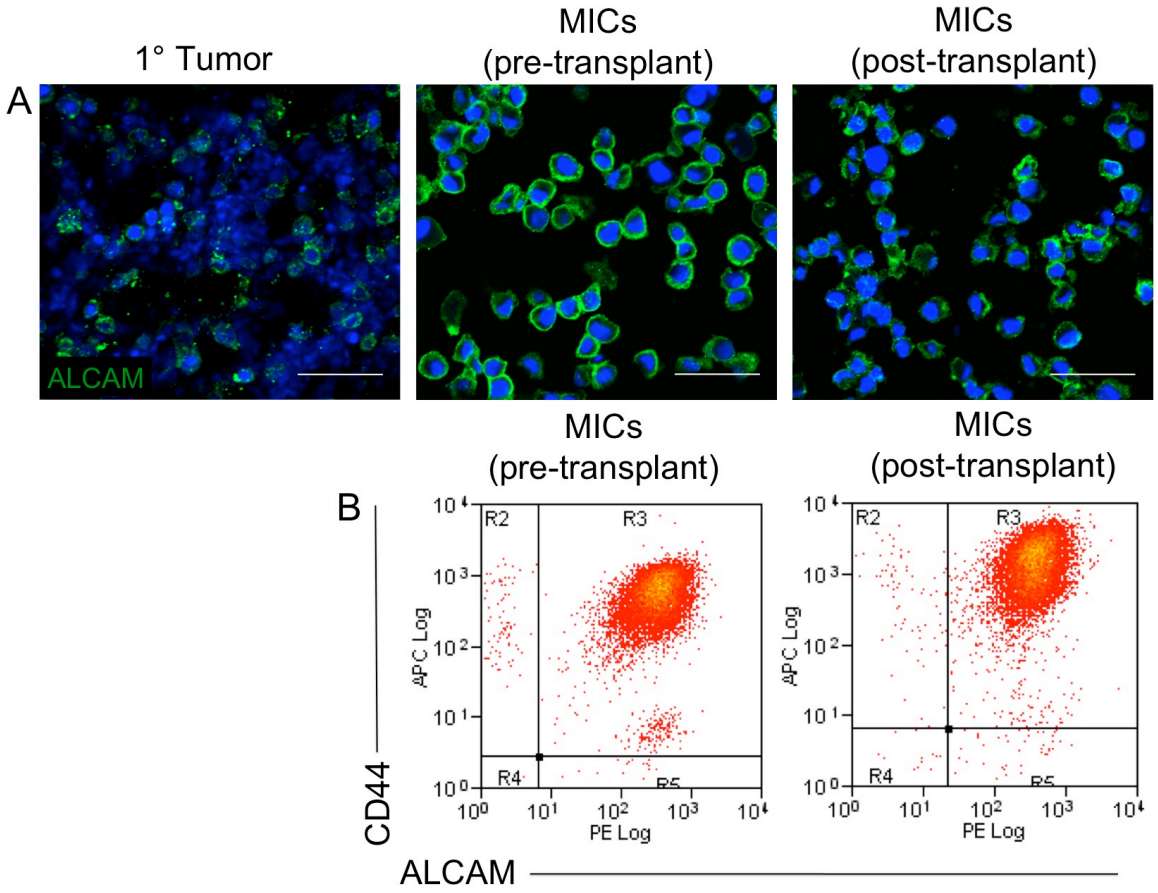
A
1° Tumor
MICs
(pre-transplant)
MICs
(post-transplant)
ALCAM
B
MICs
(pre-transplant)
MICs
(post-transplant)
R2
R3
R4
R5
APC Log
PE Log
CD44
ALCAM

Figure 24. MICs express ALCAM and CD44

Fluorescent immunohistochemistry and flow cytometric analysis show that culture medium enrich for an ALCAM+, CD44+ subpopulation of cells.

A, staining in cryosections of fresh frozen primary tumor show areas of scattered ALCAM expression (*left*) and increased abundance of cells expressing ALCAM with time in DN2L media prior to transplant (MICs pre-transplant) (*middle*). The xenograft tumor was dissociated and cultured in DN2L media until non-adherent cells remained (MICs post-transplant). Post-transplantation MICs expressed an abundance of ALCAM (*right*). *B,* Flow cytometric analysis reveals the near uniform expression of ALCAM and CD44 pre- and post-transplant. Nuclei were counterstained with DAPI (blue). Scale bars for all images 50μm.

of an ALCAM+ population of cells (derived from the primary tumor), that was either maintained or re-enriched in DN2L medium by cells derived from the xenograft.

MICs derived from the parent tumor and from the xenograft show a genomic expression pattern similar to that of the parent tumor.

Deletions or mutations in the NF2 gene, located on chromosome 22, are implicated in the tumorigenesis of many meningiomas, therefore; the NF2 gene status of MICs grown in DN2L medium and a sample from the paraffin-embedded primary tumor were analyzed to define specific cytogene changes in these cells (Testing done in the Neurofibromatosis Laboratory of Massachusetts General Hospital, Dr. Xie Win). Analysis of the coding regions of exons 1 through 17 showed no deletion of the NF2 gene in either the primary tumor specimen or the cultured cells derived from it, and no mutation (limited exon analysis). We performed aCGH and SNP genotyping analysis to determine CN and LOH for four different samples: 1) the primary parental atypical meningioma, 2) cells derived from the parental meningioma and grown in the DN2L medium, 3) the xenograft, and 4) the non-adherent population of the cells dissociated from the xenograft that had been placed in the DN2L medium **(Figure 25 *A*).** An LOH event is indicative of the genotype expressed, whereas the loss or gain of CN may influence the differential gene expression. We performed an allele-specific analysis of all the samples and confirmed that the MICs were derived from the

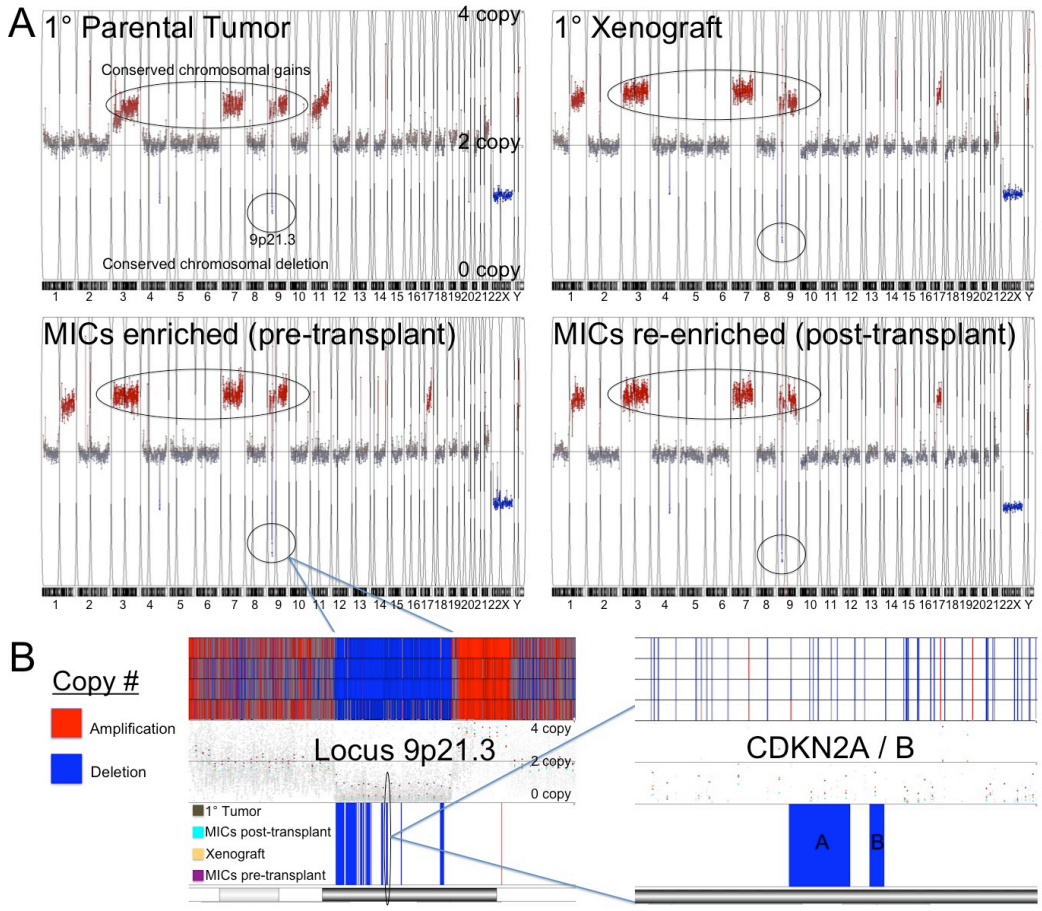
A
1° Parental Tumor
4 copy
Conserved chromosomal gains
2 copy
9p21.3
Conserved chromosomal deletion
0 copy
1° Xenograft
MICs enriched (pre-transplant)
MICs re-enriched (post-transplant)
B
Copy #
Amplification
Deletion
Locus 9p21.3
4 copy
2 copy
0 copy
1° Tumor
MICs post-transplant
Xenograft
MICs pre-transplant
CDKN2A / B
A
B

Figure 25. **Copy number variations in MICs**

Genome-wide copy number analysis suggests that the MICs are a subpopulation derived from the primary parental tumor. *A,* aCGH graphs represent genome-wide gains (*red*) and loss (*blue*) with the chromosomes distributed on the x-axis and the copy number on the y-axis. Shown are the parental tumor (*top left),* MICs pre-transplant (*bottom left*), the primary xenograft (*top right*), and the DN2L cultured cells post-transplant (*bottom right*). All conditions depicted conserved chromosomal gains (*large black oval*). *B,* region 9p21.3 (*small black oval Figure 4A)*, the location of tumor suppressor genes *CDKN2A (p16^{INK4A}), p14^{ARF},* and *CDKN2B (p15^{INK4B}),* showed a one-copy loss of heterozygosity (LOH) that was conserved in all samples.

parental tumor. The chromosomal aberrations of the primary tumor **(Figure 25 *A top left*)** included gains in regions of chromosomes 3,7,9, and 11. The MICs (pre-transplant) (**Figure 25 *A bottom left*),** subsequent xenograft **(Figure 25 *A top right*),** and cells derived from the xenograft (MICs post-transplant) **(Figure 25 *A bottom right*)** had the same gains in regions of chromosomes 3, 7, and 9. Unlike the primary tumor, the pre-transplant MICs, xenograft, and MICs post-transplant showed gains in regions of chromosomes 1 and 17, and loss of amplification in chromosome 11. There were minor regions with chromosomal deletions, generally consistent in all four samples. Of interest was region 9p21.3, the location of *CDKN2A (p16^{INK4A}), p14^{ARF},* and *CDKN2B (p15^{INK4B})*, well-known tumor suppressor genes and regulators of cell cycle progression **(Figure 25 *B left)*.** Alterations at this locus are evident in a minority of atypical meningiomas (WHO grade II) and a majority of anaplastic meningiomas (WHO grade III) *(Bostrom et al., 2001).* SNP genotyping and copy number analysis revealed a single copy LOH event for all three of these genes in the primary atypical meningioma, whereas the subsequent samples showed homozygous deletions (complete loss) **(Figure 25 *B right).***

Microarray and functional pathway analysis of MICs.

The genome-wide expression profile revealed upregulation of many epithelial to mesenchymal transition (EMT) associated genes and the deregulation of genes involved in the Wnt-signaling pathway of MICs, as compared with NSPCs. The EMT associated genes differentially upregulated were: *LEF1, SNAI2* (Slug),

TGFB3, TGFB1, TGFBR2, and TWIST1 **(Figure 26 *A*).** These 6 genes have been shown to play a part in the EMT program by contributing to the stable loss of E-cadherin, a key mechanism in the stabilization of the mesenchymal state (Polyak and Weinberg, 2009). To further investigate the presence of EMT-related genes, we performed fluorescence IHC on the MICs (DN2L medium) and analyzed Snail and Twist expression **(Figure 26 *B*).** MICs showed strong staining for both Snail and Twist, suggesting a link to a stem cell-like characteristic. To understand the biological functions associated with the MICs versus the NSPCs, we analyzed candidate genes with Ingenuity's Pathway Analysis (IPA) software. Using Partek software to integrate aCGH and gene expression microarray, we identified 1138 transcripts as being differentially expressed ($p < 0.01$). Inserting this list into IPA generated 27 gene networks. We focused on the top network associated with functions important in Cancer, Cellular Growth and Proliferation, and Connective Tissue Development and Function **(Figure 27 *A*).** This network was of particular interest due to its inclusion of many cyclin-dependant kinase-associated genes. The upregulation of cyclin D (*CCND3*) and down-regulation of cyclin D2 (*CCND2*) and cyclin-dependent kinase inhibitor B1 (*CDKN1B or p27*) identifies genes responsible for deregulation of the cell cycle for the MICs. Canonical pathway analysis revealed the Wnt/β-catenin pathway as including the most differentially expressed genes **(Figure 27 *B*).** The genes in this pathway include the upregulation of Wnt-signaling activators (*CCND1, FZD6, LEF1, TGFBR2*) and the downregulation of Wnt-signaling inhibitors (*SFRP1, SFRP2, SOX4, SOX11, SOX12*), highlighting

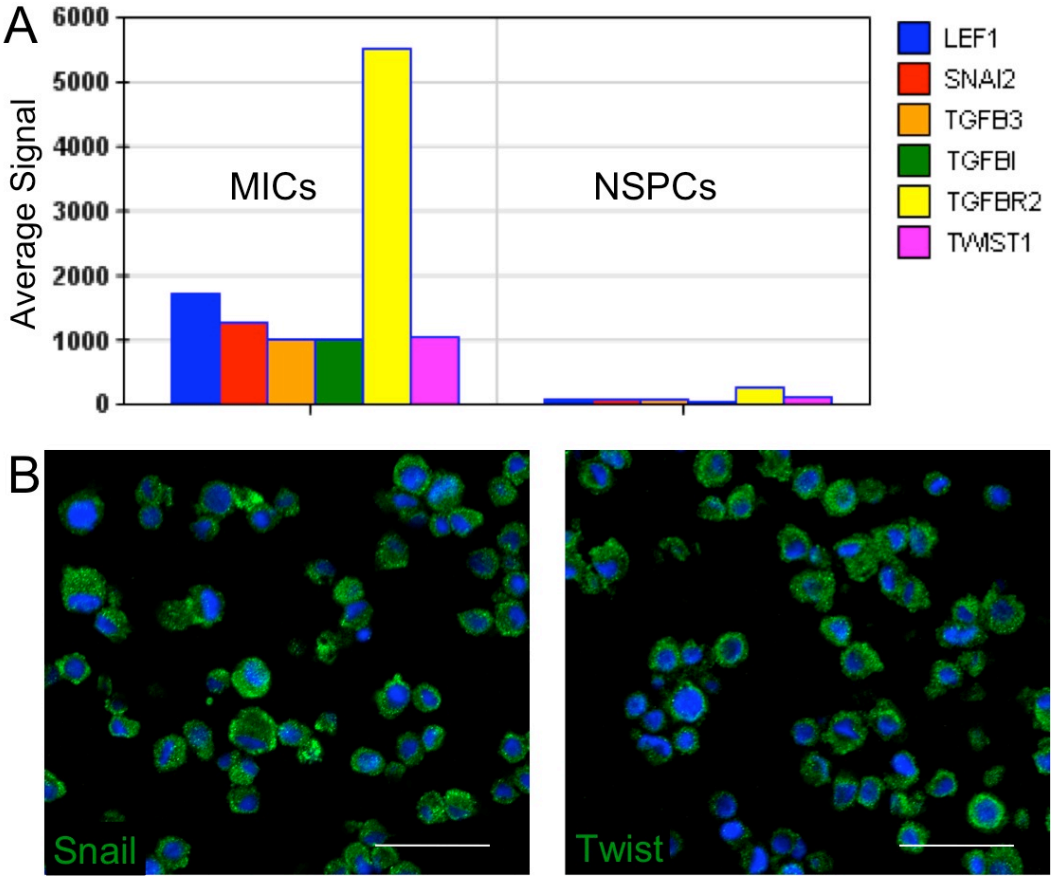

Figure 26. MICs express markers of EMT

Expression of epithelial to mesenchymal transition (EMT) genes in MICs. *A,* histogram of EMT genes shows differential upregulation in MICs as compared to NSPCs: *LEF1* (lymphoid enhancer-binding factor 1), *SNAI2* (snail homolog 2, also known as Slug), *TGFB3* (transforming growth factor, βIII), *TGFB1* (transforming growth factor, βI), *TGFBR2* (transforming growth factor, β receptor II), and *TWIST1* (twist homolog 1). *B,* fluorescent IHC expression of key EMT genes, *SNAI1* (also known as Snail) and *TWIST1* in MICs. Nuclei were counterstained with DAPI (blue). Scale bars for all images 50μm.

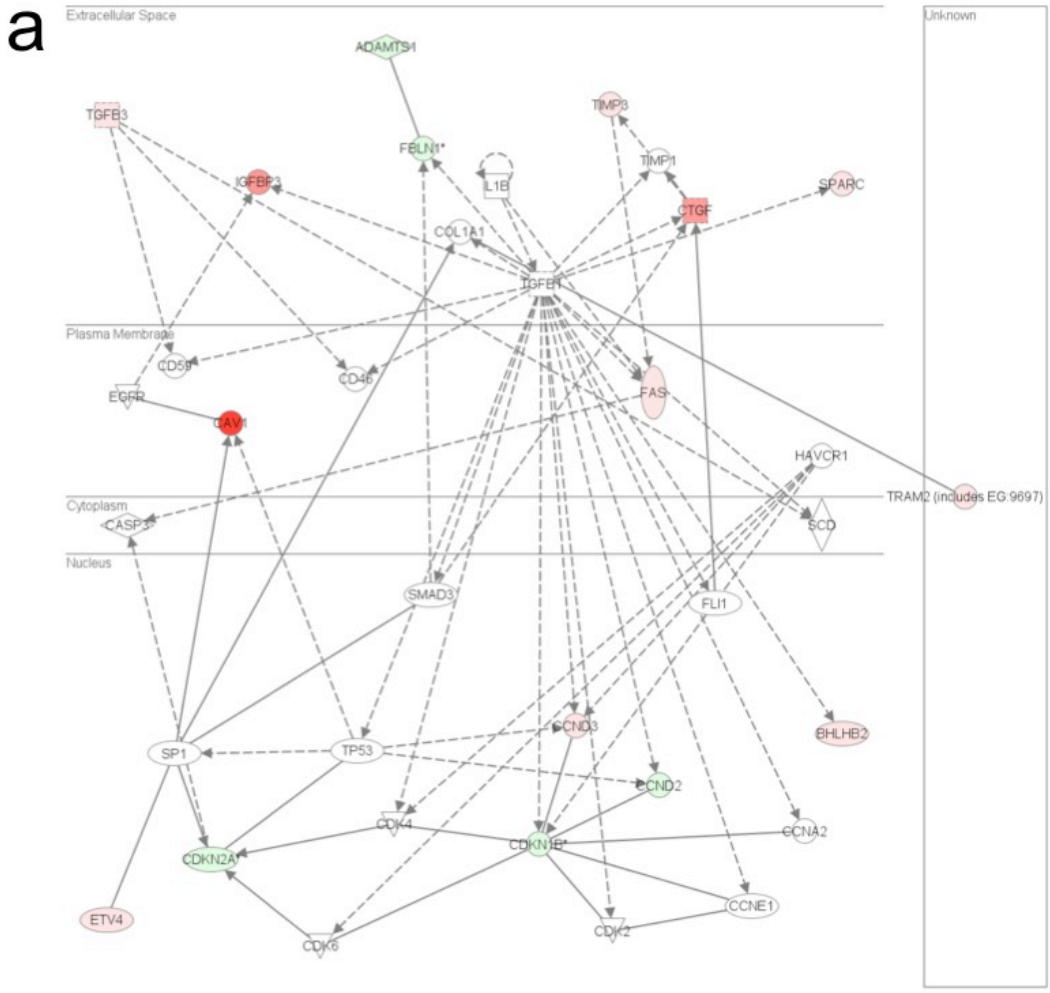
a
Extracellular Space
Unknown
Plasma Membrane
Cytoplasm
Nucleus
ADAMTS1
TGFB3
FBLN1*
TIMP3
TIMP1
IGFBP3
L1B
SPARC
CTGF
COL1A1
TGFB1
CD59
CD46
EGFR
FAS
CAV1
HAVCR1
TRAM2 (includes EG:9697)
CASP3
SCD
SMAD3
FLI1
CCND3
BHLHB2
SP1
TP53
CCND2
CDK4
CCNA2
CDKN1B*
CDKN2A
CCNE1
ETV4
CDK2
CDK6

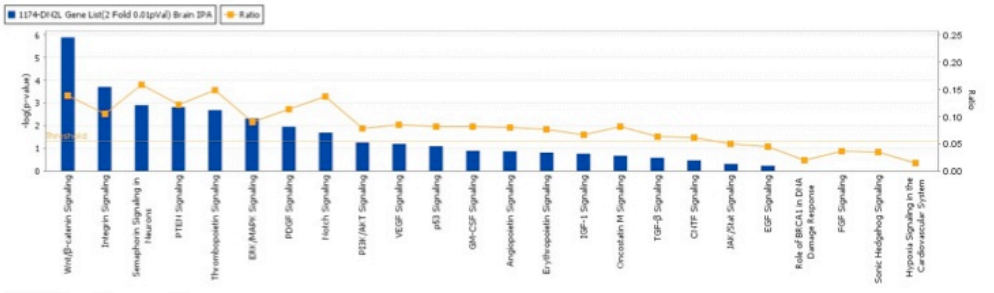
b
1174-DH2L Gene List(2 Fold 0.01pVal) Brain IPA
Ratio
-log(p-value)
Threshold
Wnt/β-catenin Signaling
Integrin Signaling
Semaphorin Signaling in Neurons
PTEN Signaling
Thrombopoietin Signaling
IL6/JAK/STAT Signaling
PDGF Signaling
Notch Signaling
PI3K/AKT Signaling
VEGF Signaling
p53 Signaling
GM-CSF Signaling
Angiopoietin Signaling
Erythropoietin Signaling
IGF-1 Signaling
Oncostatin M Signaling
TGF-β Signaling
CNTF Signaling
JAK/Stat Signaling
EGF Signaling
Role of BRCA1 in DNA Damage Response
FGF Signaling
Sonic Hedgehog Signaling
Hypoxia Signaling in the Cardiovascular System

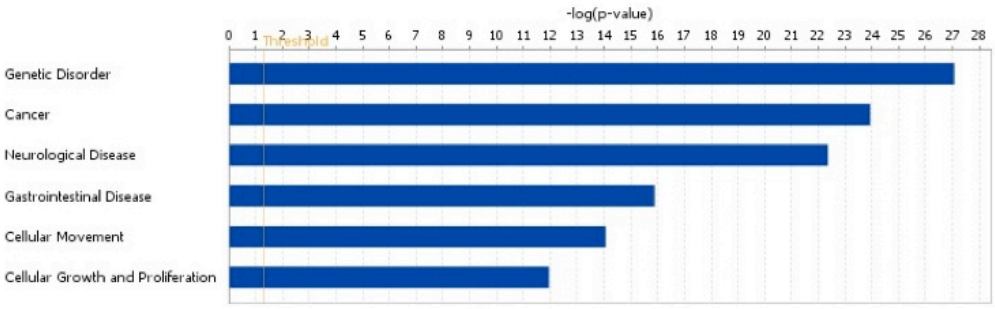
c
-log(p-value)
Threshold
Genetic Disorder
Cancer
Neurological Disease
Gastrointestinal Disease
Cellular Movement
Cellular Growth and Proliferation

Figure 27. MIC pathway analysis and gene networks

Ingenuity Pathways Analysis of the differentially expressed genes in the MICs as compared to NSPCs. A data set containing gene identities and corresponding expression values was uploaded into IPA, where each gene identifier was mapped to its corresponding gene object in the Ingenuity Pathways Knowledge Base. The genes were overlaid onto a global molecular network developed from information contained in the Ingenuity Pathways Knowledge Base where networks were then algorithmically generated based on their connectivity. ***A,*** The analysis identified 16 molecules in this network and categorized them as related to Cancer, Cellular Growth and Proliferation, Connective Tissue Development and Function. Genes shaded *red* are identified as upregulated and, *green*, downregulated. ***B,*** top canonical pathways, and ***C,*** diseases associated with the differentially expressed genes. The Functional Analysis of a network identified the biological functions and diseases that were most significant to the genes in the network. For example, Canonical pathways analysis identified the Wnt/β-catenin pathway as being the top pathway associated with the differentially expressed gene set.

the relevance of a common stem and progenitor-signaling pathway in these cells. The diseases strongly associated with the differentially expressed gene list were 'Genetic Disorder', 'Cancer' and 'Neurological Disease', appropriately identifying the core processes of these cells (**Figure 27 *C)*.**

3.5 Discussion

In this study, we describe a tumor-initiating subpopulation of cells derived from an atypical meningioma. These meningioma-initiating cells (MICs) exhibit properties of self-renewal, and upon the withdrawal of mitogens, are capable of differentiating into mature neural (neuronal and astrocytic) lineages. Upon transplantation into athymic nude mice, the resulting tumors recapitulate the histological phenotype of the parental tumor. Meningiomas are thought to arise from arachnoidal cap (meningothelial) cells (Perry A, 2007), arising embryologically from neural crest and mesoderm, rather than neural ectoderm (Catala, 1998; Perry A, 2006). However, the histogenesis has not been completely resolved, and the meningothelial phenotype has both ectodermal characteristics, frequently expressing epithelial membrane antigen (EMA) and forming desmosomes, and mesenchymal characteristics capable of synthesizing collagen (Perry A, 2006). Although there are rare descriptions of meningioma-derived cells expressing neurofilaments (Ikeda and Yoshimoto, 2003), the full neuronal and glial phenotype expressed in this study (Neurofilament, βIII-tubulin, GFAP) with simultaneous expression of neural stem cell markers (Nestin, Sox2, and CD133), has not been previously reported.

The propagation of a tumor with features of an atypical meningioma by transplanting cells derived from an atypical meningioma supports the role for a tumor-initiating cell phenotype and presupposes its use as a model for studying meningioma tumors and meningioma progression. The flank model induction of meningioma tumors, augmented by the addition of matrigel, has been shown to recapitulate the features of primary meningiomas with regard to the cytogenetic abnormalities, histological, immunohistochemical and ultrastructural features, lending support to the observations reported here (Ragel et al., 2008). Microarray analysis of gene expression and copy number variations indicates that these MICs are a sub-population derived from the original tumor (rather than a contamination by a stem- and/or progenitor cell not derived from the original neoplastic clone) and can be identified through the expression of, among other markers, ALCAM and CD44. Microarray and pathway analysis suggests the loss of tumor suppressor proteins *CDKN2A ($p16^{INK4A}$), $p14^{ARF}$,* and *CDKN2B ($p15^{INK4B}$),* and the upregulation of epithelial to mesenchymal transition (EMT) genes, as key contributors to the phenotype of these cells, and suggests a mechanistic role for tumor progression in the absence of an NF2 mutation.

Genes involved in the G1/S phase transition are important for cell cycle progression and the aCGH indicates that there is a heterozygous loss of *CDKN2A ($p16^{INK4A}$), $p14^{ARF}$,* and *CDKN2B ($p15^{INK4B}$)* in the primary tissue, and a homozygous loss in the subsequent samples. However, it is possible that the heterozygous loss reported in the bulk primary tissue is due to the contribution of two cell populations, that of cells with two normal copies, and that of a cell

population which harbors the deletion of both copies, such as the MIC population containing a homozygous deletion of this region.

An epithelial to mesenchymal transition (EMT) is believed to play a role in the pathogenesis of carcinomas, where subpopulations acquire mesenchymal features such as motility, invasiveness, and resistance to apoptosis. In meningiomas, malignant progression is seen as an increase in the frequency of genetic alterations and not defined by the type of genetic alteration (Bostrom et al., 2001; Simon et al., 2007; Weber et al., 1997). For example, the high frequency of *NF2* mutations in certain types of meningioma variants has been suggested to contribute to a mesenchymal-like phenotype (Simon et al., 2007). Although these cells do not display mutations in the *NF2* gene, we see the upregulation of genes and signaling mechanisms essential for the acquisition of a mesenchymal phenotype. In particular, the MICs upregulated genes known to be strong initiators of EMT such as TGFβ1, and the transcription factors Twist, Snail, and LEF1 (Medici et al., 2008; Polyak and Weinberg, 2009). LEF1 has recently been shown to be a pivotal molecule in the convergence of the TGF-β and Wnt/β-catenin signaling pathways and may play a strong role in the cross talk of many signaling pathways that converge upon an EMT outcome (Mani et al., 2008; Medici et al., 2008).

Interestingly, we observed expression of Neurofilament-M and GFAP in the cultured cells and in a sub-population of the xenograft tumors. One possible explanation of this phenotype, particularly the expression of the mature neural markers seen when cultured in the DN2L medium, is that of a *de novo* de-

differentiation (or reprogramming) of a mature cell type to that of a less differentiated state. In particular, GFAP expression is absent in the great majority of meningiomas, but is a common feature in neural stem cells. In culturing these cells, the DN2L medium was supplemented with LIF, common in some defined neural stem cell media (Singh et al., 2003). The addition of LIF has been shown to induce GFAP expression in mouse embryonic neural stem cell cultures, while maintaining their stem and progenitor cell traits (Bonaguidi et al., 2005). The expression of GFAP we see when culturing the cells in the DN2L medium may be explained via this LIF signaling mechanism. However, the strong labeling of GFAP seen in the mouse xenograft after residing *in vivo* for more than thirty-days suggests a LIF independent phenomena, possibly a *de novo* differentiation since the xenograft lacks the exogenous LIF provided in the DN2L media.

Together with expression of NF-M and GFAP in the DN2L medium, we observed expression of ALCAM and CD44 in almost all of the cells, which was not expected. In a study of prostate cancer xenograft tumors, the CD44+ prostate cancer cell sub-population was shown to be enriched in tumorigenic cells and share many traits of stem-like cancer cells (Patrawala et al., 2006). Additionally, a comparison of gene expression profiles between fresh-frozen primary meningiomas and their derived cell cultures, identified CD44 as being differentially upregulated in the cultured cells (although the culture medium in this study included growth in serum-containing media) (Sasaki et al., 2003). Similarly, ALCAM (CD166), a cell adhesion and cytoskeletal protein has been

described as a stem cell marker for melanomas and there was an increased ALCAM expression in metastatic melanomas compared to the primary site tumors or benign melanocytic lesions, suggesting a role for ALCAM in tumor invasion and progression (Klein et al., 2007; Lunter et al., 2005). Here we see ALCAM expression in the primary tissue and the uniform expression of CD44 and ALCAM in these cells suggests that either the culture medium augment this expression, or this expression pattern is a property of the non-adherent population of this atypical meningioma. These markers may be used to select and identify a tumor-initiating cell population in atypical meningiomas and it will be important to examine additional cases of atypical meningiomas with similar *in vivo* growth properties for the co-expression of ALCAM, CD44, and CD133 as potential biomarkers.

In addition to the expression of putative stem cell markers, IPA canonical pathway analysis revealed that the most differentially expressed genes were present in the Wnt pathway. It is known that Wnt pathway is activated in stem and progenitor cells and the deregulation of the molecules in this pathway may lead to cancer (Reya and Clevers, 2005). The association of the Wnt pathway with MICs seen here suggests an additional link to a progenitor population. In a study looking at the correlation between Wnt-signaling in atypical and anaplastic meningiomas containing losses on chromosome 10 and 14 (Wrobel et al., 2005), two Wnt pathway genes were shown to be upregulated in anaplastic compared to benign meningiomas, one of them cyclin D1 (*CCND1),* similar to the gene identified in our results. The deregulation of genes involved in the Wnt-signaling

pathway is a feature of MICs, and this signaling pathway in combination with EMT may contribute to the features of malignant progression and the presence of a stem cell-like subpopulation.

In summary, we describe a cell line derived from an atypical meningioma that is capable of expressing proteins of neuronal and glial derivation, suggesting that meningioma-initiating cells retain the potential to express a glioneuronal phenotype. These findings support the idea of an early-lineage stem cell phenotype in meningioma-initiating cells, a finding that provides new insight into the tumorigenesis and malignant progression of atypical meningiomas.

CHAPTER 4

An Integrative Microarray-based Analysis of Gene Expression, Copy Number, LOH, and DNA Methylation Profiles of Glioblastoma Stem Cells

Submitted: Prakash Rath, Alan Free, Douglas C. Miller, N. Scott Litofsky, Douglas C. Anthony, Qi Feng, Lirong Pei, Mark D. Kirk, Huidong Shi.

4.1 Abstract

Glioblastoma multiforme (GBMs) are notorious for their resistance to complete surgical resection, radiation and chemotherapy, and recur nearly 100% following treatment. There is increasing evidence that this clinical phenotype is associated with populations of stem cells that harbor within high-grade malignant gliomas, which presupposes that novel approaches for treating GBMs will come from targeting the cancer stem cell population. However, little is known about this population. Based on this hypothesis, we explored the genetic and epigenetic landscape of glioma stem cell-like cells (GSCs) derived from primary GBMs. For this study, fresh dissociated primary GBMs, and normal diencephalonic regions were placed in medium designed to enrich for cells with stem cell-like properties. Using genome-wide microarray-based platforms, we analyzed the gene expression, copy number, and LOH events. To investigate

the DNA methylation, we performed a Methylated CpG Island Amplification (MCA) coupled with a 105K custom-designed CpG island oligonucleotide array (MCAM). Integrated analysis was performed using Partek Genomics Suite software, and functional associations were derived from Ingenuity Pathway Analysis platform. Through immunohistochemical and copy number analysis, we identified the enrichment of GSCs from the parental tumor. GSC tumor spheres, and neural stem and progenitor cell (NSPC) neurospheres, exhibited the capacity of self-renewal by forming secondary spheres. Neural/embryonic stem cell properties were characterized by the presence for the molecular markers Nestin, Sox-2, Musashi, and CD133. Mitogen withdrawal resulted in the outgrowth of neurites and the expression of the neuronal lineage markers B-III tubulin and Neurofilament-M, and astrocytic marker GFAP. Expression analysis revealed the upregulation of multiple Hox family members in two GSCs. Integrative microarray analysis identified the TGF-β and the Wnt/β-Catenin signaling pathways as being the most significant pathways effected by the differentially expressed gene set, with some genes being hypo- or hypermethylated, and containing an LOH or copy number aberrations. In this study we characterized GSCs obtained from primary human specimens by microarray and immunohistochemical analysis, and profiled the aberration of genes in two common canonical pathways deregulated in GBMs. These results highlight the synchronicity between the CN, LOH events, and DNA methylation effect on gene expression. These results provide insight into the molecular mechanism of

GSCs and may have implications for tumorigenesis and the development of targeted therapies against entire pathways.

4.2 Introduction

Glioblastoma (GBMs) (WHO grade IV) are highly infiltrative, aggressive tumors, rendering complete surgical resection difficult. The remaining cells proliferate rapidly and as a result, patient survival is low. The median survival of patients with GBMs is approximately one-year with less than 4% survival five-years post-diagnosis (CBTRUS: 2007-2008 Statistical report: primary brain tumors in the United States). The remnant cells contributing to tumor recurrence are postulated to be the result of a cancer stem cell population that is refractory to all treatment modalities. According to the cancer stem cell hypothesis, a subpopulation of cells reside within the tumor is responsible for the initiation, propagation, maintenance of heterogeneity, and recurrence of high-grade gliomas such as GBMs (Vescovi et al., 2006). Little is understood about glioblastoma stem cells (GSCs) and characterizing this population has directed much attention regarding the design of targeted therapies to prevent tumor recurrence.

To isolate the stem cell-like population, gliomas are cultured in defined medium in the presence of mitogens. This methodology was initially designed for the propagation of neural stem cells and facilitates the capacity of self-renewal and differentiation (Lee et al., 2006; Singh et al., 2004; Vescovi et al., 2006). Studies have shown that GBMs cultured in defined medium facilitates the

enrichment of stem cell-like subpopulations, but more importantly, well represents the primary GBM it was derived from (Lee et al., 2006; Li et al., 2008).

During progression, GBMs accrue many aberrations that contribute to the anaplastic phenotype. Genomic and epigenomic studies have been conducted to identify abnormalities in genes and pathways, and recently, the Cancer Genome Atlas (TCGA) Research Network conducted a large-scale study of the genomic alterations in GBMs (2008; Foltz et al., 2009; Martinez et al., 2009; Yin et al., 2009). This systematic, multi-dimensional analysis confirmed previously well-known genetic events, and identified genetic alterations not previously reported in GBMs. Global studies such as these provide great insight into the molecular mechanisms of GBMs as a whole, however, analysis from bulk tumor populations potentially overlook the expression profiles of the rare cancer stem cell and may identify genes involved in the regulation of non-tumorigenic cells (Ward and Dirks, 2007).

The present study was designed to study genome and epigenome of GSCs derived from primary GBM specimens. Through immunohistochemistry and microarray technologies, we explored the genome alterations of GSCs as compared to NSPCs. The deregulation of the TGF-β and the Wnt/β-Catenin signaling pathways were identified as containing the most differentially expressed molecules from our dataset. Within these pathways, we identified DNA methylation and CN changes that may contribute the differential expression seen. These results identify aberrations found in pathway related molecules of GSCs, and their contribution to the deregulation of entire pathways.

4.3 Methods and Materials

Patient tissue

Tissue samples from GBM specimens and fetal brain-derived neural stem and progenitor cells (NSPCs) from diencephalonic regions were provided via appropriate Institutional Review Board-approved protocols of the Department of Surgery, Division of Neurological Surgery, and Pathology and Anatomical Sciences in the School of Medicine at the University of Missouri.

Cell culture

Specimens were mechanically dissociated, washed with PBS, and red blood cells removed with Histopaque (Sigma). Cells were expanded in DMEM-F12 (no phenol red, Invitrogen) containing 20% FBS (Atlanta Biologicals) and Penicillin-Streptomycin (Invitrogen) in tissue-culture flasks and maintained for no more than two passages (Liu et al., 2006). Following expansion, the cells were grown as non-adherent cultures in un-coated petri dishes in serum-free defined medium containing DMEM-F12 supplemented with 20ng/ml epidermal growth (EGF; Invitrogen), 20ng/ml basic fibroblast growth factor (bFGF; Invitrogen), 1:50 B27 supplement (Invitrogen), 1:100 N2 supplement (Invitrogen), 10ng/ml leukemia inhibitory factor (LIF; Chemicon), as a stem-cell permissive medium to facilitate the growth of neurospheres and tumorspheres, hereafter known as "DN2L medium"(Inagaki et al., 2007).

Immunohistochemistry

Neurospheres and tumorspheres were embedded in OCT, and 10μm sections were labeled with antibody as previously described (Bleau et al., 2008).

For differentiated cells, the samples were labeled and processed as described in the Human Neural Stem Cell Characterization Kit (Chemicon). Primary antibodies used were anti-Nestin, anti-Sox2, anti-Musashi, anti-*B*III Tubulin, anti-GFAP, anti-Neurofilament 150kd (all from Chemicon), and anti-CD133 (Miltenyi Biotec). Secondary antibodies used were anti-mouse Alexa Fluor 488, anti-rabbit Alexa Fluor 546, and anti-rabbit Alexa Fluor 488 (all from Invitrogen). Sections were counterstained with Vectashield (Vector Labs) mounting medium that contains the DNA counter stain DAPI, before visualization. Negative controls were processed as described above with no primary antibody.

Imaging

Brightfield images of neurospheres and tumorspheres were captured with a Nikon D100 camera through an Olympus CKx41 upright microscope. Confocal images were captured with a Zeiss 510 META NLO and a Zeiss 5 live and processed using LSM 5 Image Examiner software.

Microarrays

Total DNA and RNA were isolated (DNeasy, RNeasy kit; Qiagen) from primary tissue and DN2L cultured cells upon disruption with the TissueLyser apparatus (Qiagen). For gene expression experiments, specimens were profiled using the Human W-6 v3.0 Expression BeadChips (Illumina, Inc.) which assays >48,000 transcripts and covers >25,400 genes in the NCBI RefSeq database. For array comparative genomic hybridization (aCGH) experiments, to assess copy number (CN) and loss of heterozygosity (LOH), specimens were profiled using Affymetrix Human SNP 5.0 array (Affymetrix, Inc.), which contains over

500,000 SNP probes and 420,000 non-polymorphic copy number probes. Both platforms are whole genome arrays and assays were performed in accordance with the respective manufacturer's protocol.

For methylation analysis, Methylated CpG Island and Amplification with microarray (MCAM) was performed as previously described in (Bennett et al., 2009) **(Figure 28)**. Briefly, DNA from tumor and normal (NSPCs) samples were digested with *SmaI* and *XmaI,* ligated to adapters, then PCR amplified for methylation fragments. After purification, the amplicons, which represents the methlyated fragments in the genome, were fluorescently labeled and hybridized to a 105K custom-designed Agilent CpG island oligonucleotide array (Agilent Technologies). The tiling array was designed to cover 50bp to 2000bp *SmaI* fragments that overlap with CpG islands in the human genome. The total number of *SmaI* fragments covered is 29,875, which overlap with 13,385 annotated CpG island in the UCSC genome browser. The probe spacing for the tiling array is approximately 100bp, and a total of 99,027 probes (45-60 mer) were synthesized on each array. The microarray images were scanned by an Agilent scanner, and processed using FeatureExtraction 9.1 software (Agilent Technologies). Raw microarray data have been uploaded to Gene Omnibus database and can be accessed via accession # (pending upon acceptance) (http://www.ncbi.nlm.nih.gov/geo/).

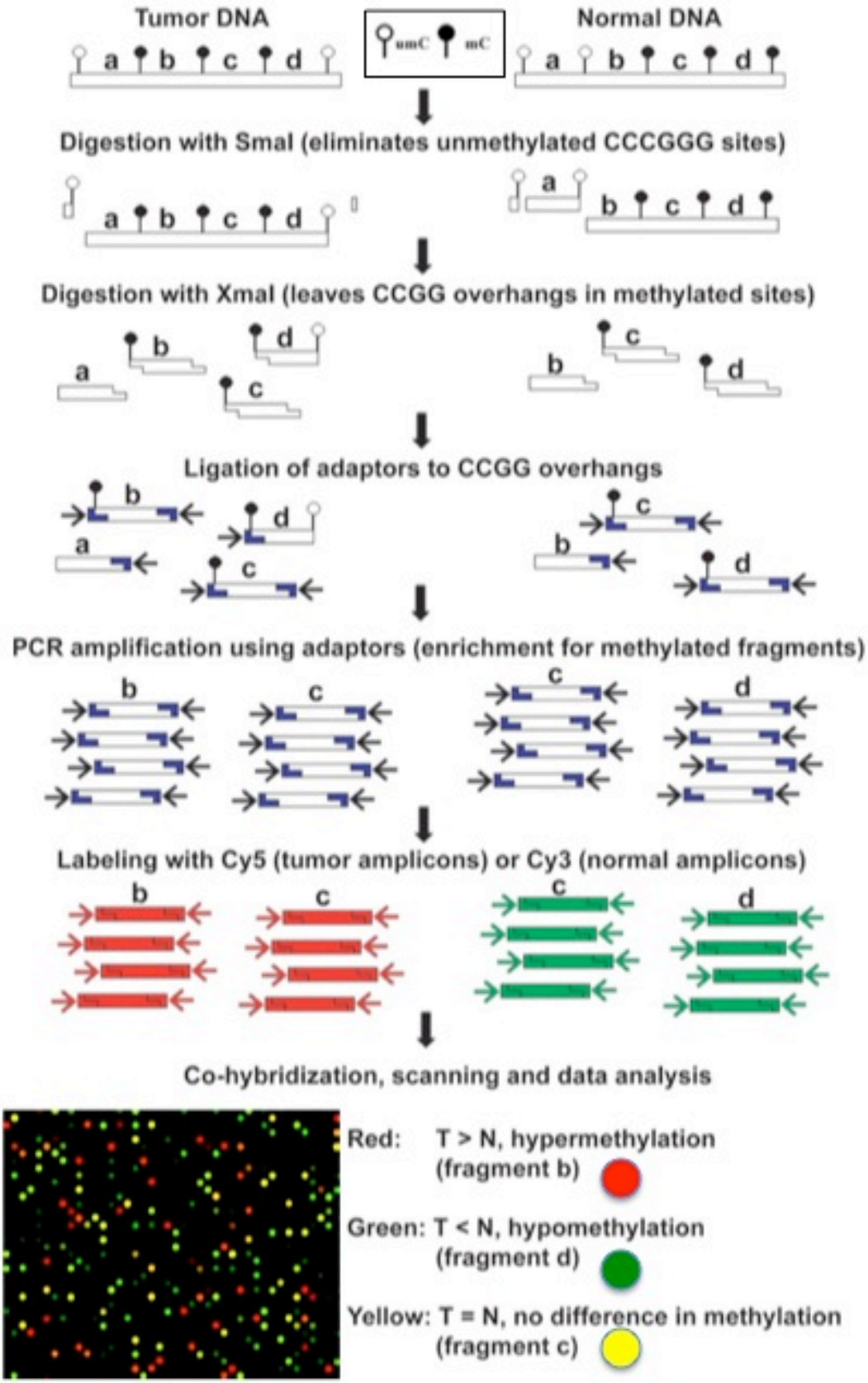
Tumor DNA
umC
mC
Normal DNA
a b c d
Digestion with SmaI (eliminates unmethylated CCCGGG sites)
Digestion with XmaI (leaves CCGG overhangs in methylated sites)
Ligation of adaptors to CCGG overhangs
PCR amplification using adaptors (enrichment for methylated fragments)
Labeling with Cy5 (tumor amplicons) or Cy3 (normal amplicons)
Co-hybridization, scanning and data analysis
Red: T > N, hypermethylation (fragment b)
Green: T < N, hypomethylation (fragment d)
Yellow: T = N, no difference in methylation (fragment c)

Figure 28. Methylated CpG island Amplification with Microarray (MCAM)

MCAM is used to detect the difference in the methylation status between a tumor and a control sample. In this schematic, a box represents the DNA and the bullets represent Sma1 specific cut sites located at CpG islands. The filled bullets represent a methylated CpG island. Sma1 cuts its recognition sequence (CCCGGG) when it is not methylated, leaving a blunt end as shown here for fragment a of the normal DNA. The samples are then digested with Xma1, which cleaves methylated CCCGGG sites resulting in sticky ends. Adaptors are then ligated to the methylated fragments and PCR amplified. The methylated amplicons are then labeled with fluorescent dyes, Cy5 for tumor amplicons and Cy3 for normal amplicons. The amplicons from each sample are then hybridized to the microarray and scanned for analysis. In this example, the red signal on the microarray indicates that fragment b is hypermethylated in the tumor sample. Similarly, the green signal indicates that fragment d is hypermethlyated in the normal sample. If both samples contain a fragment that is equally methylated, the signal readout would be yellow, such as the case for fragment c shown here. Figure adapted from (Estecio et al., 2007)

Data analysis

Gene expression, methylation, copy number (CN), and loss of heterozygosity (LOH) analyses were performed using Partek® Genomics Suite software. Briefly, CN events were reported based on Partek's Genomic Segmentation Algorithm and single nucleotide polymorphism (SNP) genotype dataset was generated through Affymetrix's Genotyping Console and compared against a standard 270 HapMap genotype dataset in Partek. Differential gene expression values were created by an Analysis of Variance (ANOVA) in Partek to create tables of differentially expressed genes. For methylation analysis, oligonucleotide probes were first grouped based on the *SmaI* fragments that they matched, and then the average of the differential $\log_2$ values of all probes represented in each *SmaI* fragment was calculated. A cutoff $\log_2$ value of ±1.3 was used to determine hypo or hypermethylation, respectively. Only *SmaI* fragments that fell within the promoter or first exon regions were considered for the pathway analysis described below.

Unique gene lists for DNA methylation, gene expression, LOH and CN were annotated to the appropriate gene for correlations between genetic and epigenetic events. Datasets were imported into Ingenuity's Pathway Analysis (IPA, Ingenuity® Systems) for constructions of networks. The differentially expressed genes were overlaid onto a global molecular network developed from information contained in Ingenuity's Pathways Knowledge Database, a repository of molecular interactions, events, and associations, used for pathway construction and functional associations.

4.4 Results

Neurospheres and tumorspheres exhibit stem cell properties

All samples were placed in DN2L medium (**Figure 29 a-c**). The NSPCs and 3/5 GBMs proliferated and were passaged multiple times, indicating the ability to self-renew. NSPCs aggregated as free-floating cell clusters and proliferated as tight spherical shapes (a). Cells from GBM sample 1239 and 1175 initially aggregated as spheroids but did not proliferate as robustly and therefore was not passaged as the other samples (data not shown). This is consistent with other reports that not all primary GBM spheres can be passaged for multiple times. GBM 1133 had a unique morphology as compared to the rest of the tumors, whereas GBM 1142 and 1063 had similar growth properties. We decided to analyze 1063 (b) and 1133 (c). GBM 1133 could be passaged for many times and aggregated as spherical clusters but in each petri dish, it was apparent that a portion of the cells appeared more 'sticky' and semi-adherent. The dual properties of non-adherent and adherent growth of stem cell-like cells derived from GBMs have been previously reported (Gunther et al., 2008), and recently, studies have shown that stem cell properties can be maintained in non-adherent and adherent conditions (Inagaki et al., 2007; Pollard et al., 2009).

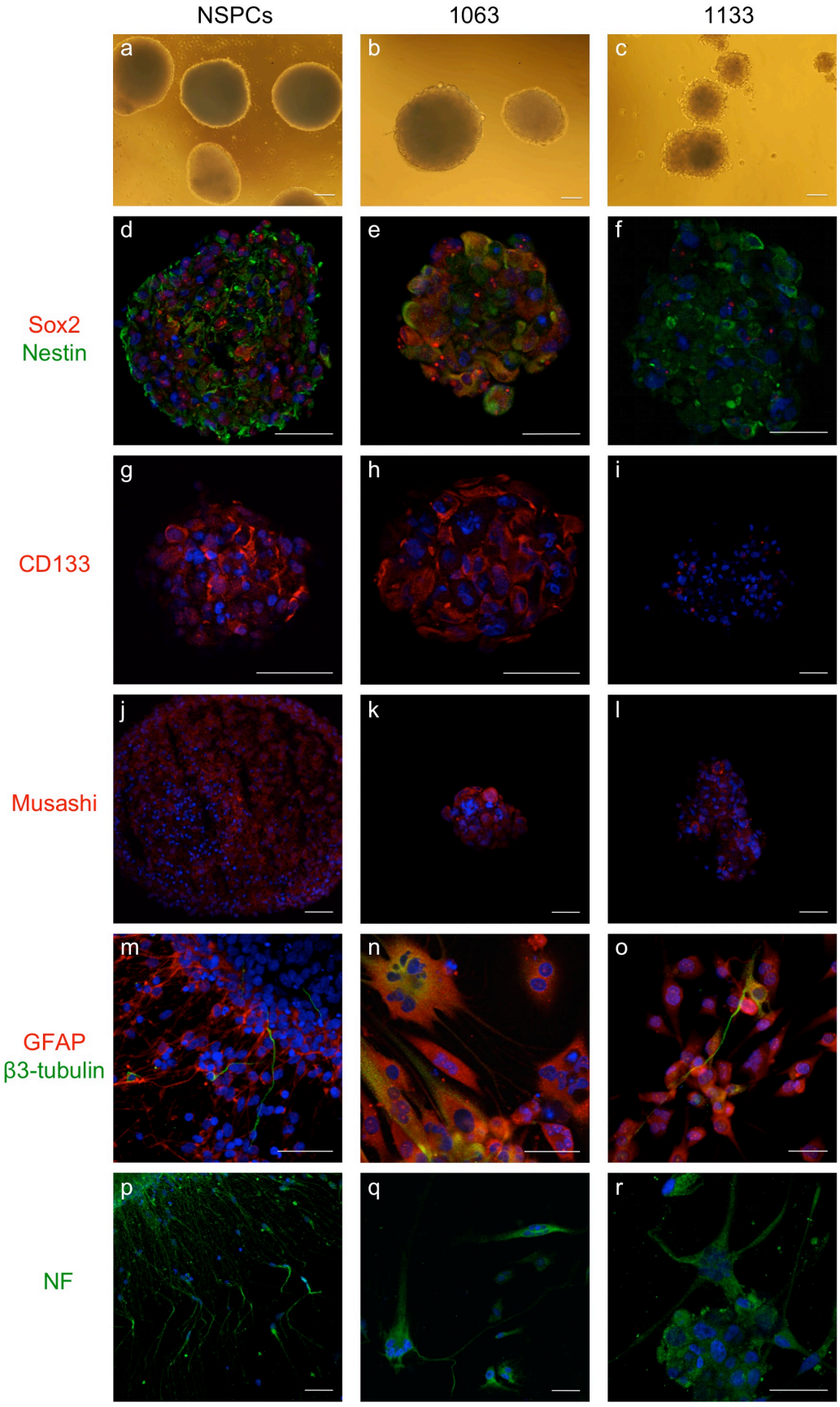
NSPCs
1063
1133
a
b
c
d
e
f
Sox2
Nestin
g
h
i
CD133
j
k
l
Musashi
m
n
o
GFAP
β3-tubulin
p
q
r
NF

Figure 29. GBM cells exhibit stem cell-like properties

GBM cells cultured in stem-cell selective medium enrich for cells capable of self-renewal and differentiation, similar to neural stem and progenitor cells. Representative bright field images show DN2L cultured NSPCs and GBMs growing as spheres (a-c). Neurospheres and tumorspheres were immuonoreactive for neural stem cell markers Sox2, Nestin (d-f), CD133 (g-i), and Musashi (j-l). Upon mitogen withdrawal, the cells extended processes and exhibited morphologies similar to neuronal and astrocytic cells. Differentiated cells expressed mature cell markers GFAP, β3-tubulin (m-o) and Neurofilament (p-r). Nuclei were counterstained with DAPI. Scale bars for all images are 50μm.

.

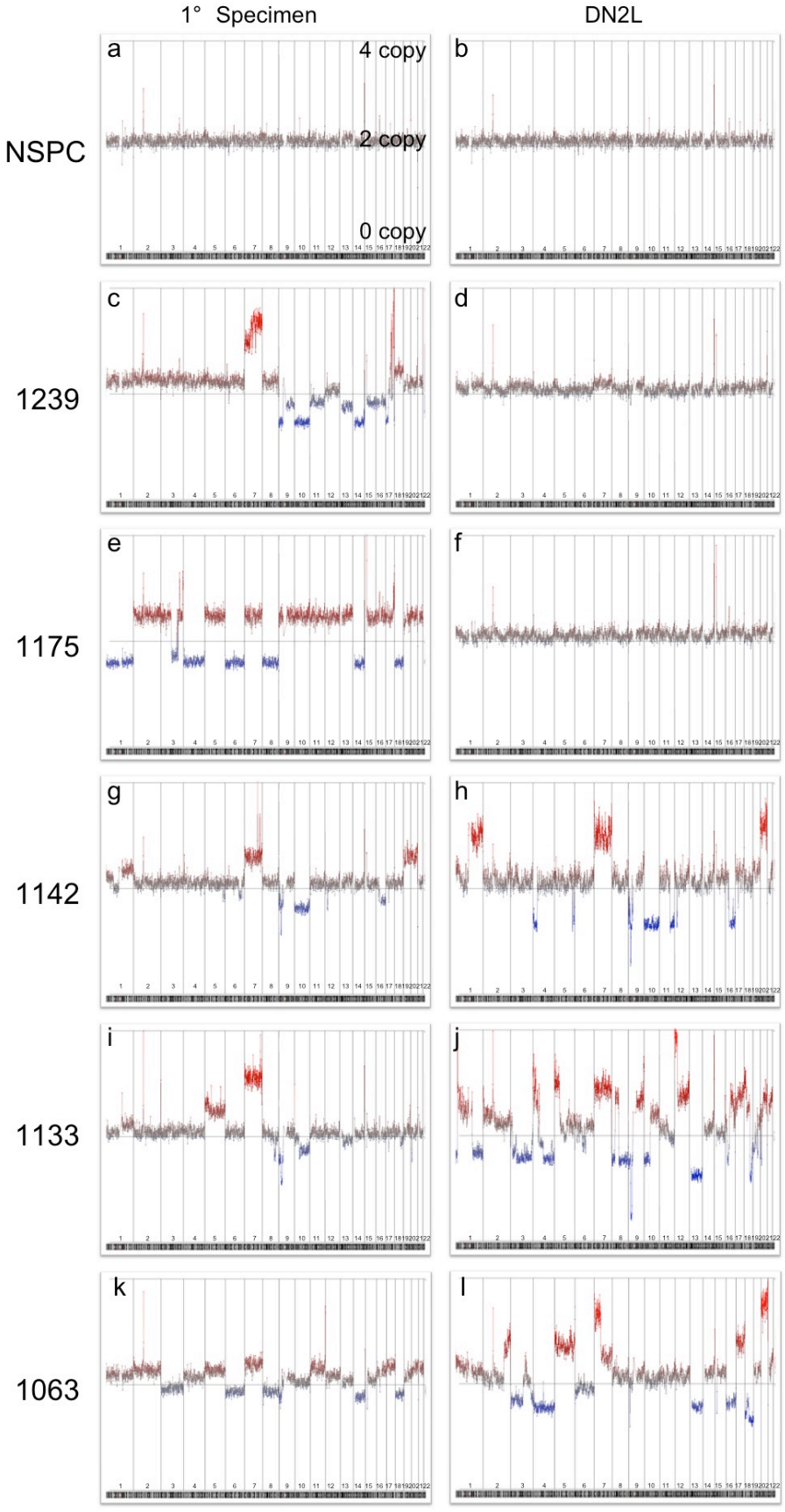
1° Specimen
DN2L
NSPC
1239
1175
1142
1133
1063
a
b
c
d
e
f
g
h
i
j
k
l
4 copy
2 copy
0 copy

Figure 30. Copy number profiles of primary and cultured GBMs

NSPCs showed a normal genome with negligible gain/loss, consistent with the DN2L cultured cells (a,b). Primary GBM specimens contained gain/loss hallmarks of GBMs (i.e. gain of ch.7) (c,e,g,i,k). Copy number analysis of DN2L cultured cells from tumors 1239 and 1175 suggests that a cell population with minor chromosomal aberrations were enriched (d,f). In contrast, cultured cells from tumors 1142, 1133, and 1063 showed a cancer genome similar to the primary parental tumor (h,j,l).

Fluorescent staining revealed immunoreactivity for stem cell markers Nestin, Sox2, CD133, and Musashi in NSPCs (d,g,j) GBM 1063 (e,h,k) and GBM 1133 (f,i,l). NSPCs and GBM 1063 uniformly expressed Sox2, Nestin and CD133, whereas GBM 1133 showed low-level expression of Sox2 and CD133. For differentiation experiments, the cells were dissociated and placed on laminin-coated glass slides in mitogen-free medium. All specimens exhibited neurite outgrowths and morphologies consistent with differentiated cells. The majority of the cells in all samples were strongly immunoreactive for astrocytic marker GFAP and mature neuronal cell marker Neurofilament (m-r), whereas a smaller subset of cells expressed β3-tubulin (Figure2 m-o).

Copy number aberrations in primary tissue and enriched populations

The results of the copy number analysis for the primary specimens and the DN2L cultured cells are shown in **Figure 30** (spikes at centromeric and telomeric regions of the chromosomes are considered artifact, i.e. ch.2, ch.14-15). Primary NSPC sample (a) and DN2L enriched sample (b) showed a normal copy number karyotype. Primary GBM specimens 1239 (c), 1175 (e), 1142 (g), 1133 (i), 1063 (k) all contained multiple chromosomal gain and loss. Recently, a comprehensive analysis of the genetic aberrations of primary GBMs identified consistent chromosomal alterations in regions of chromosome 1p, 7, 8q, 9p, 10, 12q, 13q, 19q, 20, and 22q (Bredel et al., 2009). The most frequent GBM alterations are the amplification in regions of chromosome 7, seen here for all the primary tumors, and the loss of regions in chromosome 10, seen here in GBMs 1239, 1142 and 1133. As mentioned above, GBM samples 1239 and 1175 did

not proliferate in DN2L medium; however, enough DNA was obtained from the cells that aggregated from the initial seeding. The copy number (CN) results of DN2L grown cells from GBM specimens 1239 (d) and 1175 (f) did not contain a large percentage of cells with the cancer genome as seen in the matched primary tissue. As a result, GBM 1239 and 1175 were excluded from further analysis. DN2L cultures from GBM samples 1142 (h), 1133 (j), and 1063 (l) showed cells with multiple chromosomal aberrations, similar to that of the matched primary tumors indicating that a large percentage of cells in the DN2L culture contained the cancer genome. Here we demonstrate the isolation of a glioma stem cell-like cell (GSC) that contains a cancer genome similar to the parental tumor.

Gene expressions show HOX gene network upregulation

Genome-wide microarray studies were carried out to identify the differential gene expression patterns for DN2L cultured cells, and shown as a volcano plot (**Figure 31**). Differential gene expression of the grouped tumors (GSC 1142, 1133, and 1063) versus NSPCs identified 119 genes up regulated (fold change greater than 2, p-value < 0.05) and 190 genes down regulated (fold change less than 2, p-value < 0.05). Initial analysis regarding the relationship of the differentially expressed genes indicated the up regulation of several HOX genes, therefore we focused on the entire Homeobox (HOX) gene network. Cluster analysis revealed the up regulation of many HOX family genes in GBM samples 1063 and 1133 (Figure 2B), including strong expression of HOX C4, C6, A9, and A10.

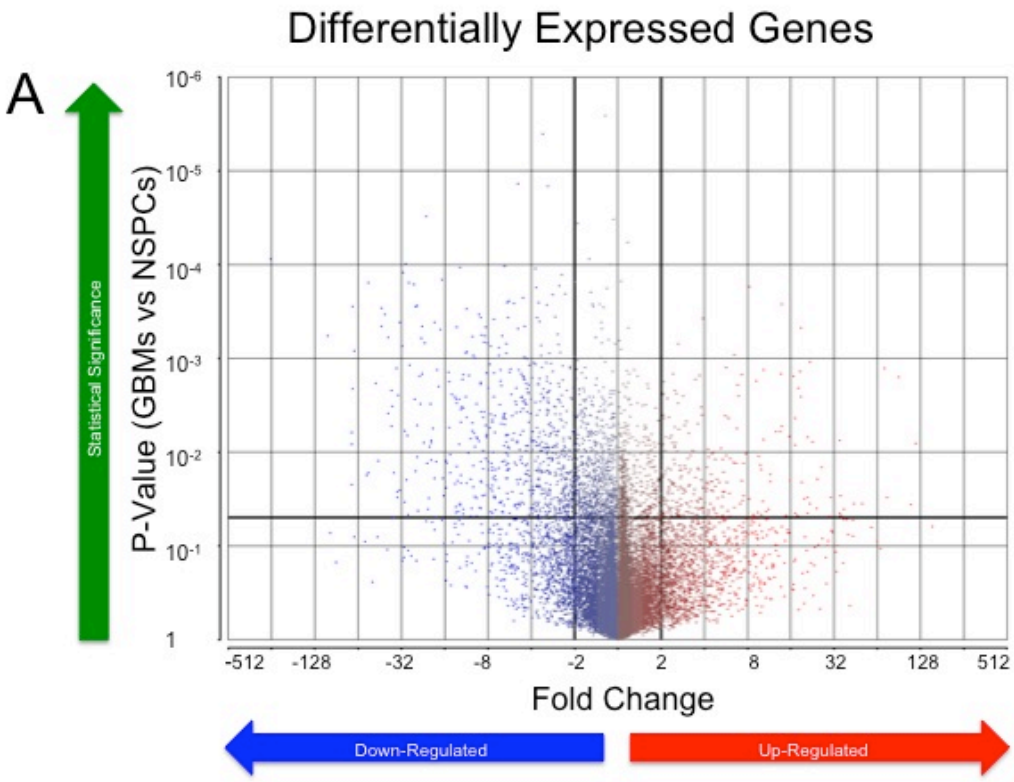
A
Differentially Expressed Genes
Statistical Significance
P-Value (GBMs vs NSPCs)
10-6
10-5
10-4
10-3
10-2
10-1
1
-512
-128
-32
-8
-2
2
8
32
128
512
Fold Change
Down-Regulated
Up-Regulated

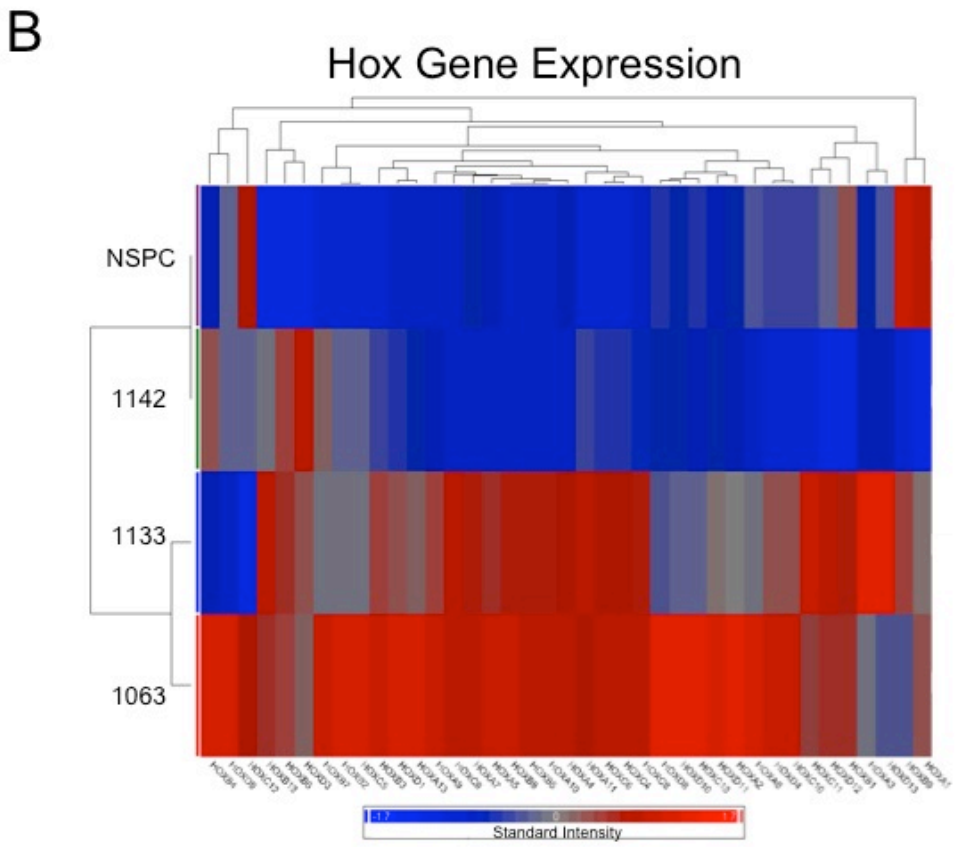
B
Hox Gene Expression
NSPC
1142
1133
1063
Standard Intensity

Figure 31. Differential gene expression profile of GSCs

Relative gene expression profile of GBM 1133, 1063, and 1142 compared to NSPCs. **(A)** Volcano plot highlights the differentially expressed genes. Each gene is represented by a single dot. Genes that have a 2-fold expression change and meet the p-value threshold (< 0.05) are considered differentially expressed **(B)** Heat map analysis identifies many HOX genes in GSC 1133 and 1063 as being up regulated.

Overall, Hox gene heat map showed GSC samples 1133 and 1063 clustered closer together and GSC 1142 and NSPCs clustered similarly.

DNA methylation profiles of GBM stem cells

In a recent study, Lee et al., identified that the epigenetic silencing of BMPR1B effects the Jak/STAT pathway in a subset of GBM initiating cells, and promoter demethylation of this gene was able to induce the loss of tumorigenicity (Lee et al., 2008). Based on this study, we sought to find out additional targets in epigenetic modulation and to understand the global relationship between the epigenome and genome, particularly the role promoter/first exon DNA methylation may contribute to the differential expression profile of GSCs. To do so, we utilized the Methylated CpG island Amplification with Microarray (MCAM) to identify hypermethylated loci. This method selectively amplifies methylated DNA fragments (Estecio et al., 2007). We used a custom designed oligonucleotide tiling array that contains probe coverage of about half of all CpG islands across the genome. The genomic DNA from GSCs and NSPCs was labeled with Alexafluor647 (Red) and co-hybridized with DNA from NSPCs labeled with Alexafluor555 (Green). Data was extracted using the Agilent Feature Extraction tool and imported into Partek Genomics Suites for methylation identification.

All probes on the custom array were first grouped based on the SmaI fragments that they matched, and then the average of the log2 ratios of all probes representing each SmaI fragment was calculated. Each fragment

(ranging from 1-5 per gene) was annotated to a particular gene to attribute methylation specific regions for each gene. For the analysis, the promoter and first exon regions of the genes were analyzed. A differential $\log_2$ value (tumor vs. normal) value > 1.3 (~2.5 fold enrichment) are considered hypermethylated and a value < -1.3 are considered hypomethylated. **Table 2** shows the hypermethylated genes common in all three GSC populations. Of the hypermethylated genes, PENK and ST8SIA3 genes were down regulated in all samples, and PENK reported a copy-neutral LOH event in GBM samples 1133 and 1063.

Integrative analysis demonstrates dysfunction of common networks.

To understand the functional associations of the molecules in the differentially expressed data set of GBM 1142,1133, and 1063, we utilized Ingenuities Pathway Analysis (IPA) platform. The grouped GBM datasets were compared to the NSPCs and showed the Wnt/β-Catenin and TGF-β signaling pathways to be the most significant based on Fischer's exact test. Each GSC sample was analyzed to understand the contribution of

Symbol	Cytoband	Gene Name
GDNF	5p13.1-p12	glial cell derived neurotrophic factor
SLC6A3	5p15.3	solute carrier family 6 (neurotransmitter transporter, dopamine), member 3
IRX2	5p15.33	iroquois homeobox protein 2
KCNK17	6p21.1	potassium channel task-4; potassium channel talk-2
TBX20	7p15-p14	t-box 20
HOXA5	7p15-p14	homeobox a5
PRR15	7p15.1	hypothetical protein loc222171
KIAA0644	7p15.1	kiaa0644 gene product
*+PENK	8q23-q24	proenkephalin
SPAG6	10p12.2	sperm associated antigen 6
CLEC14A	14q21.1	c-type lectin domain family 14, member a
BNC1	15q25.2	basonuclin 1
*ST8SIA3	18q21.31	st8 alpha-n-acetyl-neuraminide alpha-2,8-sialyltransferase 3
PROKR2	20p12.3	prokineticin receptor 2
TAF4	20q13.33	taf4 rna polymerase ii, tata box binding protein (tbp)-associated factor, 135kda
CYYR1	21q21.2	cysteine/tyrosine-rich 1

*Downregulated 3/3 +LOH 2/3

Table 2

Genes Hypermethylated in 3/3 GBM stem cells 1133, 1063, and 1142.

expression, DNA methylation, CN, and LOH events of individual molecules in these pathways. **Figure 32 A** represents the differential gene expression values were overlaid onto the canonical Wnt/β-Catenin signaling pathway for GSC 1133. Table 2A shows the integrative analysis of copy number, LOH, and DNA methylation status of the representative genes in the pathway. Of the 27 genes differentially expressed, 10 genes were up regulated and 17 genes were down regulated. Two genes, FZD8 and FZD9, were shown to be hypermethylated and down regulated with an LOH event. Seven genes contained a one-copy amplification, 8 genes a one-copy deletion, and CDKN2A reported a homozygous deletion. The genes with the highest fold change difference compared to NSPCs were SOX8 (-60 fold change) and SFRP1 (-25 fold change). Differential expression indicates an increase of Wnt activators (TGF-β, TGFBR, Wnt, Frizzled, LEF/TCF) and decrease of Wnt inhibitors (SFRP, SOX). **Figure 32 B** represents the differential gene expression of GBM 1142 overlaid onto the TGF-β signaling pathway. Integrative analyses of representative genes are shown in **Table 3.** Of the 15 differentially expressed genes represented, 12 genes were up regulated and 3 genes down regulated. One gene HRAS, is down regulated and hypermethylated, whereas three gene BMP2, SMAD7, and SOS2, were upregulated and hypomethylated. BMP2 and BMP7 genes reported a one-copy amplification whereas no

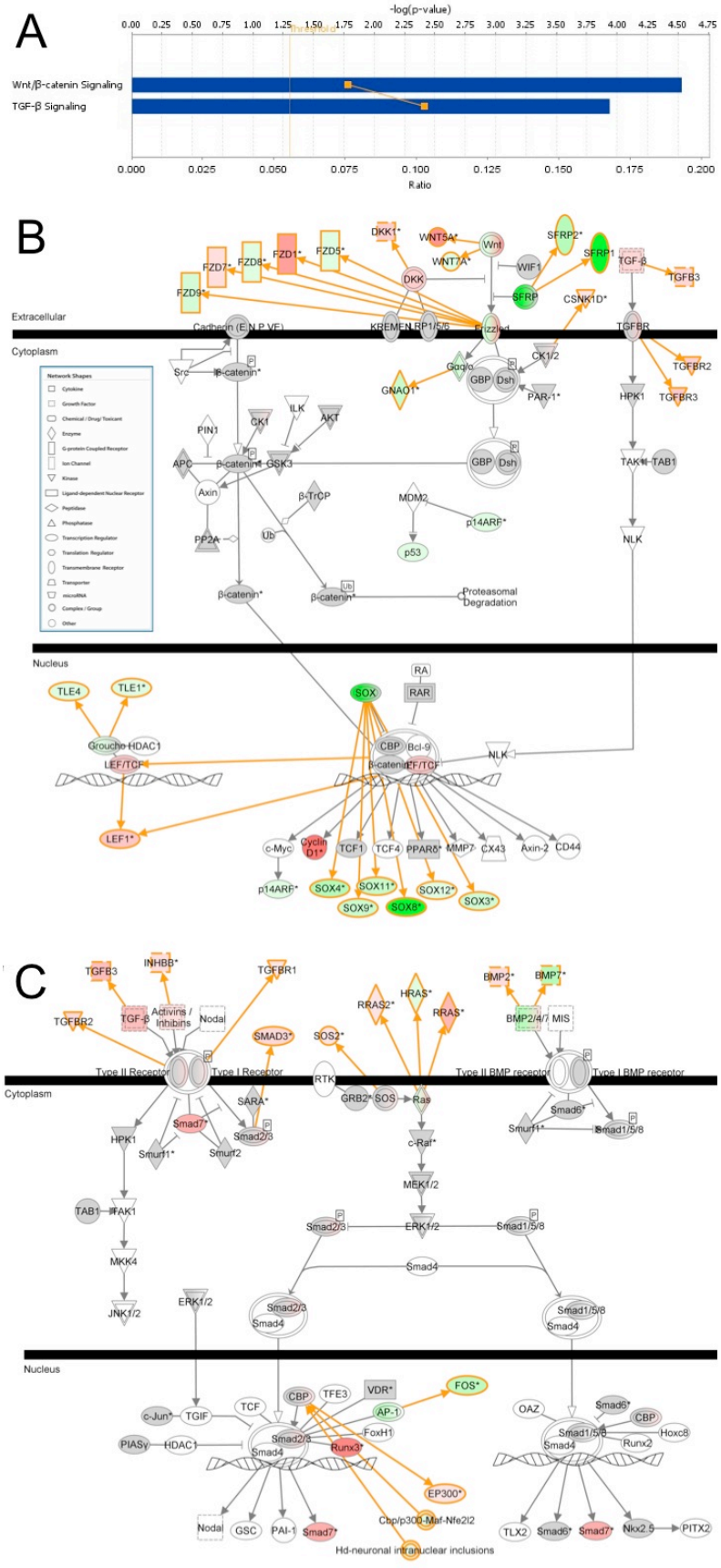
A
-log(p-value)
0.00 0.25 0.50 0.75 1.00 1.25 1.50 1.75 2.00 2.25 2.50 2.75 3.00 3.25 3.50 3.75 4.00 4.25 4.50 4.75
Threshold
Wnt/β-catenin Signaling
TGF-β Signaling
0.000 0.025 0.050 0.075 0.100 0.125 0.150 0.175 0.200
Ratio
B
Extracellular
Cytoplasm
Nucleus
DKK1*
WNT5A*
WNT7A*
Wnt
SFRP2*
SFRP1
TGF-β
TGFB3
FZD7*
FZD8*
FZD1*
FZD5*
FZD9*
DKK
WIF1
SFRP
CSNK1D*
Cadherin (E,N,P,VE)
KREMEN
LRP1/5/6
Frizzled
TGFBR
CK1/2
TGFBR2
TGFBR3
Src
β-catenin*
Gαq/o
GBP
Dsh
GNAO1*
PAR-1*
HPK1
PIN1
CK1
ILK
AKT
APC
β-catenin
GSK3
Axin
β-TrCP
Ub
PP2A
MDM2
p14ARF*
p53
TAK1
TAB1
NLK
β-catenin*
Proteasomal Degradation
TLE4
TLE1*
Groucho/HDAC1
LEF/TCF
SOX
RA
RAR
CBP
Bcl-9
β-catenin
LEF/TCF
LEF1*
c-Myc
Cyclin D1*
TCF1
TCF4
PPARδ*
MMP7
CX43
Axin-2
CD44
p14ARF*
SOX4*
SOX11*
SOX12*
SOX3*
SOX9*
SOX8*
C
Cytoplasm
Nucleus
TGFB3
INHBB*
TGFBR1
TGFBR2
TGF-β
Activins / Inhibins
Nodal
SMAD3*
Type II Receptor
Type I Receptor
SARA*
Smad7*
Smad2/3
HPK1
Smurf1*
Smurf2
TAB1
TAK1
MKK4
JNK1/2
ERK1/2
SOS2*
RTK
GRB2*
SOS
Ras
c-Raf*
MEK1/2
ERK1/2
Smad2/3
Smad4
RRAS2*
HRAS*
RRAS*
BMP2*
BMP7*
BMP2/4/7
MIS
Type II BMP receptor
Type I BMP receptor
Smad6*
Smurf1*
Smad1/5/8
Smad2/3
Smad4
Smad1/5/8
Smad4
c-Jun*
TGIF
TCF
CBP
TFE3
VDR*
FOS*
AP-1
FoxH1
Runx3*
PIASy
HDAC1
Smad2/3
Smad4
EP300*
Cbp/p300-Maf-Nfe2l2
Nodal
GSC
PAI-1
Smad7*
Hd-neuronal intranuclear inclusions
OAZ
Smad6*
CBP
Smad1/5/8
Smad4
Runx2
Hoxc8
TLX2
Smad6*
Smad7*
Nkx2.5
PITX2

Figure 32. Integrative pathway analysis of GSCs

(A) GBC 1133,1063, and 1142 gene expression analysis identified the Wnt/β-Catenin and TGF-β signaling pathways as being the most significant. **(B)** Representative molecules in the Wnt/β-Catenin signaling pathway for GSC 1133. **(C)** Representative molecules in the TGF-β signaling pathway for GSC 1142. Genes shaded gray identify present genes from the input dataset that were not differentially expressed. Red shade indicates genes that are up regulated, green shade indicate genes that are down regulated; white shaded genes were not represented but incorporated into canonical pathways. Node intensity indicates the degree of differential expression, and double-lined nodes (i.e. Wnt, not WIF1) represent family of genes. For expression values of individual genes, see **Table 3.** The asterisk symbol represents molecules represented by multiple methylation probe fragments; the most differentially methylated fragment is shown.

GSC 1133 Wnt/β-Catenin Signaling Pathway

Symbol	Cytoband	Expressed	Fold Change	Copy Number	Methylated	LOH
CCND1	11q13	Upregulated	11.380			
CDKN2A	9p21	Downregulated	-2.185	homozygous deleted		
CSNK1D	17q25	Upregulated	2.267			Yes
DKK1	10q11.2	Upregulated	4.157	1 copy deletion		Yes
FZD1	7q21	Upregulated	8.155	1 copy amplification		Yes
FZD5	2q33-q34	Downregulated	-2.309			Yes
FZD7	2q33	Upregulated	2.816			Yes
FZD8	10p11.21	Downregulated	-2.969	1 copy deletion	Hypermethylated	Yes
FZD9	7q11.23	Downregulated	-4.567	1 copy amplification	Hypermethylated	Yes
GNAO1	16q13	Downregulated	-5.673	1 copy amplification		Yes
LEF1	4q23-q25	Upregulated	4.850	1 copy deletion		Yes
SFRP1	8p12-p11.1	Downregulated	-25.188	1 copy amplification		Yes
SFRP2	4q31.3	Downregulated	-7.766	1 copy deletion		Yes
SOX3	Xq27.1	Downregulated	-5.028	1 copy deletion		Yes
SOX4	6p22.3	Downregulated	-8.035			
SOX8	16p13.3	Downregulated	-60.273			
SOX9	17q24.3-q25.1	Downregulated	-5.551	1 copy amplification		
SOX11	2p25	Downregulated	-6.087			Yes
SOX12	20p13	Downregulated	-2.402	1 copy deletion		Yes
TGFB3	14q24	Upregulated	3.566			
TGFBR2	3p22	Upregulated	4.006	1 copy deletion		
TGFBR3	1p33-p32	Upregulated	4.527			
TLE1	9q21.32	Downregulated	-2.939	1 copy amplification		
TLE4	9q21.31	Downregulated	-3.334	1 copy amplification		Yes
TP53	17p13.1	Downregulated	-2.314			
WNT5A	3p21-p14	Upregulated	9.003	1 copy deletion		
WNT7A	3p25	Downregulated	-2.170			Yes

GSC 1142 TGF-β signaling pathway

Symbol	Cytoband	Expression	Fold Change	Copy Number	Methylation	LOH
BMP2	20p12	Upregulated	4.864	1 copy amplification	Hypomethylated	
BMP7	20q13	Downregulated	-9.919	1 copy amplification		
EP300	22q13.2	Upregulated	3.245			
FOS	14q24.3	Downregulated	-8.861		Hypermethylated	
HRAS	11p15.5	Downregulated	-2.457			
INHBB	13q11	Upregulated	4.712			
RRAS	19q13.3-qter	Upregulated	10.280			
RRAS2	11p15.2	Upregulated	2.676			
RUNX3	1p36	Upregulated	16.903			Yes
SMAD3	15q22.33	Upregulated	5.572			Yes
SMAD7	18q21.1	Upregulated	11.600		Hypomethylated	
SOS2	14q21	Upregulated	2.151		Hypomethylated	
TGFB3	14q24	Upregulated	9.364			
TGFBR1	3p22	Upregulated	2.130			
TGFBR2	1p33-p32	Upregulated	5.217			

Table 3. Integrative pathway analysis of GSCs – gene list

List of genes and genetic alteration present in the Wnt/β-Catenin signaling pathway for GBM 1133 and TGF-β signaling pathways for GBM 1142.

deletions were reported for the molecules represented in this pathway. The differential gene expression indicates the deregulation of the TGF-β signaling pathway, a known occurrence in high-grade gliomas that contributes to a poor prognosis (Bruna et al., 2007).

4.5 Discussion

In this study, we examined the stem cell-like subpopulations from primary GBMs to gain a better understanding of genetic and epigenetic influences on genes and pathways. Immunohistochemistry of DN2L cultures form GBM 1133 and 1063 emphasize the enrichment of cells with similar phenotypes to that of the NSPCs. The presence of molecular markers Sox2, Nestin, CD133, and Musashi indicate the innate properties embryonic and neural stem cell. Mitogen withdrawal shows that these cells can morphologically resemble a differentiated cell, which is highlighted by the expression of mature cell markers GFAP, β3-tubulin, and NF. All primary tumor samples contained chromosomal gain/loss GBM hallmarks in multiple regions. Each DN2L culture from GBMs 1142, 1133 and 1063 contained pronounced aberrations of the respective primary tumors genome. Together with the IHC studies, these results indicate the enrichment of cancer stem cell-like cells from GBM 1142, 1133, and 1063. DN2L cultured cells from GBM 1239 and 1175 showed are relatively ordinary copy number. This result suggests that either a genetically 'normal' cell was cultured from the primary specimen, or, a heterogeneous population that includes a large percentage of normal cells and a small percentage of cancer cells is present.

Cluster analysis of the complete HOX gene network, comprising 39 genes, revealed the up regulation of many HOX genes in GSC 1133 and GSC 1063. HOX genes encode for transcription factors that modulate cellular processes such as growth and communication. Hox expression is normally seen during development, and gradually decreases as differentiation occurs. In neoplasias, HOX gene expression is re-activated and shown to contribute to cancer progression (Abate-Shen, 2002; Abdel-Fattah et al., 2006). For GBMs, HOX A6, A7, A9, A13, B13, D4, D9, AND D13 have been reported to be substantially up regulated and may contribute to malignancy (Abdel-Fattah et al., 2006; Cillo et al., 1996). Particularly, an expression signature dominated by HOX genes, which comprises Prominin-1 (CD133), emerged as a predictor for poor survival in patients treated with concomitant chemo or radiotherapy (Murat et al., 2008). Our results indicate that HOX gene up-regulation is a property of GSC 1133, and 1063, and perhaps this deregulation may be a driving force of glioma progression. Interestingly, the HOX A5 gene was shown to be hypermethylated and amplified in 3/3 GSCs analyzed. In a study investigating the DNA methylation status of 87 primary GBMs, the HOXA5 gene was shown to be hypermethylated in 26% of the samples (Martinez et al., 2009). Promoter and/or first exon hypermethylation is generally correlated with a reduction in gene expression, but for GSC 1063 and 1133, HOXA5 is hypermethylated and upregulated. The result shows the complexity of the tumor genome. The outcome of gene expression can be contributed by multiple factors. Since both GSC 1063 and 1133 reported a copy number amplification for HOXA5, one

possibility is that the copy number amplification has a greater significance on the regulation of the expression that the DNA methylation.

We identified 17 genes to be hypermethylated in either the promoter or first exon region of the genes shown in table 1. Of particular interest was the PENK gene, which was hypermethylated and contained a copy neutral LOH event. The Martinez et al. study showed PENK gene hypermethylation in 31% of the GBMs tested. The hypermethylation, down regulation, and LOH seen in here for GSCs 1133 and 1063 suggests that PENK expression may play an important role in the progression of some GBMs. Cheng et al, show that opioid growth factor ([Met5]-enkephalin or PENK) indirectly interacts with CDKN2A to increase p16 expression, resulting in a negative effect on cell growth (Cheng et al., 2007). The homozygous deletion of CDKN2A/CDKN2B (p15 and p16) deregulates the cell-cycle and is a common event seen in GBMs (Rao et al., 2009), as seen here for GSC 1133. Conversely, The loss of CDKN2A and down regulation of PENK may have a synergistic effect on the cell cycle. Additionally, for GBMs devoid of the p16 deletion, the down-regulation of PENK, either by hypermethylation or CN loss, may contribute to suppressing the activity of p16. In other studies, the down regulation of PENK in metastatic prostate cells was shown to have an association on cancer development (Goo et al., 2005), whereas PENK methylation was reported to be common event in invasive pancreatic adenocarcinoma, and an indicator of malignancy (Fukushima et al., 2002).

The suppression of genes due to DNA methylation may lead to uncontrolled cell proliferation. Frizzled homolog 9 (drosophila) (FZD9), a

member of the Frizzled gene family and receptor in the Wnt-signaling pathway, was shown to be hypermethylated and down regulated in GSC 1133 and GSC 1142. The Martinez et al. study showed that FZD9 was hypermethylated in a staggering 80% of the GBMs tested (Martinez et al., 2009). After grouping the differentially expressed gene list from 3/3 GSCs, we see that the Wnt/β-Catenin signaling pathway was the most significant pathway associated with our differentially expressed gene dataset. Wnt signaling is an important process during development and necessary for the maintenance of pluripotency in embryonic and adult stem cells (Dreesen and Brivanlou, 2007). Integrative pathway analysis of the differentially expressed genes in the Wnt/β-Catenin for GSC 1133 identified multiple genes with copy number gain/loss. The strongest indicator that proliferation is activated via this signaling pathway is the up regulation of cyclin D1 (more than 10 fold change). Although Wnt ligand-receptor family members showed various expression levels, upstream events such as the up regulation of WNT5A (9 fold change) and FZD1 (8 fold change) and down regulation of SFRP1 (25 fold change) and SOX 8 (60 fold change) suggests a synergistic effort is necessary for the activation of this pathway. For GSC 1133, both WNT7A and its cognate binding partner FZD9 are differentially down regulated. In one study, the interaction between WNT7A and FZD9 has been shown to inhibit growth and promote cellular differentiation in a subset of non-small cell lung cancer cell lines (Winn et al., 2005). The absence of this signaling cascade in GSC 1133 may contribute to the milieu of tumorigenic events.

It is not surprising that the TGF-β signaling pathway contained many genes that were differentially expressed, as there is crosstalk between this and the Wnt/β-Catenin signaling pathway, particularly the TGF-β ligand branch of signaling. TGF-β signaling pathway has long been known to be involved in embryonic stem cell self-renewal, and for regulating cellular proliferation in normal epithelial and astrocyte cells (Bruna et al., 2007). However, in some gliomas, TGF-β can promote tumorigenesis and has recently been shown, along with LIF, to be an oncogenic factor in glioblastoma initiating cells (Bruna et al., 2007; Penuelas et al., 2009; Seoane, 2006). Integrative pathway analysis of the TGF-β signaling in GSC 1142 shows BMP2, SMAD7 and SOS2 genes were hypomethylated and up regulated. BMP2 gene was also amplified suggesting multiple mechanisms contributed to the up regulation. BMP2/4 is up regulated in malignant gliomas and may promote tumor stem cell proliferation, as might be the case here (Lee et al., 2008).

Conclusions

The results of our study showing the integrative analysis of differential gene expression, DNA methylation, CN, and LOH in GBM-derived stem cell-like cell populations, highlight the genetic and epigenetic influences that may contribute to the phenotype of malignant gliomas. To summarize, a sub-population of cells derived from primary GBMs exhibit properties of stem cells with the capability of self-renewal and differentiation. Allele specific and CN analysis confirms that the cultured cells have a genomic correlation with the parental tumor, and suggests that a sub-population of cells was selected from the

heterogeneous tumor. This approach was used to gain insight into the cancer genome of GBM stem cell and how multiple aberrations contribute to malignant progression

CHAPTER 5

GENERAL DISCUSSION

Stem cells: the good and bad

The data presented here underscores the complexity of brain tumors and the necessity for developing targeted therapies. The emergence of the cancer stem cell hypothesis has redefined how we think about oncogenesis and stem cells. The function of stem cells is an important part of our everyday physiology. Stem cells are involved in the normal turnover of our skin, intestinal tract, and olfactory neurons, and are critical for replacing injured and damaged tissue. Equally, they are implicated to be a central component in many malignancies. To eliminate these rouge cells that are responsible for tumor recurrence, it is important to understand their unique molecular phenotype and develop appropriate therapies. In order to administer specific therapies, a 'personalized approach' to medicine may be necessary. Next-generation sequencing and high-throughput technologies are in place to study the full molecular spectrum of individual tumors. Furthermore, it is apparent there is significant cross-talk between genes and pathways. Identifying these unique networks will be essential for deciding what combination of drugs will have the best overall effect. In this dissertation, the studies and results presented were focused on understanding and preventing brain tumor dispersal.

Stem cells as drug-delivery vectors

We have developed an organotypic brain slice model that can be efficiently used to test the migratory ability of stem cells to glioma cells for the delivery of oncolytic agents. This *ex vivo* platform allows us to acquire data at multiple time points, and effectively visualize migratory pathways. Time-lapse images taken over the course of six weeks showed the stem cells steadily populating the glioma implant. This raises the question of whether there was a mass migration of stem cells arriving at the tumor site at different time points, or if a few migrating stem cells proliferated at the tumor site? It is likely that both of these scenarios is plausible. In any case, it is apparent that some populations of stem cells were responsive to the chemokine gradient secreted by the glioma cells, and these stem cells had the migratory machinery in place to navigate through the brain slice. For these studies, the ESCs were neuralized using the 4-/4+ retinoic acid induction protocol. Although this protocol coaxes ESCs down a neuronal lineage, the retinoic acid treatment results in a heterogeneic population of neural precursor and stem cells, as previously shown (Meyer et al., 2004). Within the neural niche, there is a well established linear progression of neural stem cells giving rise to transit amplifying cell, which give rise to migrating neuroblast cells (Alvarez-Buylla et al., 2002). When the neuralized stem cells were placed on the brain slice, the cells were possibly at different developmental states similar to the hierarchal system in the niche. In some brain slices, stem cells remained stationary at the initial site of transplant, analogous to the true NSC, some proliferated at the initial site, similar to the characteristics of the

transit amplifying cell, and some were seen associated with blood vessels and embedded in the fiber tracts of the corpus callosum (the presumptive neuroblast).

For experiments in which there was no apparent co-localization of the stem cells and the tumor cells, the site of stem cell placement and the anatomic composition of the brain slice may have played a factor. Studies have demonstrated that stem cells preferentially migrate on certain gliophilic and neurophilic pathways, and along blood vessels (Honda et al., 2007; Soares and Sotelo, 2004; Whitman et al., 2009). In our studies, we utilized brain slices from the entire brain. Some sections did not have vasculature or intact migratory pathways.

However, we were able to see stem cells associated with blood vessel-like structures and populating the corpus callosum in some slices. Although real-time data was not available in these studies, it is likely that the perivascular cells and the cells oriented toward the glioma cells in the fiber tracts are the same cells populating the glioma cells. Isolating and studying these cells may provide clues for determining which population of cells is capable of best responding to glioma associated signals, and navigating efficiently through the brain. These cells would be of most intesest to define for a drug-delivery candidate. Overall, we show that neuralized ESCs are capable of migrating directly to glioma cells and that *ex vivo* migration assays may be used to elucidate the mechanisms of stem cells for delivering oncolytic agents to brain tumors.

Throughout our migration studies on organotypic brain slices, it was apparent that the stem cells would migrate throughout the brain slice. Similarly,

we expected seeing glioma cells in fiber tracts similar to the stem cells. The SF767 glioma cells, kindly provided by Dr. Joe Loftus, have been shown to migrate and invade in brain slices (Lipinski et al., 2005). Although tumor cell proliferation was apparent in some slices, we did not see the anticipated tumor cell dispersal on the brain slice. However, it is likely that the cells invaded into the slice as described in their study. If this were the case, it was not detectable using epifluorescence microscope in our study. Another possibility is that a migratory glioma cell population was not present in the tumor cell culture. The latter possibility leads us to question whether this glioma cell line contained a cancer stem cell population, which is implicated as the migratory cell population responsible for the recurrence of malignant gliomas (Singh et al., 2003) (Singh et al., 2004) (Dirks, 2008).

Brain tumor stem cells

Studies conducted by Fine et al, have determined that the glioma cells cultured in the presence of serum for extended periods of time (as was the case for the SF767 glioma cells) poorly represent the phenotype of the primary tumor. However, fresh dissociated tumors grown in the defined culture condition often closely mimic and recapitulate the parental glioblastoma phenotypes (Lee et al., 2006; Li et al., 2008). Additional studies have corroborated these findings and the field has seemingly shifted to studying the stem cell population of malignant gliomas to better understand the mechanisms of tumor growth (Bao et al., 2006; Penuelas et al., 2009; Pollard et al., 2009). If the cancer stem cell is the root of cancer growth, as the cancer stem cell hypotheses would suggest, then

identifying and understanding the behavior of these cells will be important for developing cancer stem cell directed therapies.

Genetic and epigenetic aberrations in GBM stem cells

Our microarray-based studies with glioblastoma stem cells (GSCs) was designed to gain a global picture of how aberrant DNA methylation, copy number variation, and gene expression patterns define GSCs. Recently, various teams of researchers have provided comprehensive studies on the genetic and epigenetic variations in glioblastomas (2008; Bredel et al., 2009; Nagarajan and Costello, 2009; Parsons et al., 2008). The commonality in all of these studies is the use of primary frozen GBMs. The wealth of information provided in these studies will undoubtedly provide a deeper understanding of the molecular mechanisms regarding glioblastomas. Nonetheless, as it becomes increasingly clear that stem cells play a central role in gliomagenesis, the studies with GSCs, will become more common.

In our study, we define the deregulation of two common stem cell pathways: TGF-β and Wnt/β-catenin signaling pathways. We showed that many molecules throughout the pathway are differentially expressed, affected by DNA methylation, and copy number variation. Understanding the deregulation of the entire pathway may be necessary for designing drugs to target multiple molecules. For example, Bredel et al. point out that some GBMs upregulate certain 'hub' genes such as EGFR (upregulated in 50% of GBMs). Hub genes have such an extensive crosstalk between other genes, networks, and pathways; a monotherapeutic approach against its oncoprotein (in the case of EGFR) could

simply fail. Since the signaling cascades of hub genes are interwoven, a therapy directed against multiple hub genes would perhaps be more effective (Bredel et al., 2009). Defining the full spectrum of aberrations in glioblastomas using genomic, epigenomic, proteomic, transcriptomic, metabolomic, etc., approaches for both primary tumor and its stem cell population, is likely to be completed soon. However, the challenges ahead are developing systematic approaches for understanding the interactions of the aberrant genes and their complex networks.

Identifying meningioma initiating cells

As mentioned throughout this dissertation, understanding the initiating/stem cell population of solid tumors may prove to be of importance for developing targeted therapies. During our studies of glioblastoma stem cells, we serendipitously came upon a rapidly dividing cell population derived from a primary tumor. Not only did this population of cells thrive in the 'stem cell medium', they also grew as clusters of cells, different from the traditional neurosphere or tumorsphere growth associated with stem cell populations. Further investigations into the etiology of the tumor revealed it as an atypical meningioma.

Meningiomas are the most common primary intracranial tumor accounting for more than 32% of all reported (CBTRUS: 2007-2008 Statistical report: primary brain tumors in the United States). Atypical meningiomas are grade II tumors that may have some malignant features such as increased mitotic activity, and represent about 6-8% of all meningiomas (Wrobel et al., 2005). Virtually

nothing is known about the putative stem cell population of meningiomas, and there is question as to whether they even exist.

For our studies, we took a discovery approach and asked questions as to whether the meningioma cells we were culturing had stem cell-like properties? Could we see this growth pattern in other atypical meningioma cases? Can these cells be identified in the primary tumor? Through self-renewal and differentiation studies, we were able to establish that they had a stem cell-like phenotype, and through tumorigenic studies, we showed that they can recapitulate some of the histological features of the parental tumor.

The meningioma-initiating cells, or MICs as we refer to them, contained hallmark features of both meningiomas, and cells undergoing an epithelial to mesenchymal (EMT) program (Simon et al., 2007; Weber et al., 1997). Recently, studies have shown that EMT can generate cells with self-renewal properties, and possibly other features of stemness (Mani et al., 2008). For the MICs, EMT upregulation may be a way to identify these cells in other specimens. Additionally, we performed a gene expression array that revealed the upregulation of CD44 and CD166 in these cells, which we also identified in the primary tumor and xenograft by flow analysis and immunohistochemistry. We identified a gene network that included many differentially expressed genes including deregulated Wnt/β-catenin signaling pathway, further defining the molecular mechanisms in these cells. Currently, we are investigating additional cases of atypical meningiomas.

Conclusions

Throughout these studies, it has become clear that there is a need to establish a set of standardized methodologies to better define cancer stem cells. A seemingly important yet lightly discussed topic in the literature, is the concept of a migrating cancer stem cell (Brabletz et al., 2005). The cancer stem cell hypothesis is based on the concept that only a small population of cells within a tumor can recapitulate the heterogeneity of the parental tumor.

In the neural niches of the SVZ and SGZ, the normal neural stem cell will give rise to the transit amplifying cells, which in turn gives rise to the migrating neuroblast. If the cancer stem cell hypothesis holds to be true, this linear progression of differentiation would feasibly exist for a cancer stem cell. The 'cancer neuroblast cell' would have EMT properties (similar to the meningioma initiating cells), an acquisition that has been described as a decisive step towards malignancy (Brabletz et al., 2005). After the cell arrives in a nutrient rich area (similar to the stem cells in the brain slice study), it will establish residence and proliferate. Unlike a normal migrating cancer cell apparent during metastasis, cancer neuroblast cells would have defining features and could be traced back to the cancer stem cell of origin. Identifying the cells responsible for tumor recurrence in the brain may lead to the identification of a neuroblast cancer cell that can efficiently navigate in the brain, and help to identify cell types, for drug-delivery, with these properties that can effectively mimic this migratory pattern.

Stem cells and cancer cells share many common properties including signaling pathways and migratory abilities. The difference is the mutations that

mark the cancer cells and dictate their fate. Through next generation technologies, we are beginning to develop a better picture of this relationship. Although the CSC model may define the properties of some cancers, a combination of therapies that target the hierarchal structure of tumors maybe be necessary for combating brain tumor dispersal.

REFERENCES

2008. Comprehensive genomic characterization defines human glioblastoma genes and core pathways. Nature. 455**,** 1061-8.

Abate-Shen, C., 2002. Deregulated homeobox gene expression in cancer: cause or consequence? Nat Rev Cancer. 2**,** 777-85.

Abdel-Fattah, R., Xiao, A., Bomgardner, D., Pease, C. S., Lopes, M. B., Hussaini, I. M., 2006. Differential expression of HOX genes in neoplastic and non-neoplastic human astrocytes. J Pathol. 209**,** 15-24.

Aboody, K. S., Brown, A., Rainov, N. G., Bower, K. A., Liu, S., Yang, W., Small, J. E., Herrlinger, U., Ourednik, V., Black, P. M., Breakefield, X. O., Snyder, E. Y., 2000. Neural stem cells display extensive tropism for pathology in adult brain: evidence from intracranial gliomas. Proc Natl Acad Sci U S A. 97**,** 12846-51.

Aboody, K. S., Bush, R. A., Garcia, E., Metz, M. Z., Najbauer, J., Justus, K. A., Phelps, D. A., Remack, J. S., Yoon, K. J., Gillespie, S., Kim, S. U., Glackin, C. A., Potter, P. M., Danks, M. K., 2006. Development of a tumor-selective approach to treat metastatic cancer. PLoS ONE. 1**,** e23.

Alvarez-Buylla, A., Doetsch, F., 2002. Identification of neural stem cells in the adult vertebrate brain. Brain Research Bulletin. 57**,** 751–758.

Alvarez-Buylla, A., Seri, B., Doetsch, F., 2002. Identification of neural stem cells in the adult vertebrate brain. Brain Res Bull. 57**,** 751-8.

Bain, G., Kitchens, D., Yao, M., Huettner, J. E., Gottlieb, D. I., 1995. Embryonic stem cells express neuronal properties in vitro. Dev Biol. 168**,** 342-57.

Bao, S., Wu, Q., McLendon, R. E., Hao, Y., Shi, Q., Hjelmeland, A. B., Dewhirst, M. W., Bigner, D. D., Rich, J. N., 2006. Glioma stem cells promote radioresistance by preferential activation of the DNA damage response. Nature. 444**,** 756-60.

Barresi, V., Belluardo, N., Sipione, S., Mudo, G., Cattaneo, E., Condorelli, D. F., 2003. Transplantation of prodrug-converting neural progenitor cells for brain tumor therapy. Cancer Gene Ther. 10**,** 396-402.

Baylin, S. B., 2005. DNA methylation and gene silencing in cancer. Nat Clin Pract Oncol. 2 Suppl 1**,** S4-11.

Beier, D., Hau, P., Proescholdt, M., Lohmeier, A., Wischhusen, J., Oefner, P. J., Aigner, L., Brawanski, A., Bogdahn, U., Beier, C. P., 2007. CD133(+) and CD133(-) glioblastoma-derived cancer stem cells show differential growth characteristics and molecular profiles. Cancer Res. 67**,** 4010-5.

Belicchi, M., Pisati, F., Lopa, R., Porretti, L., Fortunato, F., Sironi, M., Scalamogna, M., Parati, E. A., Bresolin, N., Torrente, Y., 2004. Human skin-derived stem cells migrate throughout forebrain and differentiate into astrocytes after injection into adult mouse brain. J Neurosci Res. 77**,** 475-86.

Beltinger, C., Fulda, S., Kammertoens, T., Meyer, E., Uckert, W., Debatin, K. M., 1999. Herpes simplex virus thymidine kinase/ganciclovir-induced apoptosis involves ligand-independent death receptor aggregation and activation of caspases. Proc Natl Acad Sci U S A. 96**,** 8699-704.

Bennett, L. B., Schnabel, J. L., Kelchen, J. M., Taylor, K. H., Guo, J., Arthur, G. L., Papageorgio, C. N., Shi, H., Caldwell, C. W., 2009. DNA hypermethylation accompanied by transcriptional repression in follicular lymphoma. Genes Chromosomes Cancer. 48**,** 828-41.

Benninger, F., Beck, H., Wernig, M., Tucker, K. L., Brustle, O., Scheffler, B., 2003. Functional integration of embryonic stem cell-derived neurons in hippocampal slice cultures. J Neurosci. 23**,** 7075-83.

Bleau, A. M., Howard, B. M., Taylor, L. A., Gursel, D., Greenfield, J. P., Lim Tung, H. Y., Holland, E. C., Boockvar, J. A., 2008. New strategy for the analysis of phenotypic marker antigens in brain tumor-derived neurospheres in mice and humans. Neurosurg Focus. 24**,** E28.

Bonaguidi, M. A., McGuire, T., Hu, M., Kan, L., Samanta, J., Kessler, J. A., 2005. LIF and BMP signaling generate separate and discrete types of GFAP-expressing cells. Development. 132**,** 5503-14.

Bostrom, J., Meyer-Puttlitz, B., Wolter, M., Blaschke, B., Weber, R. G., Lichter, P., Ichimura, K., Collins, V. P., Reifenberger, G., 2001. Alterations of the tumor suppressor genes CDKN2A (p16(INK4a)), p14(ARF), CDKN2B (p15(INK4b)), and CDKN2C (p18(INK4c)) in atypical and anaplastic meningiomas. Am J Pathol. 159**,** 661-9.

Boucher, P. D., Im, M. M., Freytag, S. O., Shewach, D. S., 2006. A novel mechanism of synergistic cytotoxicity with 5-fluorocytosine and ganciclovir in double suicide gene therapy. Cancer Res. 66**,** 3230-7.

Brabletz, T., Jung, A., Spaderna, S., Hlubek, F., Kirchner, T., 2005. Opinion: migrating cancer stem cells - an integrated concept of malignant tumour progression. Nat Rev Cancer. 5**,** 744-9.

Bredel, M., Scholtens, D. M., Harsh, G. R., Bredel, C., Chandler, J. P., Renfrow, J. J., Yadav, A. K., Vogel, H., Scheck, A. C., Tibshirani, R., Sikic, B. I., 2009. A network model of a cooperative genetic landscape in brain tumors. JAMA. 302, 261-75.

Bruna, A., Darken, R. S., Rojo, F., Ocana, A., Penuelas, S., Arias, A., Paris, R., Tortosa, A., Mora, J., Baselga, J., Seoane, J., 2007. High TGFbeta-Smad activity confers poor prognosis in glioma patients and promotes cell proliferation depending on the methylation of the PDGF-B gene. Cancer Cell. 11, 147-60.

Cadieux, B., Ching, T. T., VandenBerg, S. R., Costello, J. F., 2006. Genome-wide hypomethylation in human glioblastomas associated with specific copy number alteration, methylenetetrahydrofolate reductase allele status, and increased proliferation. Cancer Res. 66, 8469-76.

Catala, M., 1998. Embryonic and fetal development of structures associated with the cerebro-spinal fluid in man and other species. Part I: The ventricular system, meninges and choroid plexuses. Arch Anat Cytol Pathol. 46, 153-69.

CBTRUS: 2007-2008 Statistical report: primary brain tumors in the United States, -. C., IL, Central Brain Tumor Registry of the United States of America.

Chen, H. I., Bakshi, A., Royo, N. C., Magge, S. N., Watson, D. J., 2007. Neural stem cells as biological minipumps: a faster route to cell therapy for the CNS? Curr. Stem Cell Res. & Therapy. 2, 13-22.

Cheng, F., Zagon, I. S., Verderame, M. F., McLaughlin, P. J., 2007. The opioid growth factor (OGF)-OGF receptor axis uses the p16 pathway to inhibit head and neck cancer. Cancer Res. 67, 10511-8.

Chu, P., Clanton, D. J., Snipas, T. S., Lee, J., Mitchell, E., Nguyen, M. L., Hare, E., Peach, R. J., 2009. Characterization of a subpopulation of colon cancer cells with stem cell-like properties. Int J Cancer. 124, 1312-21.

Cillo, C., Cantile, M., Mortarini, R., Barba, P., Parmiani, G., Anichini, A., 1996. Differential patterns of HOX gene expression are associated with specific integrin and ICAM profiles in clonal populations isolated from a single human melanoma metastasis. Int J Cancer. 66, 692-7.

Claes, A., Idema, A. J., Wesseling, P., 2007. Diffuse glioma growth: a guerilla war. Acta Neuropathol. 114, 443-58.

Culver, K. W., Ram, Z., Wallbridge, S., Ishii, H., Oldfield, E. H., Blaese, R. M., 1992. In vivo gene transfer with retroviral vector-producer cells for treatment of experimental brain tumors. Science. 256, 1550-2.

D'Ippolito, G., Diabira, S., Howard, G. A., Menei, P., Roos, B. A., Schiller, P. C., 2004. Marrow-isolated adult multilineage inducible (MIAMI) cells, a unique population of postnatal young and old human cells with extensive expansion and differentiation potential. J Cell Sci. 117, 2971-81.

Dalerba, P., Dylla, S. J., Park, I. K., Liu, R., Wang, X., Cho, R. W., Hoey, T., Gurney, A., Huang, E. H., Simeone, D. M., Shelton, A. A., Parmiani, G., Castelli, C., Clarke, M. F., 2007. Phenotypic characterization of human colorectal cancer stem cells. Proc Natl Acad Sci U S A. 104, 10158-63.

Danks, M. K., Yoon, K. J., Bush, R. A., Remack, J. S., Wierdl, M., Tsurkan, L., Kim, S. U., Garcia, E., Metz, M. Z., Najbauer, J., Potter, P. M., Aboody, K. S., 2007. Tumor-targeted enzyme/prodrug therapy mediates long-term disease-free survival of mice bearing disseminated neuroblastoma. Cancer Res. 67, 22-5.

Dirks, P. B., 2008. Brain tumour stem cells: the undercurrents of human brain cancer and their relationship to neural stem cells. Philos Trans R Soc Lond B Biol Sci. 363, 139-52.

Drake, R. R., Pitlyk, K., McMasters, R. A., Mercer, K. E., Young, H., Moyer, M. P., 2000. Connexin-independent ganciclovir-mediated killing conferred on bystander effect-resistant cell lines by a herpes simplex virus-thymidine kinase-expressing colon cell line. Mol Ther. 2, 515-23.

Draper, J. S., Fox, V., 2003. Human embryonic stem cells: multilineage differentiation and mechanisms of self-renewal. Arch Med Res. 34, 558-64.

Draper, J. S., Pigott, C., Thomson, J. A., Andrews, P. W., 2002. Surface antigens of human embryonic stem cells: changes upon differentiation in culture. J Anat. 200, 249-58.

Dreesen, O., Brivanlou, A. H., 2007. Signaling pathways in cancer and embryonic stem cells. Stem Cell Rev. 3, 7-17.

Elias, L. A., Wang, D. D., Kriegstein, A. R., 2007. Gap junction adhesion is necessary for radial migration in the neocortex. Nature. 448, 901-7.

Estecio, M. R., Yan, P. S., Ibrahim, A. E., Tellez, C. S., Shen, L., Huang, T. H., Issa, J. P., 2007. High-throughput methylation profiling by MCA coupled to CpG island microarray. Genome Res. 17, 1529-36.

Esteller, M., 2008. Epigenetics in cancer. N Engl J Med. 358, 1148-59.

Fabian, A., Barok, M., Vereb, G., Szollosi, J., 2009. Die hard: are cancer stem cells the Bruce Willises of tumor biology? Cytometry A. 75, 67-74.

Fang, D., Nguyen, T. K., Leishear, K., Finko, R., Kulp, A. N., Hotz, S., Van Belle, P. A., Xu, X., Elder, D. E., Herlyn, M., 2005. A tumorigenic subpopulation with stem cell properties in melanomas. Cancer Res. 65**,** 9328-37.

Foltz, G., Yoon, J. G., Lee, H., Ryken, T. C., Sibenaller, Z., Ehrich, M., Hood, L., Madan, A., 2009. DNA methyltransferase-mediated transcriptional silencing in malignant glioma: a combined whole-genome microarray and promoter array analysis. Oncogene. 28**,** 2667-77.

Fukushima, N., Sato, N., Ueki, T., Rosty, C., Walter, K. M., Wilentz, R. E., Yeo, C. J., Hruban, R. H., Goggins, M., 2002. Aberrant methylation of preproenkephalin and p16 genes in pancreatic intraepithelial neoplasia and pancreatic ductal adenocarcinoma. Am J Pathol. 160**,** 1573-81.

Gage, F. H., 2000. Mammalian neural stem cells. Science. 287**,** 1433-8.

Glass, R., Synowitz, M., Kronenberg, G., Walzlein, J. H., Markovic, D. S., Wang, L. P., Gast, D., Kiwit, J., Kempermann, G., Kettenmann, H., 2005. Glioblastoma-induced attraction of endogenous neural precursor cells is associated with improved survival. J Neurosci. 25**,** 2637-46.

Goings, G. E., Sahni, V., Szele, F. G., 2004. Migration patterns of subventricular zone cells in adult mice change after cerebral cortex injury. Brain Res. 996**,** 213-26.

Goo, Y. A., Goodlett, D. R., Pascal, L. E., Worthington, K. D., Vessella, R. L., True, L. D., Liu, A. Y., 2005. Stromal mesenchyme cell genes of the human prostate and bladder. BMC Urol. 5**,** 17.

Gritti, A., Frolichsthal-Schoeller, P., Galli, R., Parati, E. A., Cova, L., Pagano, S. F., Bjornson, C. R., Vescovi, A. L., 1999. Epidermal and fibroblast growth factors behave as mitogenic regulators for a single multipotent stem cell-like population from the subventricular region of the adult mouse forebrain. J Neurosci. 19**,** 3287-97.

Grove, J. E., Bruscia, E., Krause, D. S., 2004. Plasticity of bone marrow-derived stem cells. Stem Cells. 22**,** 487-500.

Gunther, H. S., Schmidt, N. O., Phillips, H. S., Kemming, D., Kharbanda, S., Soriano, R., Modrusan, Z., Meissner, H., Westphal, M., Lamszus, K., 2008. Glioblastoma-derived stem cell-enriched cultures form distinct subgroups according to molecular and phenotypic criteria. Oncogene. 27**,** 2897-909.

Hanemann, C. O., 2008. Magic but treatable? Tumours due to loss of merlin. Brain. 131**,** 606-15.

Hassler, M., Seidl, S., Fazeny-Doerner, B., Preusser, M., Hainfellner, J., Rossler, K., Prayer, D., Marosi, C., 2006. Diversity of cytogenetic and pathohistologic profiles in glioblastoma. Cancer Genet Cytogenet. 166, 46-55.

Herrlinger, U., Woiciechowski, C., Sena-Esteves, M., Aboody, K. S., Jacobs, A. H., Rainov, N. G., Snyder, E. Y., Breakefield, X. O., 2000. Neural precursor cells for delivery of replication-conditional HSV-1 vectors to intracerebral gliomas. Mol Ther. 1, 347-57.

Hill, R., Wu, H., 2009. PTEN, stem cells, and cancer stem cells. J Biol Chem. 284, 11755-9.

Holland, E. C., 2000. Glioblastoma multiforme: the terminator. Proc Natl Acad Sci U S A. 97, 6242-4.

Honda, S., Toda, K., Tozuka, Y., Yasuzawa, S., Iwabuchi, K., Tomooka, Y., 2007. Migration and differentiation of neural cell lines transplanted into mouse brains. Neurosci Res. 59, 124-35.

http://www.mbl.org/.

Hurwitz, R. L., Chevez-Barrios, P., Boniuk, M., Chintagumpala, M., Hurwitz, M. Y., 2003. Retinoblastoma: from bench to bedside. Expert Rev Mol Med. 5, 1-14.

Ikeda, H., Yoshimoto, T., 2003. Immunohistochemical study of anaplastic meningioma with special reference to the phenotypic change of intermediate filament protein. Ann Diagn Pathol. 7, 214-22.

Imitola, J., Raddassi, K., Park, K. I., Mueller, F. J., Nieto, M., Teng, Y. D., Frenkel, D., Li, J., Sidman, R. L., Walsh, C. A., Snyder, E. Y., Khoury, S. J., 2004. Directed migration of neural stem cells to sites of CNS injury by the stromal cell-derived factor 1alpha/CXC chemokine receptor 4 pathway. Proc Natl Acad Sci U S A. 101, 18117-22.

Inagaki, A., Soeda, A., Oka, N., Kitajima, H., Nakagawa, J., Motohashi, T., Kunisada, T., Iwama, T., 2007. Long-term maintenance of brain tumor stem cell properties under at non-adherent and adherent culture conditions. Biochem Biophys Res Commun. 361, 586-92.

Keller, A., Ludwig, N., Backes, C., Romeike, B. F., Comtesse, N., Henn, W., Steudel, W. I., Mawrin, C., Lenhof, H. P., Meese, E., 2009. Genome wide expression profiling identifies specific deregulated pathways in meningioma. Int J Cancer. 124, 346-51.

Kendall, S. E., Najbauer, J., Johnston, H. F., Metz, M. Z., Li, S., Bowers, M., Garcia, E., Kim, S. U., Barish, M. E., Aboody, K. S., Glackin, C. A., 2008.

Neural stem cell targeting of glioma is dependent on phosphoinositide 3-kinase signaling. Stem Cells. 26, 1575-86.

Kim, S. J., Cheon, S. H., Yoo, S. J., Kwon, J., Park, J. H., Kim, C. G., Rhee, K., You, S., Lee, J. Y., Roh, S. I., Yoon, H. S., 2005. Contribution of the PI3K/Akt/PKB signal pathway to maintenance of self-renewal in human embryonic stem cells. FEBS Lett. 579, 534-40.

Klein, W. M., Wu, B. P., Zhao, S., Wu, H., Klein-Szanto, A. J., Tahan, S. R., 2007. Increased expression of stem cell markers in malignant melanoma. Mod Pathol. 20, 102-7.

Koestenbauer, S., Zech, N. H., Juch, H., Vanderzwalmen, P., Schoonjans, L., Dohr, G., 2006. Embryonic stem cells: similarities and differences between human and murine embryonic stem cells. Am J Reprod Immunol. 55, 169-80.

Kokoris, M. S., Black, M. E., 2002. Characterization of herpes simplex virus type 1 thymidine kinase mutants engineered for improved ganciclovir or acyclovir activity. Protein Sci. 11, 2267-72.

Lapidot, T., Sirard, C., Vormoor, J., Murdoch, B., Hoang, T., Caceres-Cortes, J., Minden, M., Paterson, B., Caligiuri, M. A., Dick, J. E., 1994. A cell initiating human acute myeloid leukaemia after transplantation into SCID mice. Nature. 367, 645-8.

Lee, J., Kotliarova, S., Kotliarov, Y., Li, A., Su, Q., Donin, N. M., Pastorino, S., Purow, B. W., Christopher, N., Zhang, W., Park, J. K., Fine, H. A., 2006. Tumor stem cells derived from glioblastomas cultured in bFGF and EGF more closely mirror the phenotype and genotype of primary tumors than do serum-cultured cell lines. Cancer Cell. 9, 391-403.

Lee, J., Son, M. J., Woolard, K., Donin, N. M., Li, A., Cheng, C. H., Kotliarova, S., Kotliarov, Y., Walling, J., Ahn, S., Kim, M., Totonchy, M., Cusack, T., Ene, C., Ma, H., Su, Q., Zenklusen, J. C., Zhang, W., Maric, D., Fine, H. A., 2008. Epigenetic-mediated dysfunction of the bone morphogenetic protein pathway inhibits differentiation of glioblastoma-initiating cells. Cancer Cell. 13, 69-80.

Li, A., Walling, J., Kotliarov, Y., Center, A., Steed, M. E., Ahn, S. J., Rosenblum, M., Mikkelsen, T., Zenklusen, J. C., Fine, H. A., 2008. Genomic changes and gene expression profiles reveal that established glioma cell lines are poorly representative of primary human gliomas. Mol Cancer Res. 6, 21-30.

Li, L., Xie, T., 2005. Stem cell niche: structure and function. Annu Rev Cell Dev Biol. 21, 605-31.

Li, S., Tokuyama, T., Yamamoto, J., Koide, M., Yokota, N., Namba, H., 2005. Potent bystander effect in suicide gene therapy using neural stem cells transduced with herpes simplex virus thymidine kinase gene. Oncology. 69, 503-8.

Lin, J. H., Takano, T., Cotrina, M. L., Arcuino, G., Kang, J., Liu, S., Gao, Q., Jiang, L., Li, F., Lichtenberg-Frate, H., Haubrich, S., Willecke, K., Goldman, S. A., Nedergaard, M., 2002. Connexin 43 enhances the adhesivity and mediates the invasion of malignant glioma cells. J Neurosci. 22, 4302-11.

Lipinski, C. A., Tran, N. L., Menashi, E., Rohl, C., Kloss, J., Bay, R. C., Berens, M. E., Loftus, J. C., 2005. The tyrosine kinase pyk2 promotes migration and invasion of glioma cells. Neoplasia. 7, 435-45.

Liu, G., Yuan, X., Zeng, Z., Tunici, P., Ng, H., Abdulkadir, I. R., Lu, L., Irvin, D., Black, K. L., Yu, J. S., 2006. Analysis of gene expression and chemoresistance of CD133+ cancer stem cells in glioblastoma. Mol Cancer. 5, 67.

Liu, Y., Pang, J. C., Dong, S., Mao, B., Poon, W. S., Ng, H. K., 2005. Aberrant CpG island hypermethylation profile is associated with atypical and anaplastic meningiomas. Hum Pathol. 36, 416-25.

Lois, C., Garcia-Verdugo, J. M., Alvarez-Buylla, A., 1996. Chain migration of neuronal precursors. Science. 271, 978-81.

Lunter, P. C., van Kilsdonk, J. W., van Beek, H., Cornelissen, I. M., Bergers, M., Willems, P. H., van Muijen, G. N., Swart, G. W., 2005. Activated leukocyte cell adhesion molecule (ALCAM/CD166/MEMD), a novel actor in invasive growth, controls matrix metalloproteinase activity. Cancer Res. 65, 8801-8.

Mani, S. A., Guo, W., Liao, M. J., Eaton, E. N., Ayyanan, A., Zhou, A. Y., Brooks, M., Reinhard, F., Zhang, C. C., Shipitsin, M., Campbell, L. L., Polyak, K., Brisken, C., Yang, J., Weinberg, R. A., 2008. The epithelial-mesenchymal transition generates cells with properties of stem cells. Cell. 133, 704-15.

Marshall, C. A., Suzuki, S. O., Goldman, J. E., 2003. Gliogenic and neurogenic progenitors of the subventricular zone: who are they, where did they come from, and where are they going? Glia. 43, 52-61.

Martinez, R., Martin-Subero, J. I., Rohde, V., Kirsch, M., Alaminos, M., Fernandez, A. F., Ropero, S., Schackert, G., Esteller, M., 2009. A microarray-based DNA methylation study of glioblastoma multiforme. Epigenetics. 4, 255-64.

Medici, D., Hay, E. D., Olsen, B. R., 2008. Snail and Slug promote epithelial-mesenchymal transition through beta-catenin-T-cell factor-4-dependent expression of transforming growth factor-beta3. Mol Biol Cell. 19**,** 4875-87.

Mesnil, M., Piccoli, C., Tiraby, G., Willecke, K., Yamasaki, H., 1996. Bystander killing of cancer cells by herpes simplex virus thymidine kinase gene is mediated by connexins. Proc Natl Acad Sci U S A. 93**,** 1831-5.

Meyer, J. S., Katz, M. L., Maruniak, J. A., Kirk, M. D., 2004. Neural differentiation of mouse embryonic stem cells in vitro and after transplantation into eyes of mutant mice with rapid retinal degeneration. Brain Res. 1014**,** 131-44.

Meyer, J. S., Katz, M. L., Maruniak, J. A., Kirk, M. D., 2006. Embryonic stem cell-derived neural progenitors incorporate into degenerating retina and enhance survival of host photoreceptors. Stem Cells. 24**,** 274-83.

Moolten, F. L., Wells, J. M., 1990. Curability of tumors bearing herpes thymidine kinase genes transferred by retroviral vectors. J Natl Cancer Inst. 82**,** 297-300.

Muller, F. J., Snyder, E. Y., Loring, J. F., 2006. Gene therapy: can neural stem cells deliver? Nat Rev Neurosci. 7**,** 75-84.

Murat, A., Migliavacca, E., Gorlia, T., Lambiv, W. L., Shay, T., Hamou, M. F., de Tribolet, N., Regli, L., Wick, W., Kouwenhoven, M. C., Hainfellner, J. A., Heppner, F. L., Dietrich, P. Y., Zimmer, Y., Cairncross, J. G., Janzer, R. C., Domany, E., Delorenzi, M., Stupp, R., Hegi, M. E., 2008. Stem cell-related "self-renewal" signature and high epidermal growth factor receptor expression associated with resistance to concomitant chemoradiotherapy in glioblastoma. J Clin Oncol. 26**,** 3015-24.

Nagarajan, R. P., Costello, J. F., 2009. Epigenetic mechanisms in glioblastoma multiforme. Semin Cancer Biol. 19**,** 188-97.

Nakamizo, A., Marini, F., Amano, T., Khan, A., Studeny, M., Gumin, J., Chen, J., Hentschel, S., Vecil, G., Dembinski, J., Andreeff, M., Lang, F. F., 2005. Human bone marrow-derived mesenchymal stem cells in the treatment of gliomas. Cancer Res. 65**,** 3307-18.

Namba, H., Iwadate, Y., Kawamura, K., Sakiyama, S., Tagawa, M., 2001. Efficacy of the bystander effect in the herpes simplex virus thymidine kinase-mediated gene therapy is influenced by the expression of connexin43 in the target cells. Cancer Gene Ther. 8**,** 414-20.

NIAAA.NIH.GOV., D. G. a.

Noble, M., 2000. Can neural stem cells be used to track down and destroy migratory brain tumor cells while also providing a means of repairing tumor-associated damage? Proc Natl Acad Sci U S A. 97**,** 12393-5.

Oh, S. K., Choo, A. B., 2006. Human embryonic stem cells: technological challenges towards therapy. Clin Exp Pharmacol Physiol. 33**,** 489-95.

Parsons, D. W., Jones, S., Zhang, X., Lin, J. C., Leary, R. J., Angenendt, P., Mankoo, P., Carter, H., Siu, I. M., Gallia, G. L., Olivi, A., McLendon, R., Rasheed, B. A., Keir, S., Nikolskaya, T., Nikolsky, Y., Busam, D. A., Tekleab, H., Diaz, L. A., Jr., Hartigan, J., Smith, D. R., Strausberg, R. L., Marie, S. K., Shinjo, S. M., Yan, H., Riggins, G. J., Bigner, D. D., Karchin, R., Papadopoulos, N., Parmigiani, G., Vogelstein, B., Velculescu, V. E., Kinzler, K. W., 2008. An integrated genomic analysis of human glioblastoma multiforme. Science. 321**,** 1807-12.

Patrawala, L., Calhoun, T., Schneider-Broussard, R., Li, H., Bhatia, B., Tang, S., Reilly, J. G., Chandra, D., Zhou, J., Claypool, K., Coghlan, L., Tang, D. G., 2006. Highly purified CD44+ prostate cancer cells from xenograft human tumors are enriched in tumorigenic and metastatic progenitor cells. Oncogene. 25**,** 1696-708.

Paxinos, G., Franklin, K. B. J., 2004. The mouse brain in stereotaxic coordinates. Elsevier Academic Press, Amsterdam ; Boston.

Penuelas, S., Anido, J., Prieto-Sanchez, R. M., Folch, G., Barba, I., Cuartas, I., Garcia-Dorado, D., Poca, M. A., Sahuquillo, J., Baselga, J., Seoane, J., 2009. TGF-beta increases glioma-initiating cell self-renewal through the induction of LIF in human glioblastoma. Cancer Cell. 15**,** 315-27.

Perry A, Menigiomas. In: R. M. McLendon RE, Bigner DD, (Ed.), Russell and Rubinstein's Pathology of Tumors of the Nervous System. Hodder Arnold, London, 2006, pp. 427-474.

Perry A, L. D., Scheithauer BW, BudkaH, von Deimling A, Menigiomas. In: O. H. Louis DN, Wiestler OD, Cavenee WK, (Ed.), WHO Classification of Tumours of the Central Nervous System. International Agency for Research on Cancer, Lyon, France, 2007.

Pollard, S. M., Yoshikawa, K., Clarke, I. D., Danovi, D., Stricker, S., Russell, R., Bayani, J., Head, R., Lee, M., Bernstein, M., Squire, J. A., Smith, A., Dirks, P., 2009. Glioma stem cell lines expanded in adherent culture have tumor-specific phenotypes and are suitable for chemical and genetic screens. Cell Stem Cell. 4**,** 568-80.

Polyak, K., Weinberg, R. A., 2009. Transitions between epithelial and mesenchymal states: acquisition of malignant and stem cell traits. Nat Rev Cancer. 9**,** 265-73.

Ragel, B. T., Couldwell, W. T., Gillespie, D. L., Wendland, M. M., Whang, K., Jensen, R. L., 2008. A comparison of the cell lines used in meningioma research. Surg Neurol. 70, 295-307; discussion 307.

Rainov, N. G., 2000. A phase III clinical evaluation of herpes simplex virus type 1 thymidine kinase and ganciclovir gene therapy as an adjuvant to surgical resection and radiation in adults with previously untreated glioblastoma multiforme. Hum Gene Ther. 11, 2389-401.

Ram, Z., Culver, K. W., Oshiro, E. M., Viola, J. J., DeVroom, H. L., Otto, E., Long, Z., Chiang, Y., McGarrity, G. J., Muul, L. M., Katz, D., Blaese, R. M., Oldfield, E. H., 1997. Therapy of malignant brain tumors by intratumoral implantation of retroviral vector-producing cells. Nat Med. 3, 1354-61.

Ramaswamy, S., Goings, G. E., Soderstrom, K. E., Szele, F. G., Kozlowski, D. A., 2005. Cellular proliferation and migration following a controlled cortical impact in the mouse. Brain Res. 1053, 38-53.

Rao, S. K., Edwards, J., Joshi, A. D., Siu, I. M., Riggins, G. J., 2009. A survey of glioblastoma genomic amplifications and deletions. J Neurooncol.

Reardon, J. E., 1989. Herpes simplex virus type 1 and human DNA polymerase interactions with 2'-deoxyguanosine 5'-triphosphate analogues. Kinetics of incorporation into DNA and induction of inhibition. J Biol Chem. 264, 19039-44.

Reports, S. C., Regenerative Medecine. Stem Cells: Scientific Progress and Future Research Directions 2006.

Reya, T., Clevers, H., 2005. Wnt signalling in stem cells and cancer. Nature. 434, 843-50.

Reynolds, B. A., Weiss, S., 1992. Generation of neurons and astrocytes from isolated cells of the adult mammalian central nervous system. Science. 255, 1707-10.

Robertson, K. D., 2005. DNA methylation and human disease. Nat Rev Genet. 6, 597-610.

Rodenhiser, D., Mann, M., 2006. Epigenetics and human disease: translating basic biology into clinical applications. CMAJ. 174, 341-8.

Sanson, M., Marcaud, V., Robin, E., Valery, C., Sturtz, F., Zalc, B., 2002. Connexin 43-mediated bystander effect in two rat glioma cell models. Cancer Gene Ther. 9, 149-55.

Sasaki, T., Hankins, G. R., Helm, G. A., 2003. Comparison of gene expression profiles between frozen original meningiomas and primary cultures of the meningiomas by GeneChip. Neurosurgery. 52, 892-8; discussion 898-9.

Scott, C. T., 2006. Stem cell now : from the experiment that shook the world to the new politics of life. Pi Press, New York.

Seoane, J., 2006. Escaping from the TGFbeta anti-proliferative control. Carcinogenesis. 27, 2148-56.

Serfozo, P., Schlarman, M. S., Pierret, C., Maria, B. L., Kirk, M. D., 2006. Selective migration of neuralized embryonic stem cells to stem cell factor and media conditioned by glioma cell lines. Cancer Cell Int. 6, 1.

Shah, K., Tung, C. H., Breakefield, X. O., Weissleder, R., 2005. In vivo imaging of S-TRAIL-mediated tumor regression and apoptosis. Mol Ther. 11, 926-31.

Simon, M., Bostrom, J. P., Hartmann, C., 2007. Molecular genetics of meningiomas: from basic research to potential clinical applications. Neurosurgery. 60, 787-98; discussion 787-98.

Singh, S. K., Clarke, I. D., Terasaki, M., Bonn, V. E., Hawkins, C., Squire, J., Dirks, P. B., 2003. Identification of a cancer stem cell in human brain tumors. Cancer Res. 63, 5821-8.

Singh, S. K., Hawkins, C., Clarke, I. D., Squire, J. A., Bayani, J., Hide, T., Henkelman, R. M., Cusimano, M. D., Dirks, P. B., 2004. Identification of human brain tumour initiating cells. Nature. 432, 396-401.

Smith, A. G., 2001. Embryo-derived stem cells: of mice and men. Annu Rev Cell Dev Biol. 17, 435-62.

Soares, S., Sotelo, C., 2004. Adult neural stem cells from the mouse subventricular zone are limited in migratory ability compared to progenitor cells of similar origin. Neuroscience. 128, 807-17.

Son, M. J., Woolard, K., Nam, D. H., Lee, J., Fine, H. A., 2009. SSEA-1 is an enrichment marker for tumor-initiating cells in human glioblastoma. Cell Stem Cell. 4, 440-52.

Srivastava, A. S., Shenouda, S., Mishra, R., Carrier, E., 2006. Transplanted embryonic stem cells successfully survive, proliferate, and migrate to damaged regions of the mouse brain. Stem Cells. 24, 1689-94.

Stiles, C. D., Rowitch, D. H., 2008. Glioma stem cells: a midterm exam. Neuron. 58, 832-46.

Stoppini, L., Buchs, P. A., Muller, D., 1991. A simple method for organotypic cultures of nervous tissue. J Neurosci Methods. 37, 173-82.

Takahashi, K., Yamanaka, S., 2006. Induction of pluripotent stem cells from mouse embryonic and adult fibroblast cultures by defined factors. Cell. 126, 663-76.

Tang, Y., Shah, K., Messerli, S. M., Snyder, E., Breakefield, X., Weissleder, R., 2003. In vivo tracking of neural progenitor cell migration to glioblastomas. Hum Gene Ther. 14, 1247-54.

Vescovi, A. L., Galli, R., Reynolds, B. A., 2006. Brain tumour stem cells. Nat Rev Cancer. 6, 425-36.

Ward, R. J., Dirks, P. B., 2007. Cancer stem cells: at the headwaters of tumor development. Annu Rev Pathol. 2, 175-89.

Watson, M. A., Gutmann, D. H., Peterson, K., Chicoine, M. R., Kleinschmidt-DeMasters, B. K., Brown, H. G., Perry, A., 2002. Molecular characterization of human meningiomas by gene expression profiling using high-density oligonucleotide microarrays. Am J Pathol. 161, 665-72.

Weber, R. G., Bostrom, J., Wolter, M., Baudis, M., Collins, V. P., Reifenberger, G., Lichter, P., 1997. Analysis of genomic alterations in benign, atypical, and anaplastic meningiomas: toward a genetic model of meningioma progression. Proc Natl Acad Sci U S A. 94, 14719-24.

Whitman, M. C., Fan, W., Rela, L., Rodriguez-Gil, D. J., Greer, C. A., 2009. Blood vessels form a migratory scaffold in the rostral migratory stream. J Comp Neurol. 516, 94-104.

Wichterle, H., Lieberam, I., Porter, J. A., Jessell, T. M., 2002. Directed differentiation of embryonic stem cells into motor neurons. Cell. 110, 385-97.

Willis, J., Smith, C., Ironside, J. W., Erridge, S., Whittle, I. R., Everington, D., 2005. The accuracy of meningioma grading: a 10-year retrospective audit. Neuropathol Appl Neurobiol. 31, 141-9.

Winn, R. A., Marek, L., Han, S. Y., Rodriguez, K., Rodriguez, N., Hammond, M., Van Scoyk, M., Acosta, H., Mirus, J., Barry, N., Bren-Mattison, Y., Van Raay, T. J., Nemenoff, R. A., Heasley, L. E., 2005. Restoration of Wnt-7a expression reverses non-small cell lung cancer cellular transformation through frizzled-9-mediated growth inhibition and promotion of cell differentiation. J Biol Chem. 280, 19625-34.

Wrobel, G., Roerig, P., Kokocinski, F., Neben, K., Hahn, M., Reifenberger, G., Lichter, P., 2005. Microarray-based gene expression profiling of benign,

atypical and anaplastic meningiomas identifies novel genes associated with meningioma progression. Int J Cancer. 114**,** 249-56.

Yadav, A. K., Renfrow, J. J., Scholtens, D. M., Xie, H., Duran, G. E., Bredel, C., Vogel, H., Chandler, J. P., Chakravarti, A., Robe, P. A., Das, S., Scheck, A. C., Kessler, J. A., Soares, M. B., Sikic, B. I., Harsh, G. R., Bredel, M., 2009. Monosomy of chromosome 10 associated with dysregulation of epidermal growth factor signaling in glioblastomas. JAMA. 302**,** 276-89.

Yin, D., Ogawa, S., Kawamata, N., Tunici, P., Finocchiaro, G., Eoli, M., Ruckert, C., Huynh, T., Liu, G., Kato, M., Sanada, M., Jauch, A., Dugas, M., Black, K. L., Koeffler, H. P., 2009. High-resolution genomic copy number profiling of glioblastoma multiforme by single nucleotide polymorphism DNA microarray. Mol Cancer Res. 7**,** 665-77.

Ying, V., Haverstick, K., Page, R. L., Saltzman, W. M., 2007. Efficacy of camptothecin and polymer-conjugated camptothecin in tumor spheroids and solid tumors. J Biomater Sci Polym Ed. 18**,** 1283-99.

Yip, S., Sabetrasekh, R., Sidman, R. L., Snyder, E. Y., 2006. Neural stem cells as novel cancer therapeutic vehicles. Eur J Cancer. 42**,** 1298-308.

Zhang, S., Balch, C., Chan, M. W., Lai, H. C., Matei, D., Schilder, J. M., Yan, P. S., Huang, T. H., Nephew, K. P., 2008. Identification and characterization of ovarian cancer-initiating cells from primary human tumors. Cancer Res. 68**,** 4311-20.

VITA

Prakash Rath was born on September 3rd 1979 in Buffalo, NY. He graduated from Fayetteville High School in 1997. He received a Bachelors of Science degree in Zoology from the University of Arkansas, Fayetteville, in 2002 and Masters of Science degree from the same University in 2004. In 2009 he received his Ph.D in Biological Sciences from the University of Missouri, Columbia. During his Ph.D studies, he worked in the Department of Patholgy and Anatomical Sciences in the Missouri School of Medicine, and at the Medical College of Georgia, Augusta. Beginning in 2010, he will begin post-doctoral research in the Department of Neurology at The Johns Hopkins University, Baltimore.